RESEARCH MEMORANDUM

EFFECT OF WING SLATS AND INBOARD WING FENCES ON THE LONGITUDINAL STABILITY CHARACTERISTICS OF THE DOUGLAS D-558-II RESEARCH AIRPLANE IN ACCELERATED MANEUVERS AT SUBSONIC AND TRANSONIC SPEEDS

By Jack Fischel

Langley Aeronautical Laboratory
Langley Field, Va.

NATIONAL ADVISORY COMMITTEE
FOR AERONAUTICS

WASHINGTON

February 8, 1954

NACA RM L53L16

NATIONAL ADVISORY COMMITTEE FOR AERONAUTICS

RESEARCH MEMORANDUM

EFFECT OF WING SLATS AND INBOARD WING FENCES ON THE LONGITUDINAL STABILITY CHARACTERISTICS OF THE DOUGLAS D-558-II RESEARCH AIRPLANE IN ACCELERATED MANEUVERS AT SUBSONIC AND TRANSONIC SPEEDS

By Jack Fischel

SUMMARY

Previous flight tests of the Douglas D-558-II research airplane indicated an instability and "pitch-up" in accelerated longitudinal maneuvers which is a characteristic of swept-wing airplanes at subsonic and transonic speeds. In an attempt to alleviate this instability, the airplane was tested with the wing slats fully extended, with and without inboard wing fences, and with the wing slats half extended and wing fences removed. Also, in order to improve the stick-force characteristics at moderate and large angles of attack, additional tests were conducted with two bungees of differing stiffness alternately attached to the control column. These tests were performed at Mach numbers up to about 1.0, and at altitudes between 10,000 and 35,000 feet.

Opening the wing slats to the fully extended position improved the stability characteristics of the airplane by alleviating pitch-up at Mach numbers below approximately 0.8; however, at Mach numbers of 0.80 and 0.85 the severity of the pitch-up remained unaltered. At Mach numbers of about 0.98 and 1.00, maneuvers performed up to relatively high values of normal-force coefficient with slats fully extended exhibited no evidence of pitch-up; however, this effect has since been duplicated with the clean-wing configuration (no fences, slats retracted).

Removing the wing fences from the airplane configuration with slats fully extended caused the reduction in stick-fixed stability to become more pronounced and, generally, to occur at approximately the same or slightly lower values of normal-force coefficient.

With wing slats half extended and no wing fences, the airplane exhibited instability characteristics and pitch-up similar to that exhibited by the airplane with slats retracted and with wing fences.

With slats fully extended and wing fences removed, use of a bungee in the control system to alleviate or eliminate the stick-free instability caused the airplane to appear more controllable to the pilot and caused the decrease in stick-fixed stability to become less apparent and less objectionable.

In general, the pilots' opinions corroborated the aforementioned statements in that the airplane was generally controllable with fully extended slats and was uncontrollable with half-extended slats. In any configuration, when pitch-up was experienced, the behavior was extremely undesirable and would prevent precision flight.

INTRODUCTION

The use of sweptback wings on aircraft has introduced a problem pertaining to longitudinal stability and control. The problem manifests itself by a sizable decrease in the stability as the airplane angle of attack increases, and by an uncontrolled pitching of the airplane to large angles of attack (refs. 1 to 4).

In order to alleviate this problem, and thereby enable the swept-wing airplane to be usable throughout the range of normal-force coefficient and Mach number of which it is capable, as well as to avoid the danger of exceeding airplane structural limits, the National Advisory Committee for Aeronautics is investigating in flight various modifications to the Douglas D-558-II swept-wing research airplane. The effects of outboard wing fences on the airplane longitudinal stability characteristics were previously investigated and were reported (ref. 2) to provide only a slight improvement in stability over the original airplane configuration. As an extension of that investigation, as well as to obtain slat loads on a swept-wing airplane, the airplane was tested with the leading-edge wing slats locked open in the fully extended position and also in the half-extended position. Data were obtained during accelerated longitudinal maneuvers up to high values of normal-force coefficient and at speeds up to a Mach number of approximately 1.0. The slat-load data obtained during the course of this investigation are presented in reference 5, whereas the longitudinal stability data are presented herein. From these data, a normal-force-coefficient—Mach number boundary for the occurrence of the decay in stick-fixed and/or stick-free stability was determined for each airplane configuration and is compared with a similar stick-fixed stability boundary for the original airplane configuration. The effects on stability of removing the inboard wing fence, included on the airplane in the original configuration, were also determined with the slats fully extended. In addition, because of the adverse effect of a stick-free instability on the handling qualities and pilots' opinion of the airplane, the effects of adding a

"soft" and a "stiff" bungee to the longitudinal control column in order to improve the stick-free stability were determined with the slats fully extended and inboard wing fences removed.

SYMBOLS

b	wing span, ft
C_{N_A}	airplane normal-force coefficient, nW/qS
c	wing chord, ft
$\bar{c}$	wing mean aerodynamic chord, ft
F_e	elevator control force, lb
g	acceleration due to gravity, ft/sec^2
h_p	pressure altitude, ft
i_t	stabilizer setting with respect to fuselage center line, positive when leading edge of stabilizer is up, deg
M	free-stream Mach number
n	normal acceleration, g units
q	free-stream dynamic pressure, lb/sq ft
S	wing area, sq ft
t	time, sec
V_c	calibrated airspeed, mph
W	airplane weight, lb
α	angle of attack of airplane center line, deg
δ_e	elevator deflection with respect to stabilizer, deg
$\delta_{e(\ddot{\theta}=0)}$	elevator deflection corrected to zero pitching acceleration, deg
$\dot{\theta}$	pitching velocity, radians/sec
$\ddot{\theta}$	pitching acceleration, radians/sec^2

[redacted]

AIRPLANE

The Douglas D-558-II airplanes have sweptback wing and tail surfaces and were designed for combination turbojet and rocket power. The airplane used in the present investigation (Bu.Aero No. 37975 or NACA 145) is equipped with a Westinghouse J-34-WE-40 turbojet engine, which exhausts out of the bottom of the fuselage between the wing and tail, and with a Reaction Motors, Inc. LR8-RM-6 rocket engine, which exhausts out of the rear of the fuselage. The airplane is air-launched from a Boeing B-29 mother airplane. A photograph of the airplane is shown as figure 1 and a three-view drawing is shown as figure 2. Pertinent airplane dimensions and characteristics are listed in table I.

The wing slats, which extended from 0.434 semispan to the wing tips, may be normally free floating or locked in either the open or closed position. When in the unlocked free-floating condition, the slats are normally closed at low values of angle of attack or normal-force coefficient and open with increase in angle of attack. At Mach numbers below approximately 0.72, the slats opened for values of α above approximately 3° to 5° (unpublished data); at Mach numbers in excess of 0.72 and up to approximately 0.98, the data of reference 5 indicate that the slats would also tend to open with increase in α, starting at moderate values of α or C_{N_A}. For the investigation reported herein, the wing slats were locked open in either the fully extended or half-extended position. Wing fences located at 0.36 semispan, incorporated in the original airplane configuration to improve the longitudinal stability characteristics of the airplane at high angles of attack ($\alpha > 10^\circ$) when the wing slats were fully extended (ref. 6), were removed from the airplane for a part of the investigation reported herein. Figures 3 to 6 illustrate the wing slat and fence configurations investigated.

The airplane is equipped with an adjustable stabilizer. No aerodynamic balance or control-force booster system is used on the elevator. Hydraulic dampers are installed on all the control surfaces to aid in the prevention of control-surface "buzz."

For a part of the investigation reported herein, two different bungees were included in the longitudinal control system to increase the pull forces at up-elevator deflections above about 8° (under no-load conditions) and were slack at smaller up-elevator deflections. The position of the control column at which the bungee commenced stretching was indicated by a control-position transmitter attached to the control column. The bungees provided stick forces of approximately 6 pounds and 22 pounds per inch of control-wheel movement, which roughly corresponded to about 2 pounds and 8 pounds per degree of elevator deflection, respectively, depending on the aerodynamic elevator load

and control-system deflection. Because of stretch in the control system under flight conditions, the bungees employed increased the control forces commencing at up-elevator deflections somewhat less than 8°, depending on the aerodynamic elevator load, as will be shown in the data figures.

INSTRUMENTATION

Standard NACA recording instruments were installed in the airplane to measure the following quantities which were pertinent to this investigation:

Airspeed
Altitude
Elevator wheel force
Normal acceleration
Pitching velocity
Pitching acceleration
Angle of attack
Stabilizer and elevator positions
Control-column position (included during tests with bungee)

All of the instruments were synchronized by means of a common timer.

The elevator position was measured at the inboard end of the control surface, and the stabilizer position was measured at the plane of symmetry. All control positions were measured perpendicular to the control hinge line.

An NACA high-speed pitot-static tube (type A-6 of ref. 7) was mounted on a boom $4\frac{3}{4}$ feet forward of the nose of the airplane. The vane used to measure the angle of attack was mounted on the same boom about $3\frac{1}{2}$ feet forward of the nose of the airplane. The angle-of-attack data have not been corrected for the effects of upwash ahead of the nose of the airplane nor for the effects of airplane pitching velocity. The maximum error attributable to the effects of pitching velocity was of the order of 1.2° (obtained during a pitch-up with the slats half extended). The airspeed system was calibrated up to $M = 0.80$ by the "fly-by" method and at speeds in excess of $M = 0.80$ by the NACA radar phototheodolite method (ref. 8).

[redacted]

TESTS, RESULTS, AND DISCUSSION

The longitudinal stability characteristics of the D-558-II airplane were determined in turning flight, with flaps and landing gear up, for a range of Mach numbers from about 0.4 to 1.0 and for the operating conditions shown for each configuration in the following table:

Configuration		Stabilizer setting, i_t, deg	Center-of-gravity location, percent mean aerodynamic chord	Altitude range, ft
Slat position	Inboard wing fences			
Fully extended	On	1.6 to 2.3*	25.4 to 26.2	14,000 to 35,100
Fully extended	Removed	1.3 to 1.6*	25.2 to 26.9	10,800 to 33,000
Half extended	Removed	1.6*	28.5 to 28.6	29,000 to 35,000

*Exception noted below.

Except where otherwise noted (at $M > 0.9$), the turns were performed by the use of elevator alone, the stabilizer remaining stationary during the maneuvers. Additional data were obtained during 1g stalls with slats fully extended, inboard fences on and removed, in the landing condition (flaps and gear down) at an altitude of approximately 20,000 feet, for a center-of-gravity location of about $0.25\bar{c}$, and at $i_t = 1.6^\circ$.

Data obtained in turns with the airplane configurations incorporating fully extended slats, with and without inboard wing fences, are plotted in the form of time histories and as functions of angle of attack in figures 7 to 14. Comparative data obtained during 1 g stalls in the landing condition with slats fully extended and inboard wing fences on and removed are presented in figures 15 and 16. For the condition with wing fences removed and the slat half extended, longitudinal-maneuvering data are presented in figures 17 and 18. For convenience in comparing the data, the flight conditions and figure numbers of the data presented are tabulated in table II. Summary plots, showing the Mach number—normal-force-coefficient boundaries for the decay in stick-fixed and stick-free longitudinal stability for each slat and wing-fence configuration investigated are shown in figures 19 to 21. Because one of the major purposes of the tests reported herein was to determine an airplane configuration with improved longitudinal stability characteristics, data obtained with each

configuration do not exhaustively cover a large Mach number range inasmuch as tests with a given configuration were terminated when that configuration did not appear to provide the desired improvement.

It will be observed that two sets of elevator-deflection data are presented in the figures where the data are plotted as functions of angle of attack (figs. 8, 10, 12, 14, and 18): the measured values of δ_e shown in the time-history plots, and values of δ_e corrected to zero pitching acceleration to represent static trimmed-flight conditions. This correction was applied to the measured values of δ_e because the slope $d\delta_e/d\alpha$ does not indicate the true airplane stability when relatively high pitching accelerations are obtained. The trimmed-flight values of δ_e were computed by means of the following equation:

$$\delta_{e(\ddot{\theta}=0)} = \delta_e - \frac{I_Y\ddot{\theta}}{C_{m_{\delta_e}} qS\bar{c}}$$

where

I_Y airplane moment of inertia in pitch; varied from about 33,400 to about 37,500 slug-feet^2 (depending on airplane weight and balance) for the tests reported herein

$C_{m_{\delta_e}}$ variation of airplane pitching-moment coefficient with elevator deflection, obtained from unpublished flight data; varied from about -0.022 at $M = 0.5$ to about -0.012 at $M = 0.95$

Inasmuch as the values of $C_{m_{\delta_e}}$ employed for these calculations were measured at low values of α and are probably invalid for high values of α, the values of $\delta_{e(\ddot{\theta}=0)}$ were computed only over a sufficiently large range of α to show the onset of adverse stick-fixed stability effects.

Airplane Configuration Incorporating Fully Extended Slats and Inboard Wing Fences

The time histories of figure 7 show that the airplane with slats fully extended and fences on is generally stable, stick-fixed, up to moderate values of normal-force coefficient, with up movement of the

[redacted]

elevator (or nose-down movement of the stabilizer, fig. 7(o)) producing an almost proportional increase in the airplane angle of attack and normal-force coefficient. Throughout the Mach number range of these tests (except at $M = 0.98$), the stick forces lightened at moderately large angles of attack prior to reversal of the elevator control to effect recovery from the maneuver. At Mach numbers below approximately 0.65, the lightening of the elevator stick forces produced an inadvertent increase in the rate of change of elevator deflection; however, the increase in α appears only slightly greater than the increase in δ_e, compared to these variations at smaller values of C_{N_A}, indicating only a small reduction in stick-fixed stability. At Mach numbers between approximately 0.65 and 0.85 when the elevator was moved at an approximately constant rate, there was at moderate lifts a measurable increase in the rate of change of α, after which the stick force lightened and the control was reversed to effect recovery from the maneuver. An example of this may be seen in figure 7(m) where rapid increase of the angle of attack appears to start slightly after 3.5 seconds, although the up-elevator movement appears to be at a constant rate. Over most of the speed range covered, the time-history data indicate that the airplane is generally controllable, except possibly near the highest angles of attack attained, where there is a small region of apparent instability which is probably a dynamic effect.

These aforementioned effects are also shown in figure 8, where the data shown in figure 7, as well as other measured quantities, are presented as functions of angle of attack. These data show that up to about $M = 0.74$, the variation of $\delta_{e(\ddot{\theta}=0)}$ with α is linear up to about $\alpha \approx 8^\circ$ at which point a decrease occurs, indicating a reduction in the apparent stick-fixed static longitudinal stability. At $\alpha \approx 12^\circ$ to 14° a further decrease in apparent stick-fixed stability occurs which is sometimes followed by a region of almost neutral stability. This latter decrease in stability is accompanied by large pitching rates and is preceded by or occurs coincident with a decay in the stick-free stability which would accentuate the decrease in stick-fixed stability to the pilot. For convenience, the angle of attack at which the first decrease in stick-fixed stability occurs and at which the stick-free stability decays is indicated by a tick adjacent to the $\delta_{e(\ddot{\theta}=0)}$ and F_e curves, respectively.

At Mach numbers of about 0.8 and 0.85 (figs. 8(m) and 8(n)) the apparent longitudinal stick-fixed static stability decreases sharply at values of $\alpha \approx 5^\circ$ or 6°, and an instability (or pitch-up) follows, accompanied by a decay in the stick-free stability and large pitching accelerations. At both Mach numbers, an almost uncontrollable pitch-up is apparent after the reduction in stick-fixed stability; and large values of α and C_{N_A} were obtained prior to recovery from the maneuver at $M = 0.85$. No data were obtained with slats out between Mach numbers of

[redacted]

about 0.85 and 0.95, so the stability characteristics of this configuration in this range are not known; however, in the maneuver performed at $M \approx 0.98$, a value of $C_{N_A} = 0.85$ was attained with no apparent decay in stick-fixed stability. This latter effect has since been duplicated on the basic clean-wing configuration (no fences, slats retracted), for which a value of $C_{N_A} \approx 1.0$ was attained during a maneuver at $M \approx 1.0$ with no evidence of a pitch-up.

The effects of extending the wing slats may be observed by comparing the data of figures 7 and 8 with the data of reference 2 for the original airplane configuration incorporating retracted wing slats and inboard wing fences. Inasmuch as the elevator data of reference 2 were not corrected to $\ddot{\theta} = 0$, comparison with the stick-fixed stability data contained herein should be limited to measured values of δ_e. (Comparison was also made by correcting the δ_e data of reference 2 for pitching-acceleration effects and comparing with $\delta_{e_{(\ddot{\theta}=0)}}$ data of the present paper.) In general, after the initial decay in stability, slat extension caused the reduction of stick-fixed stability to be milder, which for Mach numbers below approximately 0.8 alleviated the uncontrollable pitch-up obtained with the slats retracted. Also, in general, the airplane appeared more controllable at high values of α and C_{N_A} with the slats extended. Although the wing slats improved the stick-fixed stability, the stick-free stability with slats fully extended was still reduced at moderately high angles of attack and was similar to that with slats retracted. (See ref. 2.) Study of reference 9 shows that elevator hinge moments would tend to get more positive (pull force) as up-elevator deflection increased, and would tend toward more negative values (push force) as α increased. Consideration of these opposite effects of α and δ_e on the hinge moments, as well as the probability of a reduction in dynamic pressure at the tail as α increased, indicates that the elevator pull forces could be expected to lighten and even decrease at moderate values of α.

In general, these results agree with the low-speed wind-tunnel data of reference 6, which showed the airplane model experienced a decay of stability and a highly unstable region at moderate values of α with slats retracted and either a neutrally stable or a slightly stable region at comparable values of α with slats extended.

Airplane Configuration Incorporating Fully Extended Slats With Inboard Wing Fences Removed

Data obtained with the airplane over a Mach number range from about 0.4 to about 1.0 after removal of the wing fences, with the slats fully

extended, are shown in figures 9 to 14. These data were obtained without a bungee attached to the control column (figs. 9 and 10), with a soft bungee (figs. 11 and 12), and with a stiff bungee (figs. 13 and 14).

A comparison of the data of figures 7 and 8 with the data of figures 9 to 14 shows that removal of the inboard wing fences with slats fully extended caused the reduction of stick-fixed static stability occurring at moderate values of α ($\alpha \approx 8^\circ$) to be somewhat more pronounced, for Mach numbers below about 0.7, but had a negligible effect on the values of α at which this decay in stability occurred. Removal of the wing fences also tended to accentuate the almost neutral stability region occurring at $\alpha \approx 10^\circ$ to 17° and even produced regions of stick-fixed static instability. At Mach numbers between about 0.80 and 0.95, the decay in stability was more pronounced, similar to the effect noted for the airplane with fences, and stick-fixed static instability with accompanying large pitching accelerations - indicating severe pitch-up - were obtained. At a Mach number of about 1.0, a value of $C_{N_A} = 0.56$ was attained with no indication of an instability. In both configurations, however, the airplane appeared about equally controllable at high angles of attack and appeared to respond similarly to reversal of the controls. The angles of attack for stick-fixed and stick-free stability reduction are indicated by ticks on figures 10, 12, and 14.

In general, removal of the wing fences had little or no effect on the stick-free stability characteristics of the airplane. Because of the possible effect the decay in stick-force characteristics may have had in causing the pilot to aggravate the decay in apparent stick-fixed stability at Mach numbers below about 0.8 and thus influence the flight behavior, a soft bungee and a stiff bungee were alternately attached to the control column to alleviate the stick-free instability. Although the bungees were installed to increase the stick forces at $M \approx 0.7$ for up-elevator deflections above about 8° (under no-load conditions), stretch in the control system under flight conditions caused the effects of the bungee to be initiated at low values of up-elevator deflection. The angle of attack at which the effects of the bungee were initiated during each maneuver is indicated on figures 12 and 14 by the tick on the F_e curve.

The effect of the soft bungee on the stick-free instability, which occurred after the stick-fixed stability had decayed, was generally negligible. The stick-free instability occurred at approximately the same values of α and δ_e as with no bungee present. As a result, it was concluded that the soft bungee did not increase the stick forces sufficiently in the range of δ_e desired and a heavier or stiffer bungee should be utilized. The stiff bungee employed was selected to provide almost linear increases in stick force with increase in elevator deflection

for values of δ_e above about 8° at $M \approx 0.7$. In general, the stiff bungee tended to improve the stick-free stability characteristics of the airplane at the higher angles of attack. Although the stick forces leveled off, and, in many cases, decreased slightly at about the same values of α and δ_e as when no bungee was present, the forces did not decrease rapidly with further increase in α and δ_e as they did without a bungee. In most instances, as was intended, the forces increased with increase in the stick-fixed stability at the high angles of attack.

Inasmuch as the data of reference 6 showed that removal of the inboard wing fences with the slats extended would cause the airplane to be unstable for a small range of angles of attack at moderate values of α, additional flight data were obtained in order to determine the characteristics of the airplane with inboard fences on and removed in the landing condition. Level flight stalls were performed at an altitude of about 20,000 feet with the slat fully extended and flaps and gear extended and the resulting data are presented in figures 15 and 16. The airplane exhibited greater stick-fixed stability with inboard fences removed at speeds above 150 miles per hour; but, at lower speeds, the airplane appeared unstable with fences removed and exhibited a region of slight instability or neutral stability with fences on. In addition, the pilot reported the airplane to have marginal dynamic lateral stability at speeds below 150 miles per hour with the fences removed. With either fence configuration and for the stabilizer position used ($i_t = 1.6^\circ$), the airplane exhibited a neutral variation of stick force with airspeed over most of the speed range shown, and an unstable variation at the lower speeds. To avoid the poor longitudinal and lateral characteristics encountered at lower speeds when the fences were removed, the pilot landed the airplane at approximately 150 miles per hour; however, this landing speed was well within the customary range of landing speeds ($V_c \approx 140$ to 170 mph) employed with this airplane.

Airplane Configuration Incorporating Half-Extended Slats and No Wing Fences

An appreciable increase in airplane drag occurred at low and moderate lift coefficients in going from the slats-retracted to the slats fully extended condition (unpublished data). In order to determine if the improved stability characteristics which resulted when going from the slats-retracted to the slats fully extended condition might not be obtained with a smaller drag increase, flight measurements were made with the slats in the half-extended position. The data obtained are presented in figures 17 and 18. The limited data obtained with the fences removed and slats half extended indicate that large changes in stability are

encountered at moderate values of α and C_{N_A}, and that the airplane experiences an uncontrollable pitch-up when performing longitudinal maneuvers at Mach numbers between approximately 0.85 and 0.96. At $M = 0.85$ the value of α for the decrease in stick-fixed stability is quite apparent; however, this is not as obvious at $M = 0.96$ because of the use of both stabilizer and elevator to perform the turn. At both speeds tested, the value of α at which the decay in stability is felt to occur is indicated by the tick. The subsequent uncontrollable pitch-up is apparent from the fact that an almost constant elevator position or a reduction in control position is accompanied by a rapid pitching to high angles of attack and large normal accelerations. The large pitching velocities noted for the higher Mach number maneuver are approximately the largest obtained to date on this airplane.

Comparison of figures 17 and 18 with figures 9 and 14 indicates that the decay in airplane stability was more pronounced and a large degree of stick-fixed static instability existed at moderate values of α with slats half extended. In addition, control reversal effected a more rapid recovery of the airplane with slats fully extended than with slats half extended.

Boundary for the Decay in Airplane Stability

From the data shown in figures 7 to 14, 17, and 18, the normal-force coefficients corresponding to the value of α at which the stick-free instability or decay of stick-fixed static stability occur have been determined and are presented as functions of Mach number in figures 19 to 21. In figures 19 and 20, the boundary for decay of stick-fixed stability is shown dashed at the highest Mach numbers because no data were obtained in this range and a stick-fixed instability is not clearly apparent at the highest Mach number. (See figs. 8(o) and 12(k).) For comparative purposes, the boundary for the decay in stick-fixed stability of the original airplane configuration of reference 2, corrected to $\ddot{\theta} = 0$, has been included on figure 19.

For each configuration investigated, the decay in stick-fixed static stability is observed to occur at lower values of C_{N_A} than the stick-free instability, the incremental difference in C_{N_A} being about 0.2 over most of the Mach number range. In general, the values of C_{N_A} for both the stick-fixed and stick-free stability boundaries showed little change for Mach numbers below $M \approx 0.7$. Above $M = 0.7$ the values of C_{N_A} defining the stability boundaries are seen to vary in an irregular manner. As may be noted, extending the wing slats had little effect on the boundary. However, these boundaries do not reflect the generally

more favorable behavior of the airplane with slats extended, as discussed previously, particularly the fact that the uncontrollable pitch-up obtained with slats retracted was considerably alleviated for $M < 0.8$, and the airplane appeared more controllable in the pitch-up region with slats extended. Removal of the wing fences with slats extended had a small unfavorable effect on the stick-fixed stability boundary. With slats half extended, the stick-fixed stability boundary at $M \approx 0.86$ occurs at about the same C_{N_A} as for slats retracted or fully extended; however, at a Mach number of 0.95, the stability boundary occurs at a higher value of C_{N_A} than for the airplane with inboard wing fences and with slats retracted.

Peak values of C_{N_A} obtained during the reported maneuvers are also shown in figures 19 to 21. It is felt that in some instances these peak values of C_{N_A} may correspond to maximum values attainable at the given Mach number. At higher Mach numbers, the difference between peak C_{N_A} and the value of C_{N_A} for decay in stability is appreciably larger than at low values of M; consequently, the magnitude and the potential danger of the stability decay is greater in this speed range.

In the speed range in which pitch-up was encountered and the airplane appeared uncontrollable, the stability problem would be aggravated for airplanes having high wing loadings and for flight at high altitude. For such airplanes, level flight would necessarily be performed at higher angles of attack and normal-force coefficients. This would allow for little or no maneuvering lift margin prior to experiencing the pitch-up, in some cases pitch-up being encountered in level flight which would be both intolerable and dangerous. Because the reported flights were generally performed at reasonably high altitudes, no excessive airframe loads were encountered; however, at lower altitudes, the possibility and danger of such excessive loads are apparent (ref. 10).

Pilots' Impressions

In general, the pilots' reports corroborated the data and conclusions reached for the maneuvers performed. With slats fully extended at all Mach numbers below $M \approx 0.8$, it is the pilot's opinion that the airplane stability did not deteriorate appreciably after the initial decay, and as a consequence control was regained more rapidly than in the original slats-retracted configuration (ref. 2). At $M \approx 0.98$ (wing fences on) and $M \approx 1.0$ (wing fences removed), the airplane appeared controllable up to the maximum value of α attained. In both fence configurations with slats fully extended the stability change most apparent to the pilot was the lightening of stick forces at moderate angles of attack. The pilots reported a stick-fixed stability change at moderate values of angle of attack which became somewhat more apparent when the inboard wing fences were removed from the slats fully

extended configuration. The pilots thought that the airplane configurations with slats fully extended were a definite improvement over the airplane configurations flown with slats retracted (ref. 2), for the reasons discussed.

Because the soft bungee had little or no effect on the stick forces, the character of the stick-free and stick-fixed instability of the airplane appeared to the pilot to be about the same as when no bungee was used. In both instances, the lightening of the stick forces at moderate angles of attack tended to increase the control rate, which in turn would aggravate any pitching. With the stiff bungee, however, the character of the decay in stability appeared much improved, for now the stick-free stability was improved and the airplane appeared to have a lower pitch divergence rate than previously; thus, the change in stick-fixed stability was somewhat less apparent and less objectionable.

In the configuration with slats half extended, the pilot thought the airplane behavior was similar to that encountered with slats retracted, and the pitch-up encountered was equally uncontrollable. Although data obtained in this configuration were limited to two high-speed maneuvers, the pilot reported that pitch-up was also encountered in other maneuvers performed at lower speeds (down to $M < 0.7$), at lower values of normal acceleration as the Mach number was decreased.

As was reported in reference 2, when the pitch-up occurred at high speeds, it was rather abrupt and more severe than at low speeds. If the pilot does not check the pitch-up by use of the elevator as soon as it is noticed, the angle of attack increases rapidly and violent rolling and yawing motions are experienced at large values of α. In addition, the occurrence of a reduction in stick-free stability almost simultaneously with the reduction in stick-fixed stability tended to accentuate the pitch-up to the pilot. In any case, when a reduction in stick-fixed stability was followed by a pitch-up, the airplane behavior was considered undesirable and objectionable. If the stick-fixed stability is made acceptable, the provision of a bob weight, bungee, or artificial feel system to supply more satisfactory stick-force characteristics would be desirable.

CONCLUSIONS

Results of a longitudinal stability investigation of several wing-slat and inboard wing-fence configurations of the swept-wing D-558-II airplane at subsonic and transonic Mach numbers gave the following conclusions:

[redacted]

1. Fully extended wing slats improved the stability characteristics of the airplane by alleviating pitch-up at Mach numbers below approximately 0.8; however, at Mach numbers between 0.80 and 0.85 the severity of the pitch-up remained unaltered. At Mach numbers of about 0.98 and 1.00, maneuvers performed up to relatively high values of normal-force coefficient with slats fully extended exhibited no evidence of pitch-up; however, this effect has since been duplicated with the clean-wing configuration (no fences, slats retracted).

2. Removing the wing fences from the airplane configuration with slats fully extended caused the reduction in stick-fixed stability to become slightly more pronounced.

3. With wing slats half extended and no wing fences, the airplane exhibited instability characteristics and pitch-up similar to that exhibited by the airplane with slats retracted and with wing fences.

4. In general, the pilots' opinions corroborated the aforementioned statements in that the airplane was generally controllable with fully extended slats and was uncontrollable with half-extended slats. In any configuration, when pitch-up was experienced, the behavior was extremely undesirable and would prevent precision flight in this region.

5. With slats fully extended and wing fences removed, use of a bungee in the control system to alleviate or eliminate the stick-free instability caused the airplane to appear more controllable to the pilot and caused the decrease in stick-fixed stability to become less apparent and less objectionable.

Langley Aeronautical Laboratory,
National Advisory Committee for Aeronautics,
Langley Field, Va., December 1, 1953.

[redacted]

REFERENCES

1. Sjoberg, S. A., Peele, James R., and Griffith, John H.: Flight Measurements With the Douglas D-558-II (BuAero No. 37974) Research Airplane. Static Longitudinal Stability and Control Characteristics at Mach Numbers up to 0.87. NACA RM L50K13, 1951.

2. Fischel, Jack, and Nugent, Jack: Flight Determination of the Longitudinal Stability in Accelerated Maneuvers at Transonic Speeds for the Douglas D-558-II Research Airplane Including the Effects of an Outboard Wing Fence. NACA RM L53A16, 1953.

3. Anderson, Seth B., and Bray, Richard S.: A Flight Evaluation of the Longitudinal Stability Characteristics Associated With the Pitch-Up of a Swept-Wing Airplane in Maneuvering Flight at Transonic Speeds. NACA RM A51I12, 1951.

4. McFadden, Norman M., Rathert, George A., Jr., and Bray, Richard S.: The Effectiveness of Wing Vortex Generators in Improving the Maneuvering Characteristics of a Swept-Wing Airplane at Transonic Speeds. NACA RM A51J18, 1952.

5. Peele, James R.: Transonic Flight Measurement of the Aerodynamic Load on the Extended Slat of the Douglas D-558-II Research Airplane. NACA RM L53F29, 1953.

6. Queijo, M. J., and Jaquet, Byron M.: Wind-Tunnel Investigation of the Effect of Chordwise Fences on Longitudinal Stability Characteristics of an Airplane Model With a 35° Sweptback Wing. NACA RM L50K07, 1950.

7. Gracey, William, Letko, William, and Russell, Walter R.: Wind-Tunnel Investigation of a Number of Total-Pressure Tubes at High Angles of Attack. Subsonic Speeds. NACA TN 2331, 1951. (Supersedes NACA RM L50G19.)

8. Zalovcik, John A.: A Radar Method of Calibrating Airspeed Installations on Airplanes in Maneuvers at High Altitudes and at Transonic and Supersonic Speeds. NACA Rep. 985, 1950. (Supersedes NACA TN 1979.)

9. Kolbe, Carl D., and Bandettini, Angelo: Investigation in the Ames 12-Foot Pressure Wind Tunnel of a Model Horizontal Tail of Aspect Ratio 3 and Taper Ratio 0.5 Having the Quarter-Chord Line Swept Back 45°. NACA RM A51D02, 1951.

[redacted]

10. Drake, Hubert M., Robinson, Glenn H., and Kuhl, Albert E.: Loads Experienced in Flights of Two Swept-Wing Research Airplanes in the Angle-of-Attack Range of Reduced Stability. NACA RM L53D16, 1953.

[redacted]

TABLE I.- PHYSICAL CHARACTERISTICS OF THE

DOUGLAS D-558-II AIRPLANE

Wing:	
Root airfoil section (normal to 0.30 chord of unswept panel)	NACA 63-010
Tip airfoil section (normal to 0.30 chord of unswept panel)	NACA 63_1-012
Total area, sq ft	175.0
Span, ft	25.0
Mean aerodynamic chord, in.	87.301
Root chord (parallel to plane of symmetry), in.	108.51
Tip chord (parallel to plane of symmetry), in.	61.18
Taper ratio	0.565
Aspect ratio	3.570
Sweep at 0.30 chord of unswept panel, deg	35.0
Incidence at fuselage center line, deg	3.0
Dihedral, deg	-3.0
Geometric twist, deg	0
Total aileron area (rearward of hinge line), sq ft	9.8
Aileron travel (each), deg	±15
Total flap area, sq ft	12.58
Flap travel, deg	50
Horizontal tail:	
Root airfoil section (normal to 0.30 chord of unswept panel)	NACA 63-010
Tip airfoil section (normal to 0.30 chord of unswept panel)	NACA 63-010
Area (including fuselage), sq ft	39.9
Span, in.	143.6
Mean aerodynamic chord, in.	41.75
Root chord (parallel to plane of symmetry), in.	53.6
Tip chord (parallel to plane of symmetry), in.	26.8
Taper ratio	0.50
Aspect ratio	3.59
Sweep at 0.30 chord line of unswept panel, deg	40.0
Dihedral, deg	0
Elevator area, sq ft	9.4
Elevator travel, deg	
Up	25
Down	15
Stabilizer travel, deg	
Leading edge up	4
Leading edge down	5

[redacted]

TABLE I.- PHYSICAL CHARACTERISTICS OF THE

DOUGLAS D-558-II AIRPLANE - Concluded

Vertical tail:	
Airfoil section (normal to 0.30 chord of unswept panel)	NACA 63-010
Area, sq ft	36.6
Height from fuselage center line, in.	98.0
Root chord (parallel to fuselage center line), in.	146.0
Tip chord (parallel to fuselage center line), in.	44.0
Sweep angle at 0.30 chord of unswept panel, deg	49.0
Rudder area (aft of hinge line), sq ft	6.15
Rudder travel, deg	±25
Fuselage:	
Length, ft	42.0
Maximum diameter, in.	60.0
Fineness ratio	8.40
Speed-retarder area, sq ft	5.25
Engines:	
Turbojet	J-34-WE-40
Rocket	LR8-RM-6
Airplane weight, lb:	
Full jet and rocket fuel	15,131
Full jet fuel	11,942
No fuel	10,382
Center-of-gravity locations, percent M.A.C.:	
Full jet and rocket fuel (gear up)	23.5
Full jet fuel (gear up)	25.2
No fuel (gear up)	27.0
No fuel (gear down)	26.4

[redacted]

TABLE II.- INDEX TO DATA FIGURES

Airplane configuration	Altitude, ft	Mach number (approx.)	Maneuver	Figure number
Slats fully extended, inboard wing fences on, flaps and gear retracted	18,300	0.45	Wind-up turn	7(a), 8(a)
	19,200	.46		7(b), 8(b)
	17,000	.48		7(c), 8(c)
	19,700	.49		7(d), 8(d)
	15,700	.50		7(e), 8(e)
	20,000	.55		7(f), 8(f)
	14,000	.56		7(g), 8(g)
	21,000	.59		7(h), 8(h)
	23,000	.66		7(i), 8(i)
	21,500	.71		7(j), 8(j)
	19,600	.73		7(k), 8(k)
	23,800	.74		7(l), 8(l)
	28,500	.80		7(m), 8(m)
	33,000	.85		7(n), 8(n)
	35,100	.98		7(o), 8(o)
Slats fully extended, inboard wing fences removed, flaps and gear retracted	19,700	.50	Wind-up turn	9(a), 10(a)
	20,700	.50		9(b), 10(b)
	20,700	.55		9(c), 10(c)
	21,800	.55		9(d), 10(d)
	22,100	.61		9(e), 10(e)
	23,400	.61		9(f), 10(f)
	24,000	.70		9(g), 10(g)
	26,500	.72		9(h), 10(h)
Slats fully extended, inboard wing fences removed, flaps and gear retracted, soft bungee attached to control column	14,900	.41	Wind-up turn	11(a), 12(a)
	15,900	.45		11(b), 12(b)
	16,500	.50		11(c), 12(c)
	17,200	.54		11(d), 12(d)
	16,000	.56		11(e), 12(e)
	18,000	.61		11(f), 12(f)
	19,000	.77		11(g), 12(g)
	23,000	.80		11(h), 12(h)
	27,300	.85		11(i), 12(i)
	27,000	.90		11(j), 12(j)
	33,000	1.0		11(k), 12(k)
Slats fully extended, inboard wing fences removed, flaps and gear retracted, stiff bungee attached to control column	12,700	.40	Wind-up turn	13(a), 14(a)
	13,600	.40		13(b), 14(b)
	14,200	.45		13(c), 14(c)
	15,500	.45		13(d), 14(d)
	16,500	.52		13(e), 14(e)
	18,000	.52		13(f), 14(f)
	10,800	.54		13(g), 14(g)
	16,100	.54		13(h), 14(h)
	18,300	.57		13(i), 14(i)
	22,000	.72		13(j), 14(j)
	26,500	.77		13(k), 14(k)
Slats fully extended, inboard wing fences on, flaps and gear extended	20,000	----	1 g stall	15
Slats fully extended, inboard wing fences removed, flaps and gear extended	19,250	----	1 g stall	16
Slats half extended, inboard wing fences removed, flaps and gear retracted	29,000	.85	Wind-up turn	17(a), 18(a)
	35,000	.96		17(b), 18(b)

[redacted]

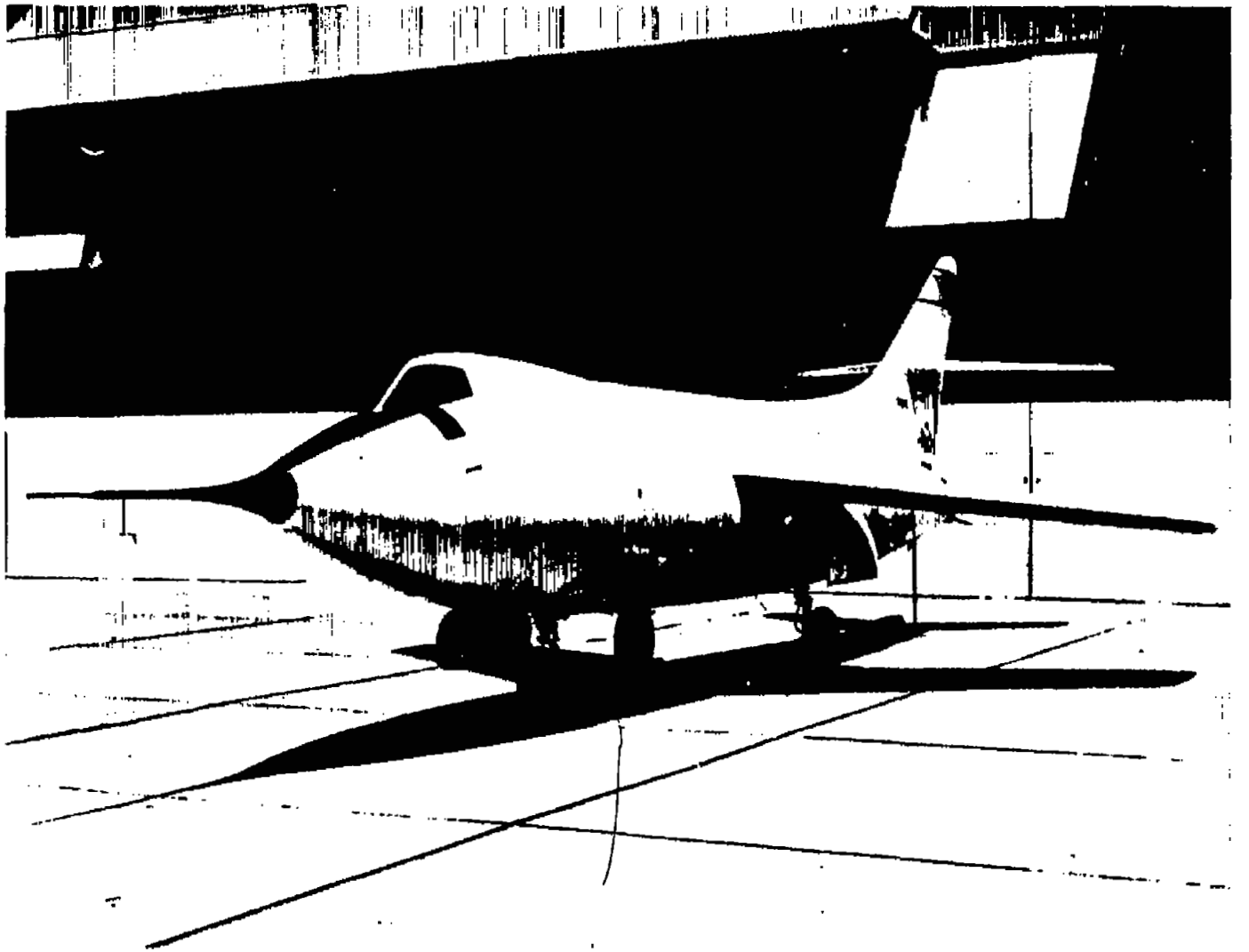

L-70947

Figure 1.- Three-quarter front view of Douglas D-558-II airplane.

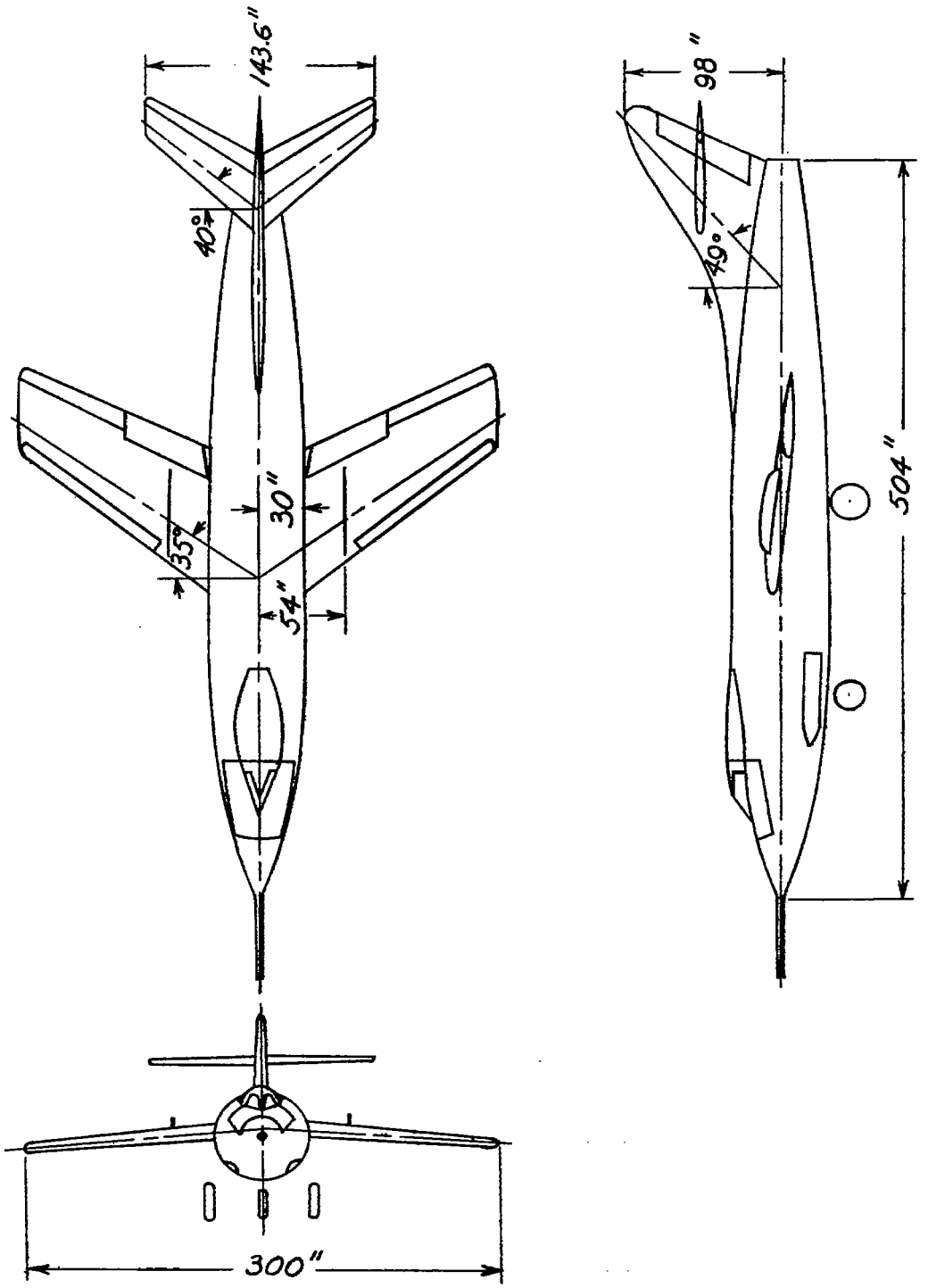

Figure 2.- Three-view drawing of Douglas D-558-II (NACA 145) research airplane.

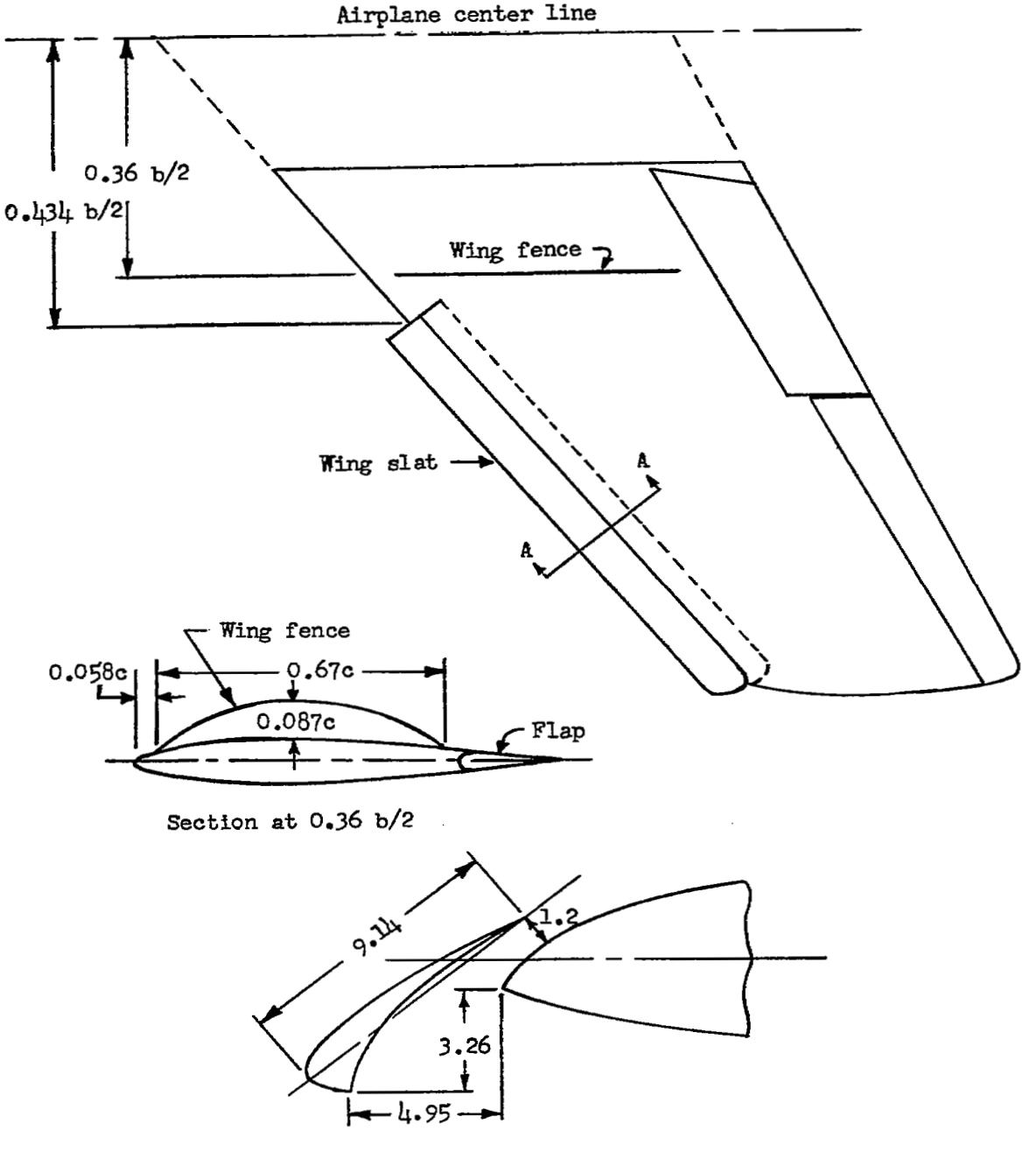

Figure 3.- Plan form and section of the wing of the Douglas D-558-II airplane showing the location of the slat in the fully extended position. All dimensions in inches except as noted.

[redacted]

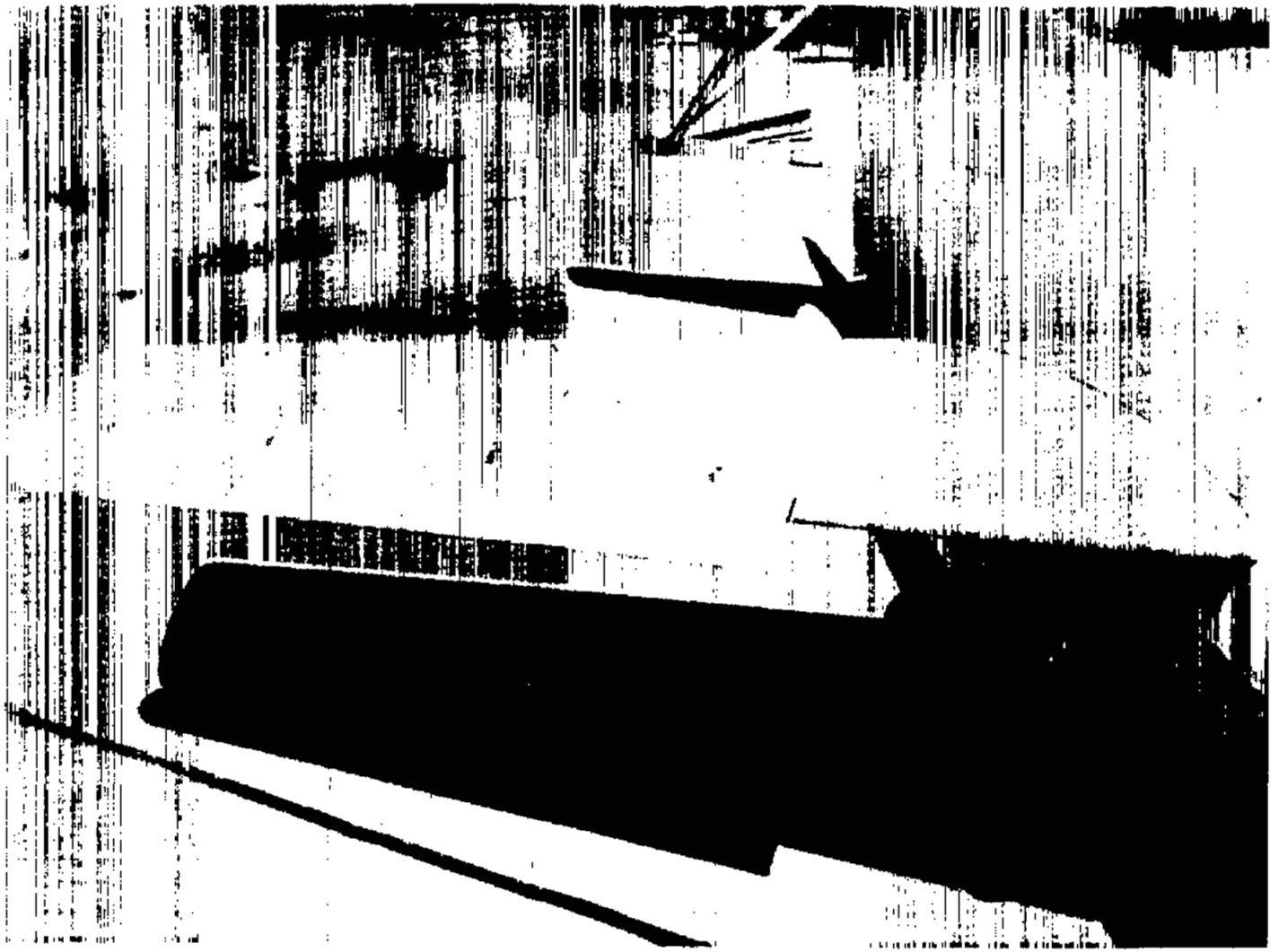

LE-817

Figure 4.- Photograph of right wing of D-558-II airplane, showing slat in fully extended position and inboard fence on wing.

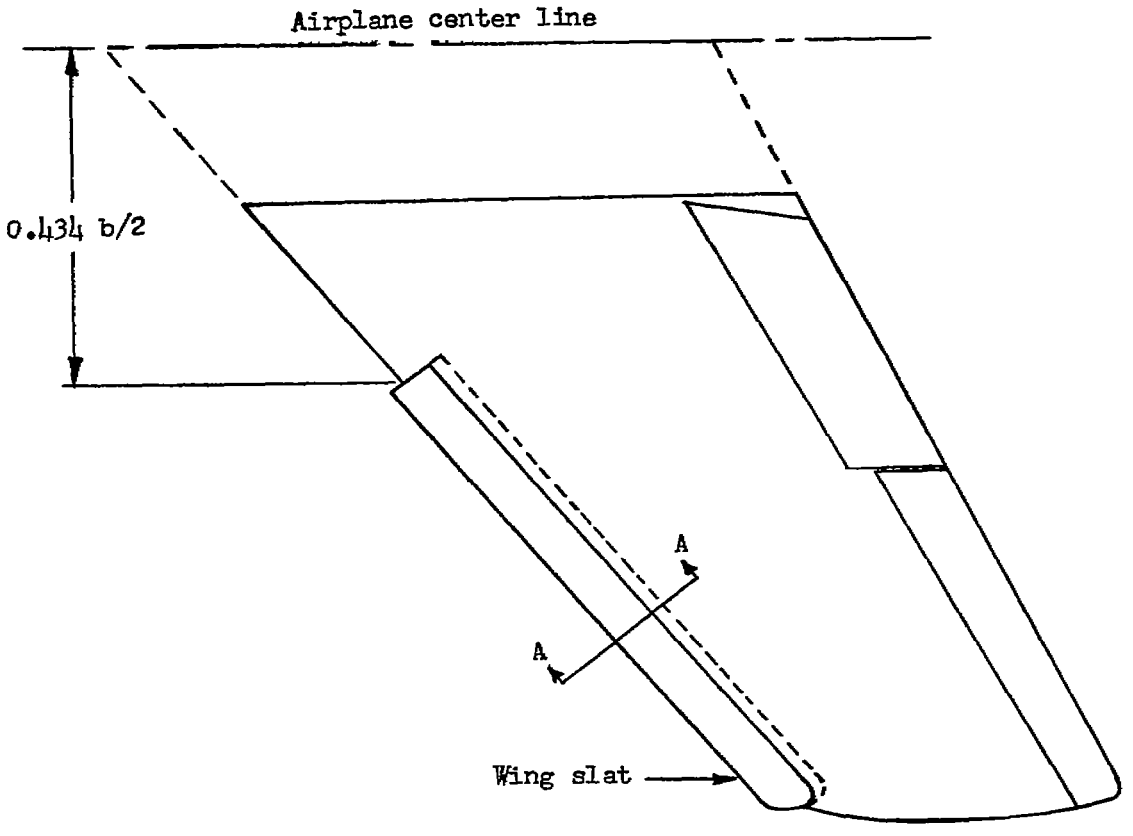

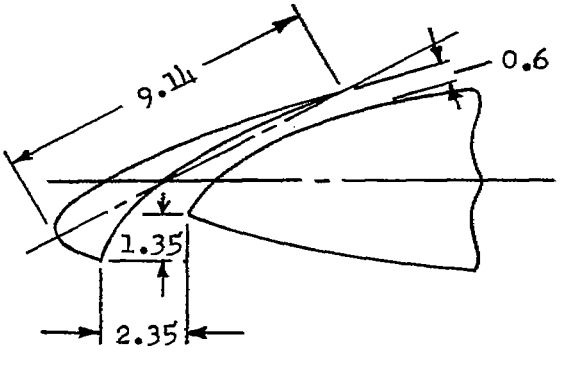

Section A-A (enlarged)

Figure 5.- Plan form and section of the wing of the Douglas D-558-II airplane showing the location of the slat in the half-extended position. All dimensions in inches except as noted.

[redacted]

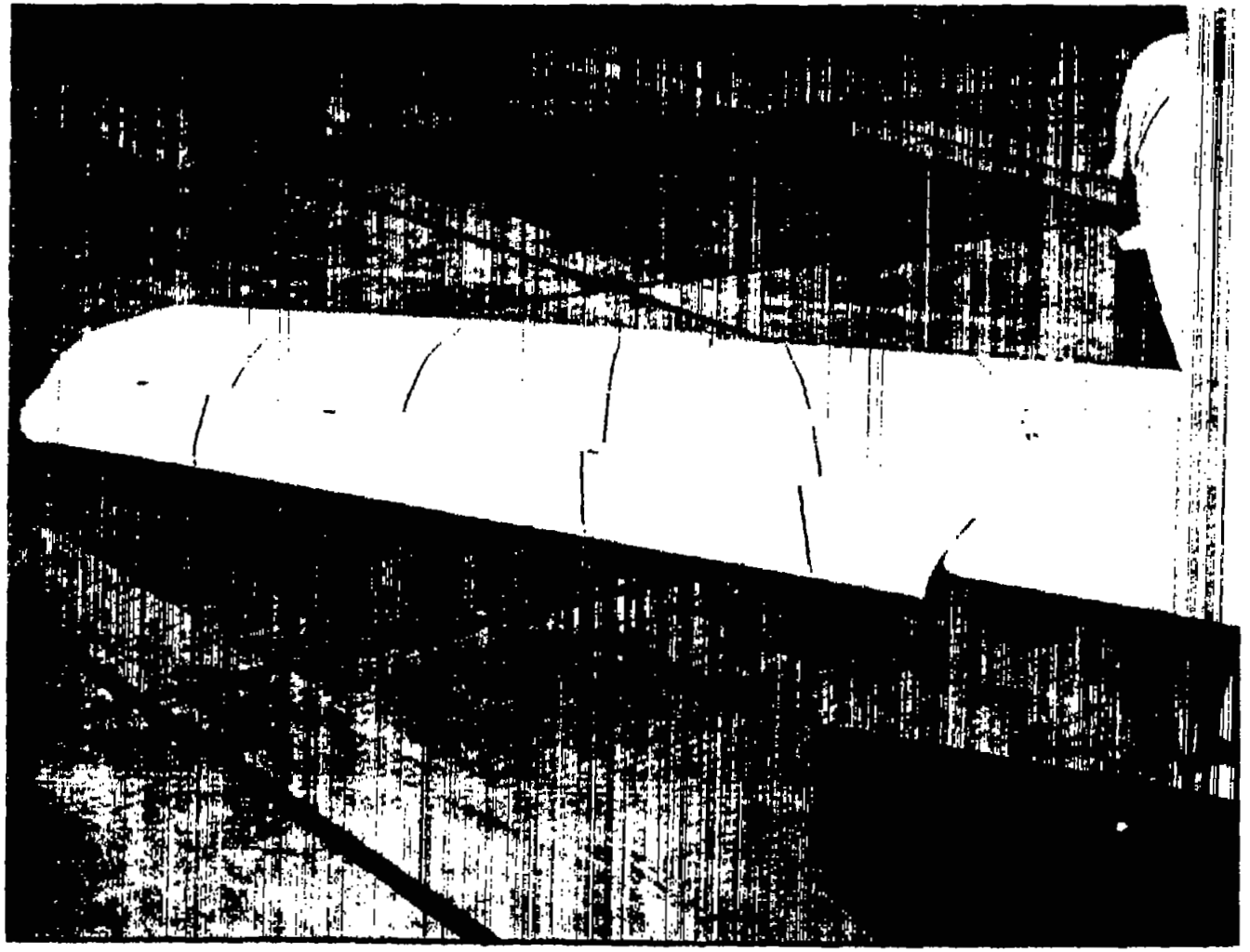

LE-816

Figure 6.- Photograph of right wing of D-558-II airplane, showing slat in half-extended position with inboard wing fences removed.

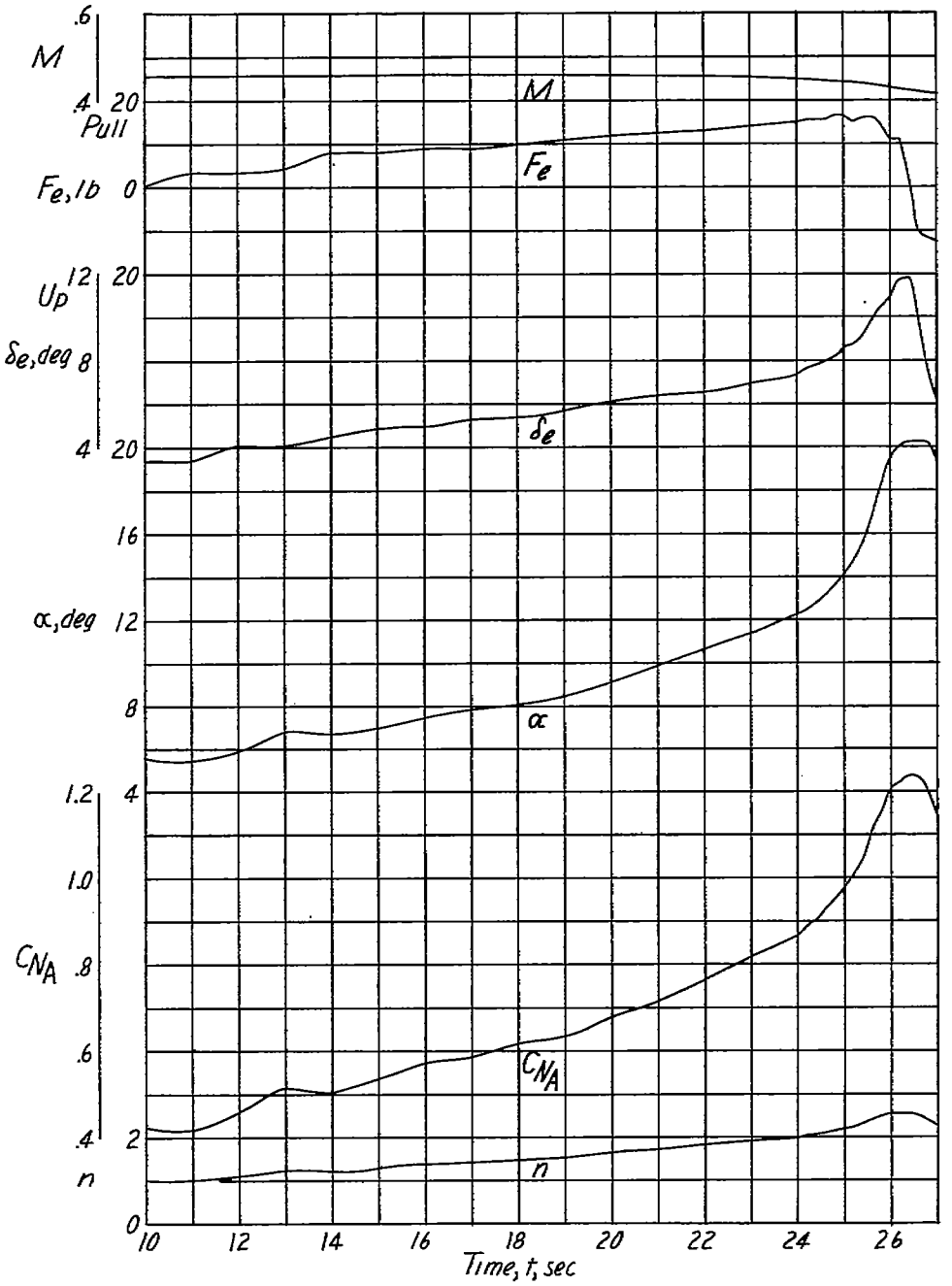

(a) $h_p \approx 18{,}300$ feet; $i_t = 1.6^\circ$; center of gravity at 26.0 percent mean aerodynamic chord.

Figure 7.- Time histories of wind-up turns with the Douglas D-558-II research airplane with slats fully extended and inboard fences on the wings.

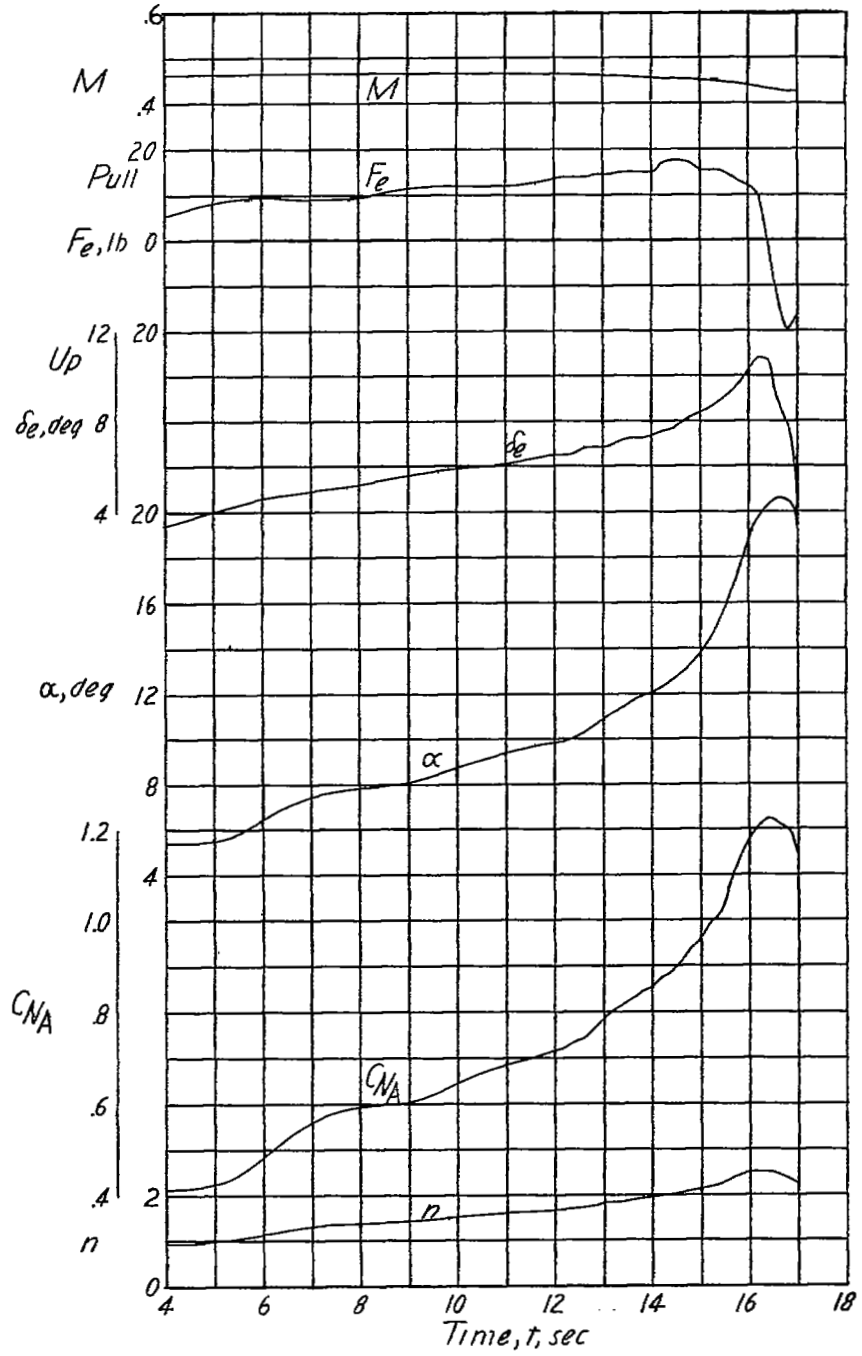

(b) $h_p \approx 19{,}200$ feet; $i_t = 1.6^\circ$; center of gravity at 25.9 percent mean aerodynamic chord.

Figure 7.- Continued.

[redacted]

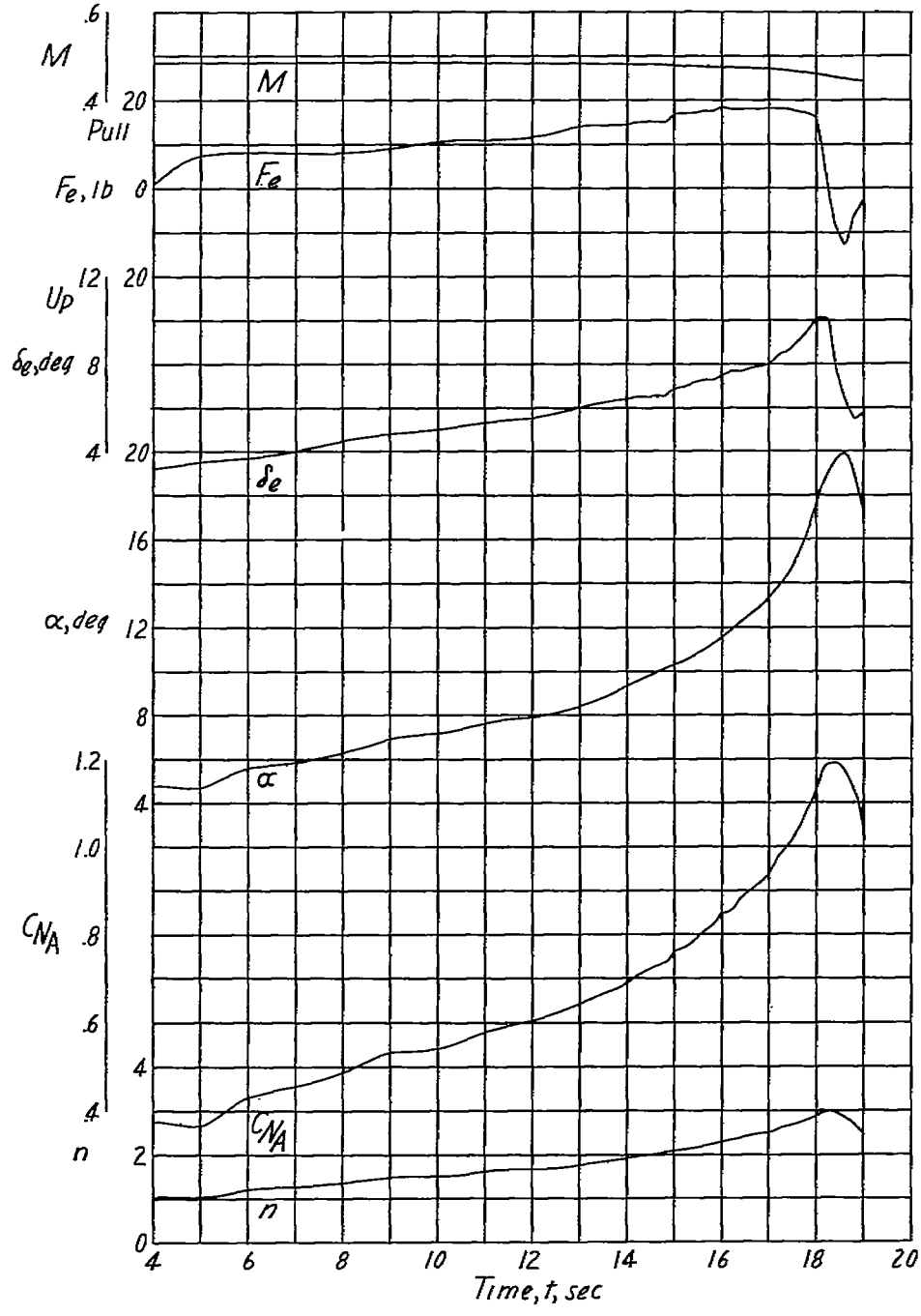

(c) $h_p \approx 17{,}000$ feet; $i_t = 1.6°$; center of gravity at 26.1 percent mean aerodynamic chord.

Figure 7.- Continued.

[redacted]

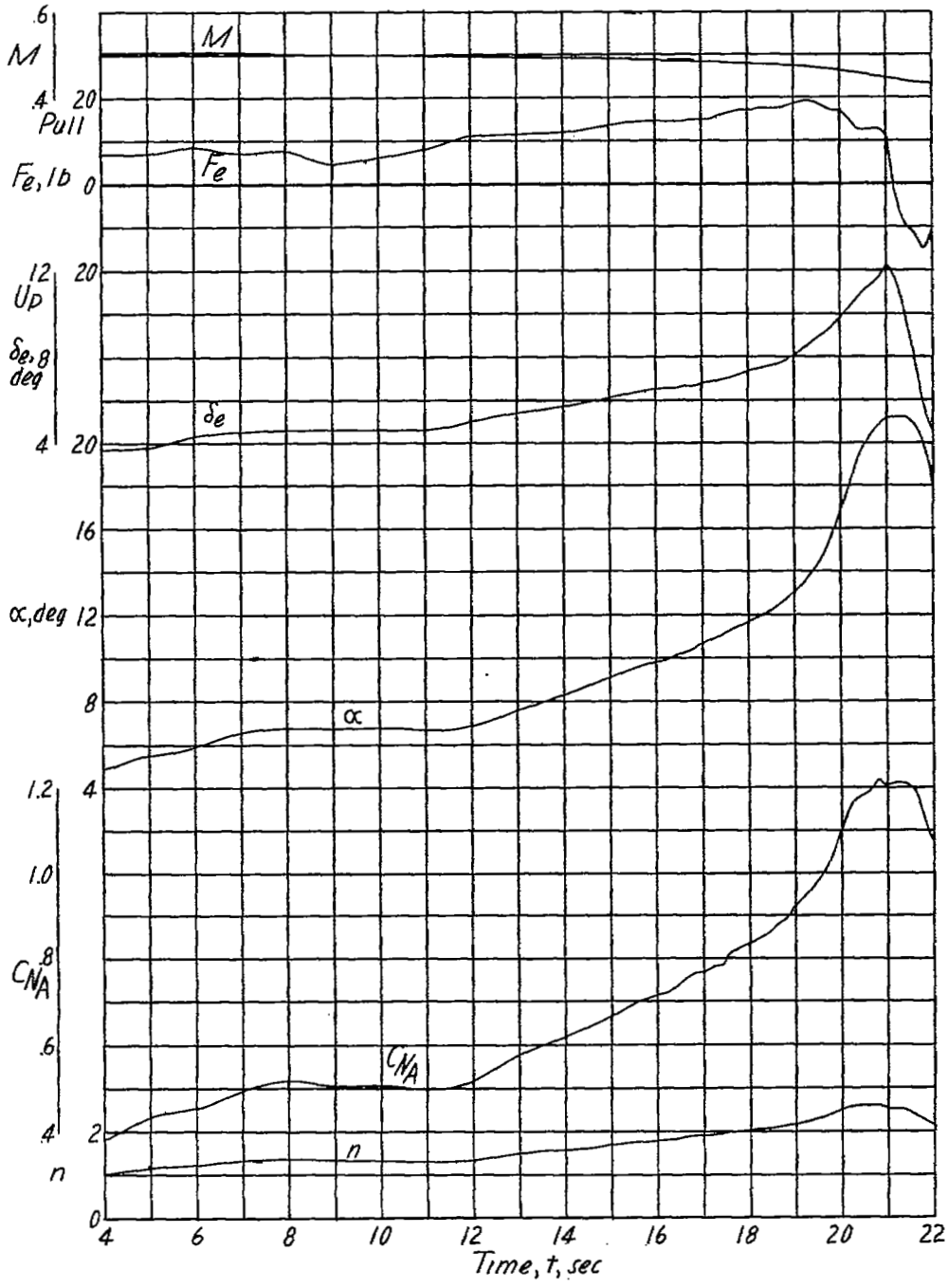

(d) $h_p \approx 19{,}700$ feet; $i_t = 1.6°$; center of gravity at 25.8 percent mean aerodynamic chord.

Figure 7.- Continued.

[redacted]

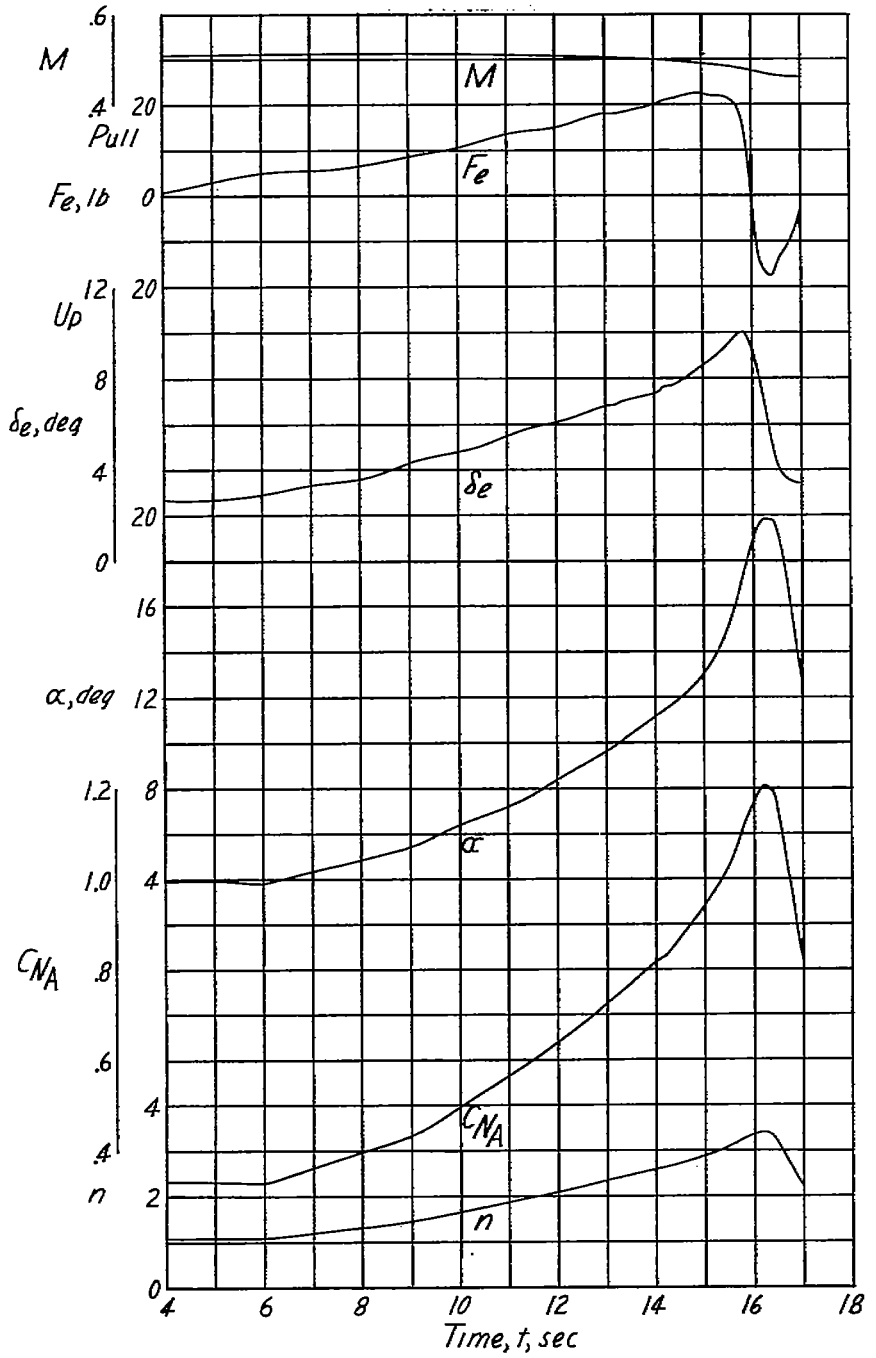

(e) $h_p \approx 15{,}700$ feet; $i_t = 1.6°$; center of gravity at 26.1 percent mean aerodynamic chord.

Figure 7.- Continued.

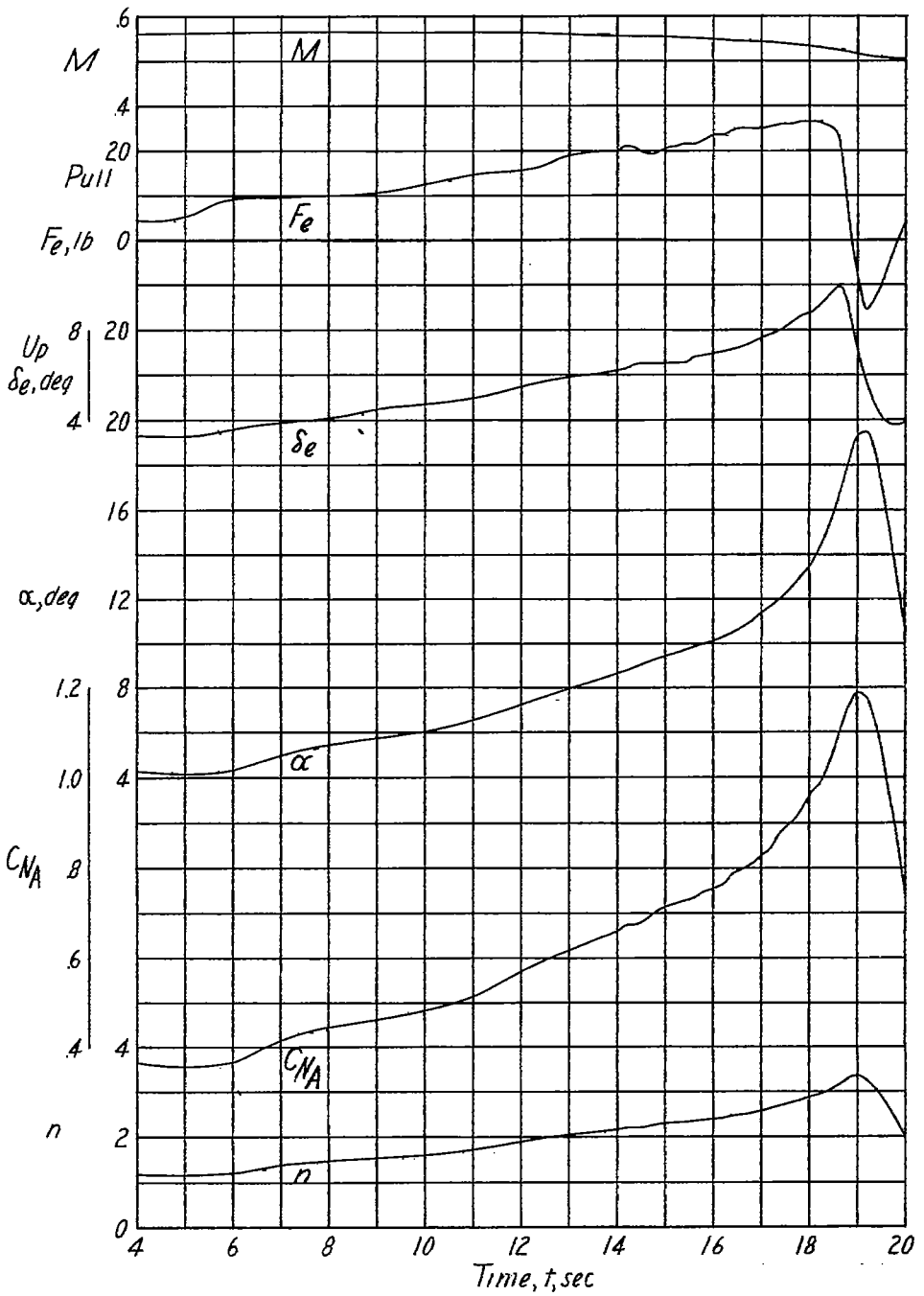

(f) $h_p \approx 20{,}000$ feet; $i_t = 1.6^\circ$; center of gravity at 25.8 percent mean aerodynamic chord.

Figure 7.- Continued.

[redacted]

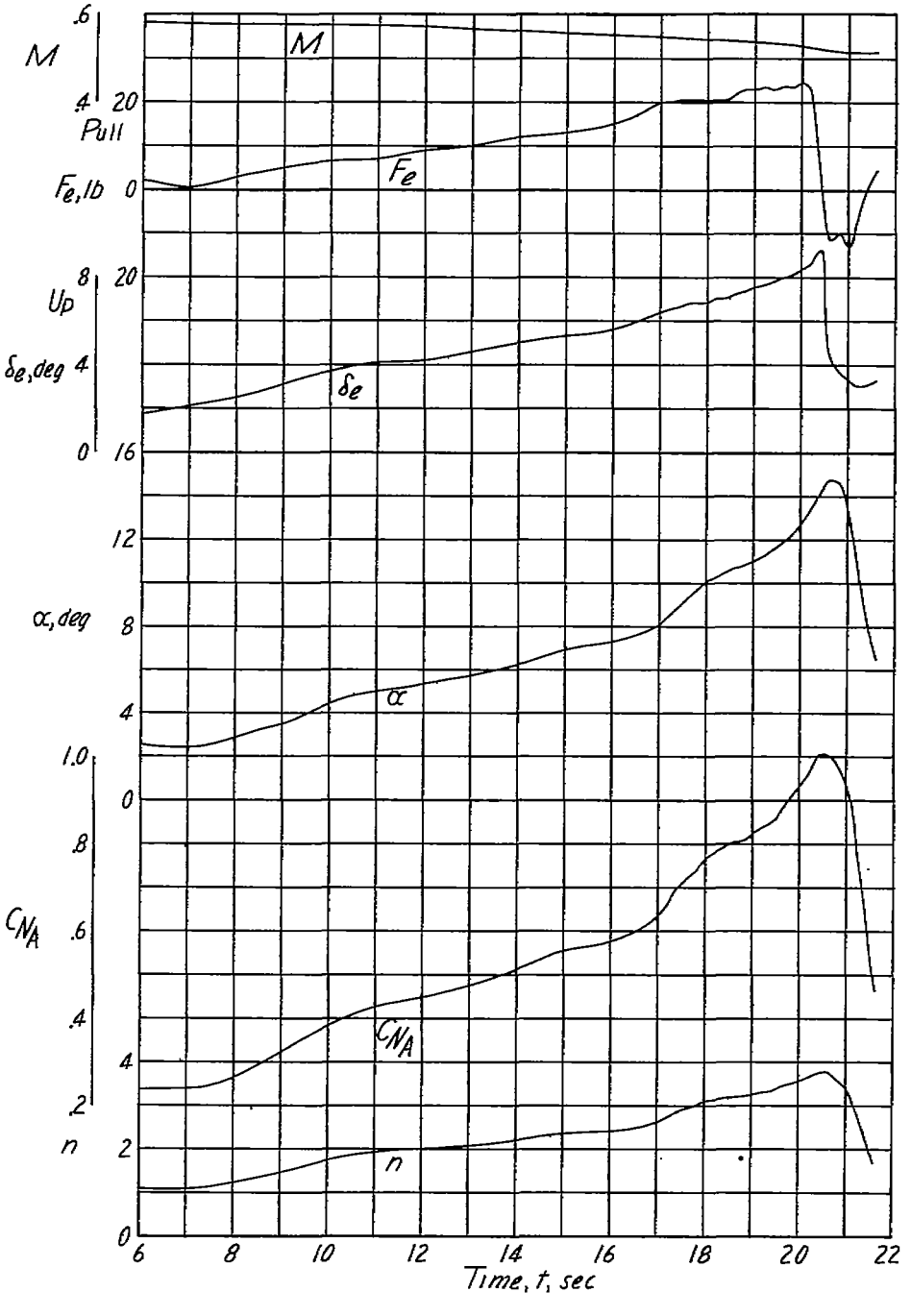

(g) $h_p \approx 14{,}000$ feet; $i_t = 1.6°$; center of gravity at 26.2 percent mean aerodynamic chord.

Figure 7.- Continued.

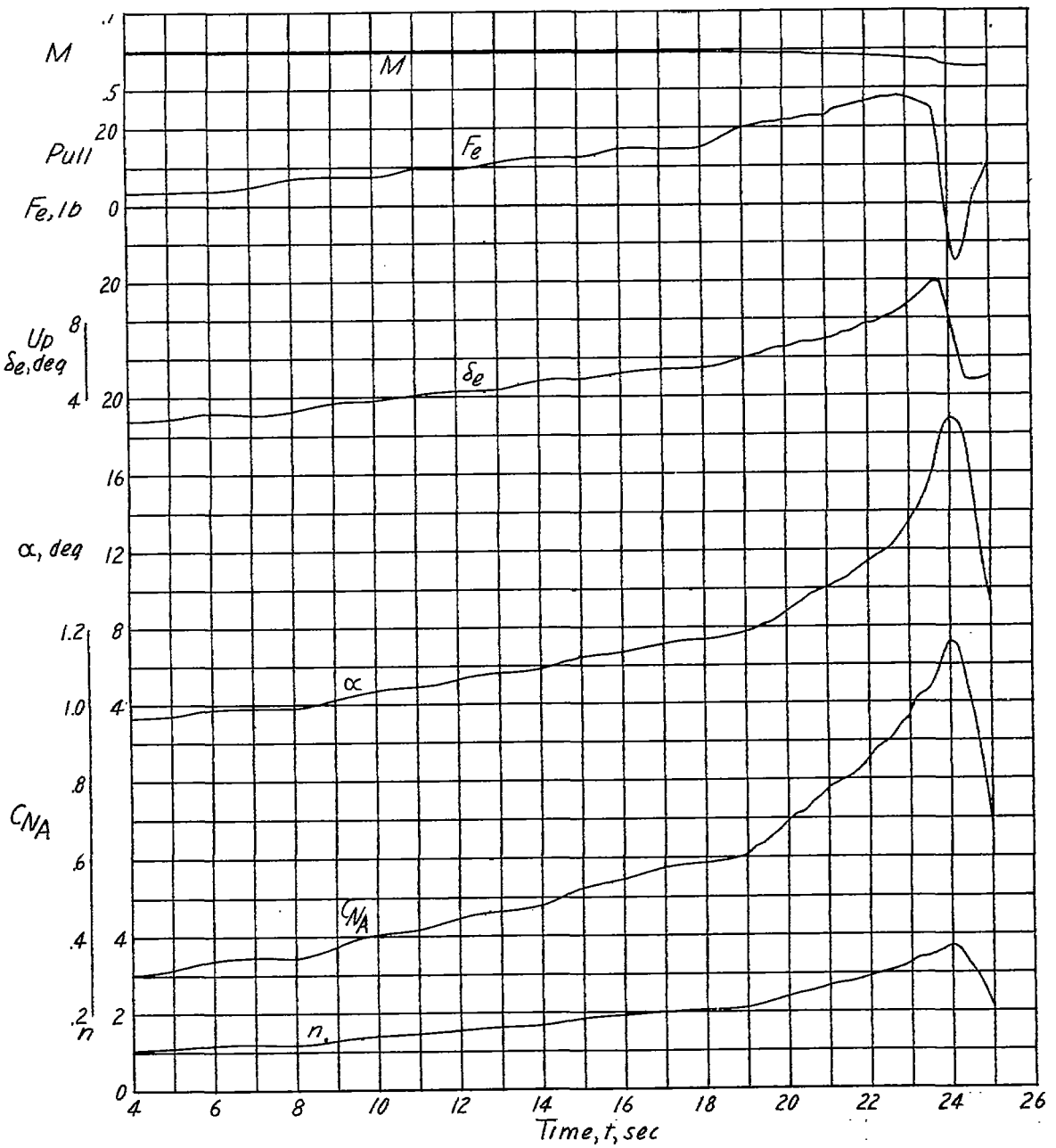

(h) $h_p \approx 21{,}000$ feet; $i_t = 1.6°$; center of gravity at 25.8 percent mean aerodynamic chord.

Figure 7.- Continued.

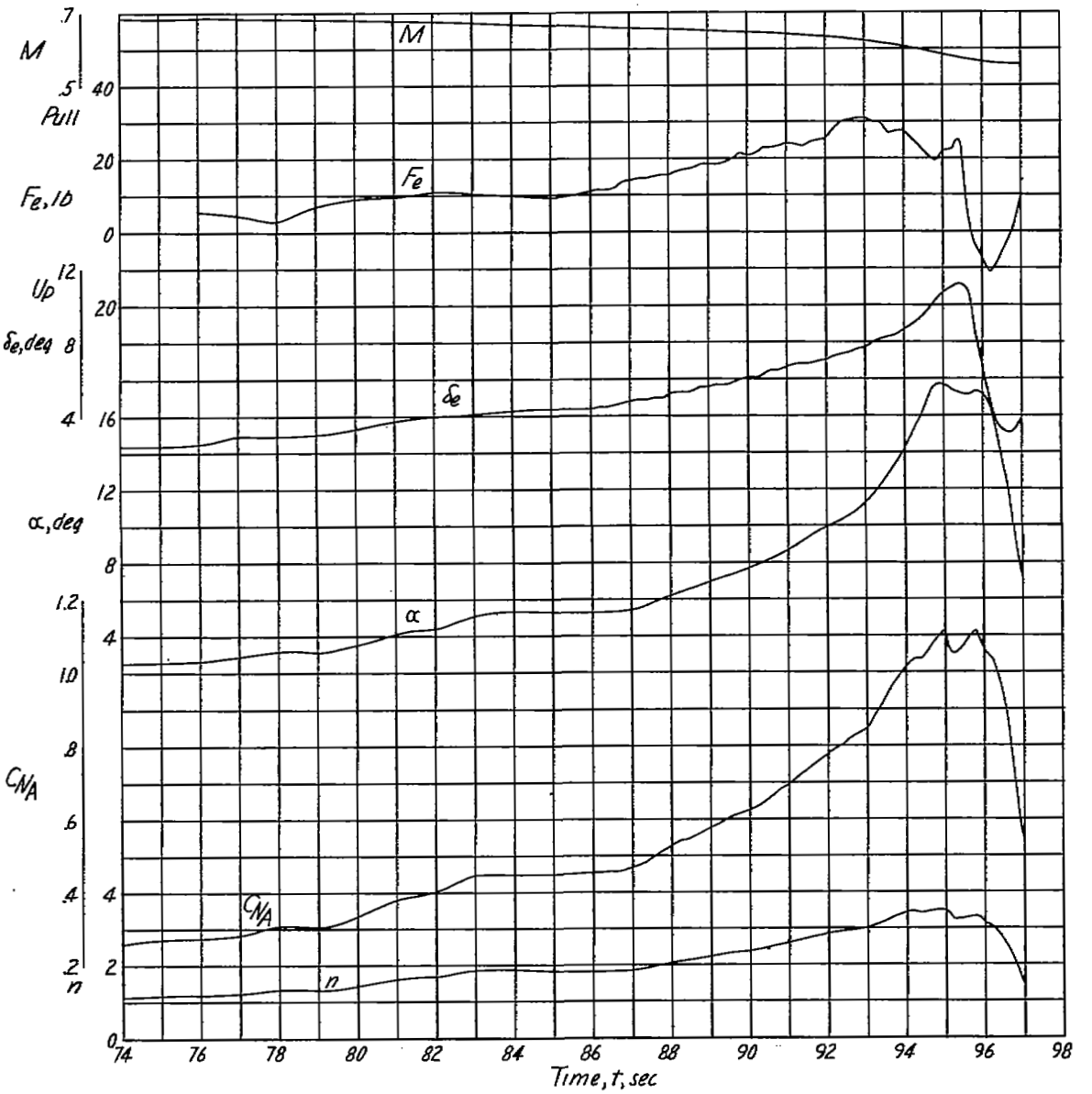

(i) $h_p \approx 23{,}000$ feet; $i_t = 1.6°$; center of gravity at 25.8 percent mean aerodynamic chord.

Figure 7.- Continued.

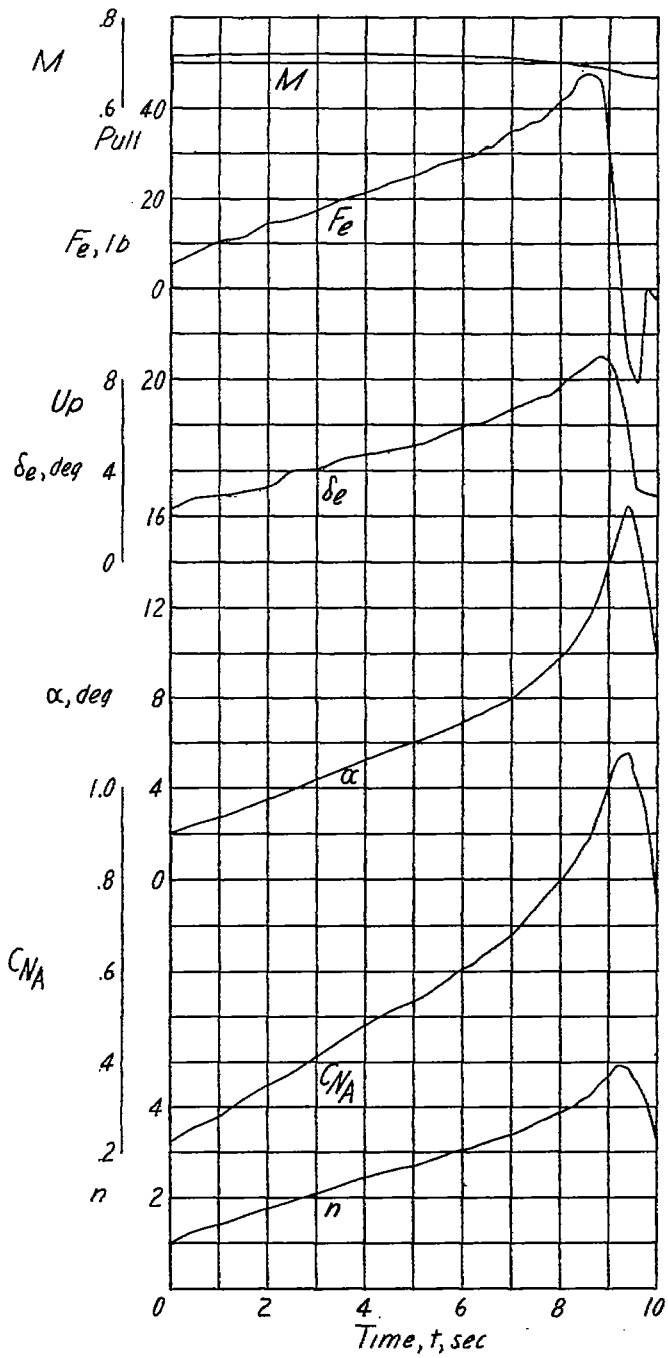

(j) $h_p \approx 21{,}500$ feet; $i_t = 1.6^\circ$; center of gravity at 25.4 percent mean aerodynamic chord.

Figure 7.- Continued.

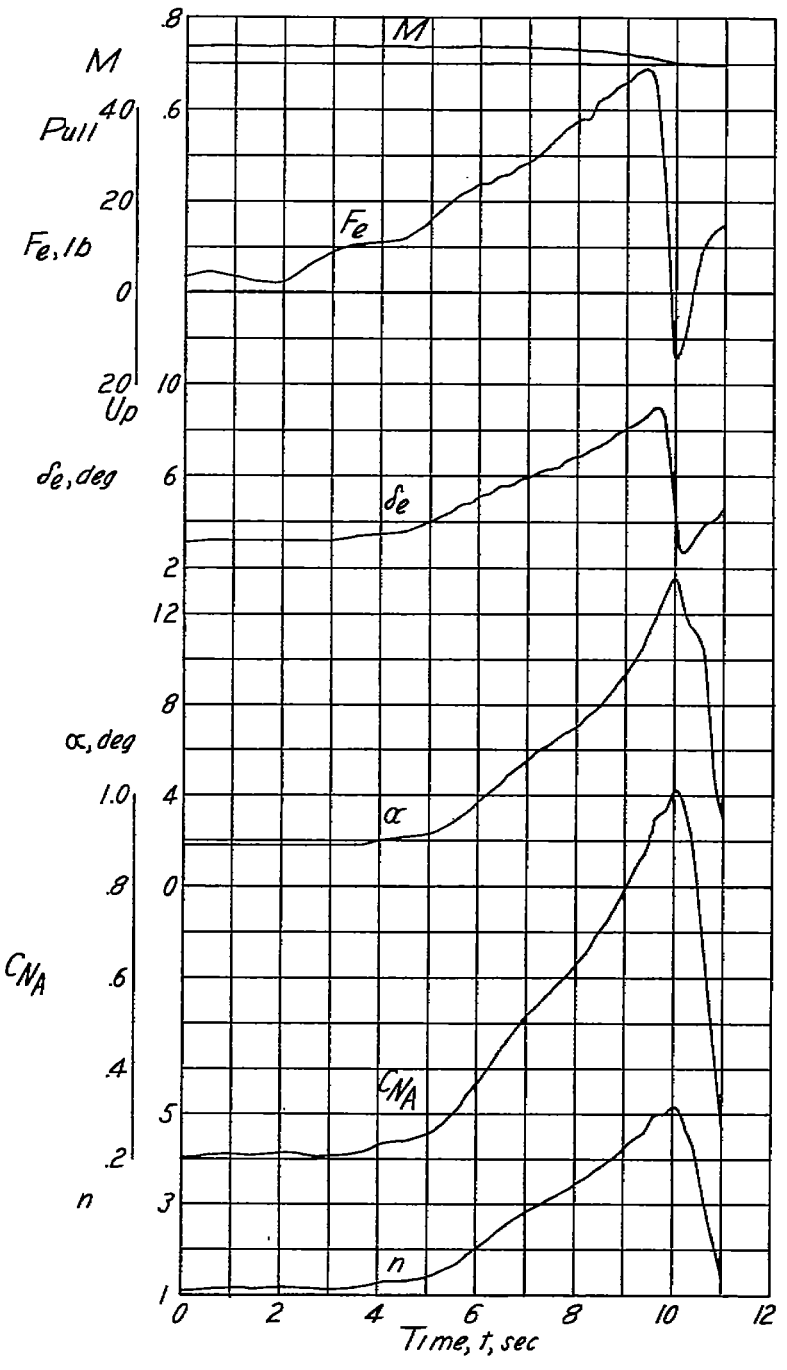

(k) $h_p \approx 19{,}600$ feet; $i_t = 2.2^\circ$; center of gravity at 25.9 percent mean aerodynamic chord.

Figure 7.- Continued.

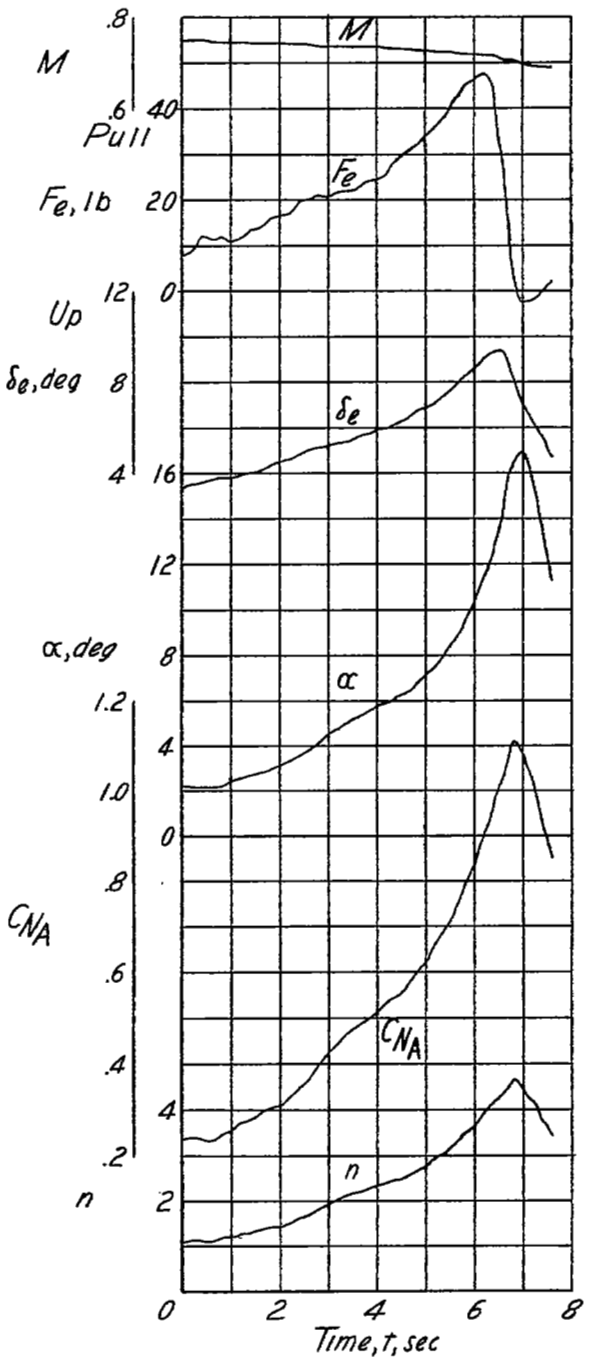

(l) $h_p \approx 23{,}800$ feet; $i_t = 2.3°$; center of gravity at 25.8 percent mean aerodynamic chord.

Figure 7.- Continued.

[redacted]

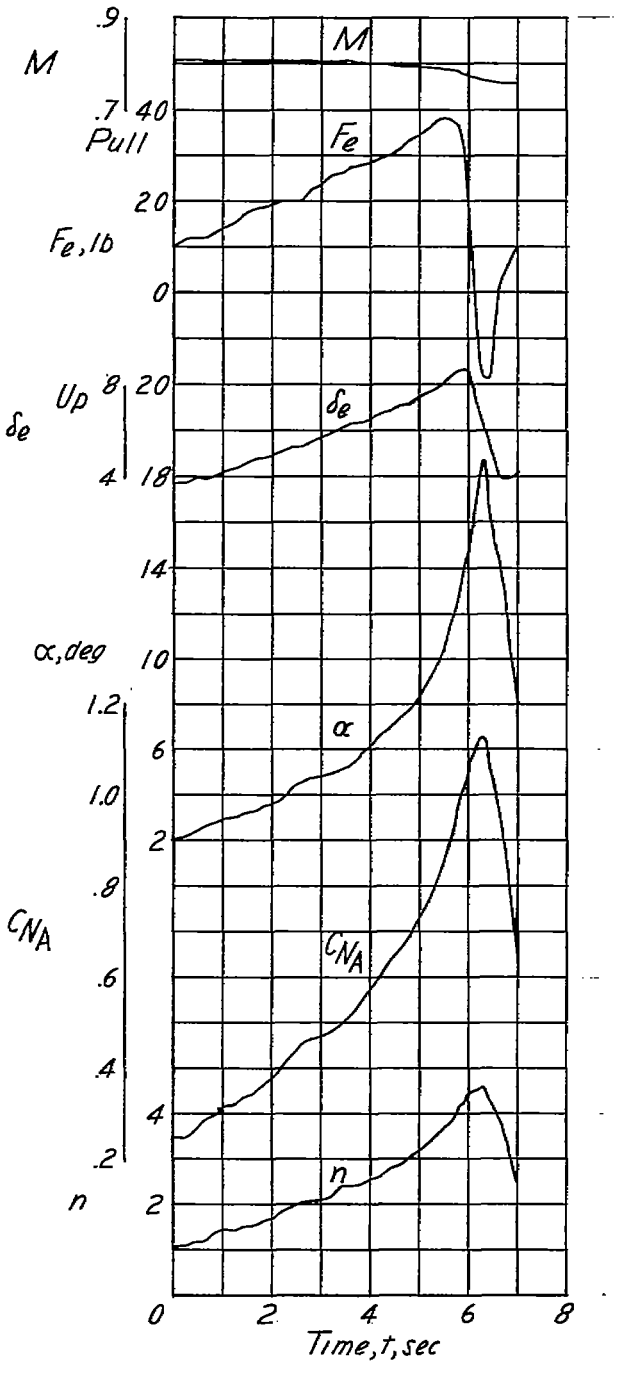

(m) $h_p \approx 28{,}500$ feet; $i_t = 2.3°$; center of gravity at 25.8 percent mean aerodynamic chord.

Figure 7.- Continued.

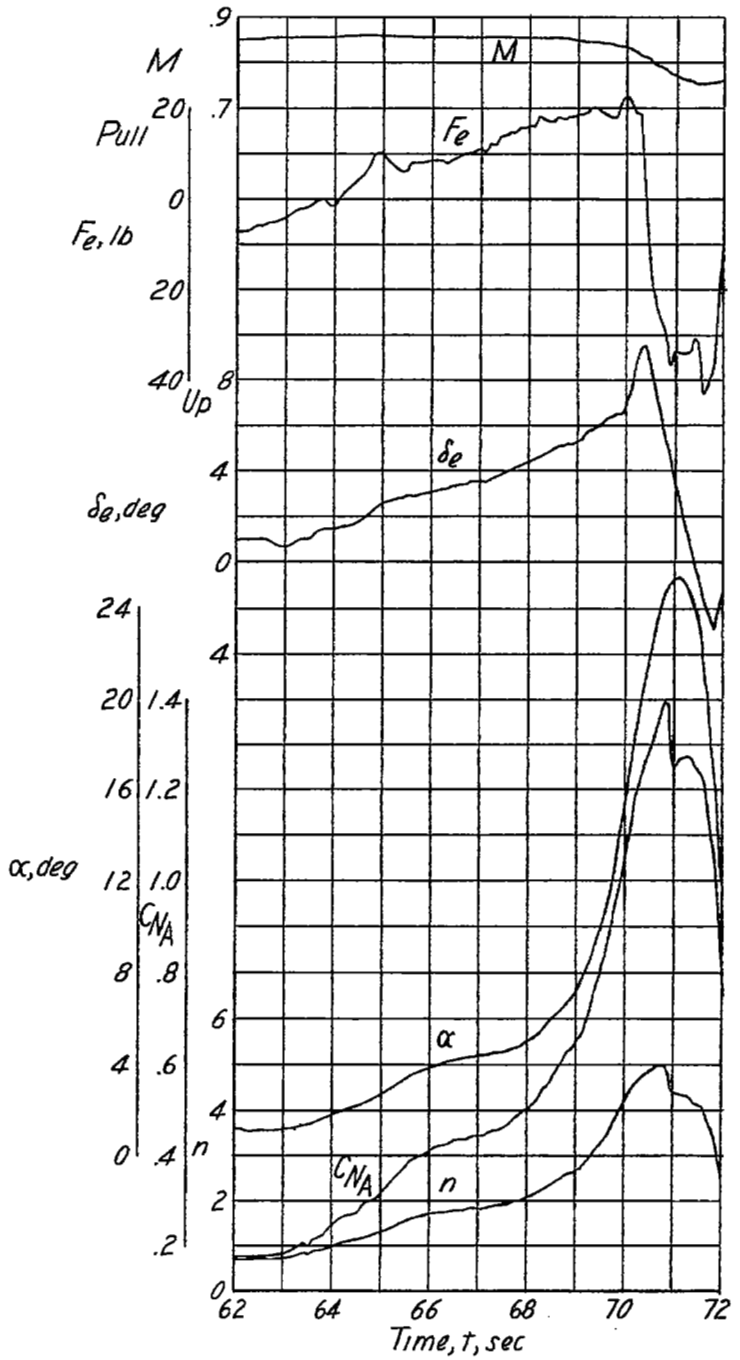

(n) $h_p \approx 33{,}000$ feet; $i_t = 1.6°$; center of gravity at 25.8 percent mean aerodynamic chord.

Figure 7.- Continued.

[redacted]

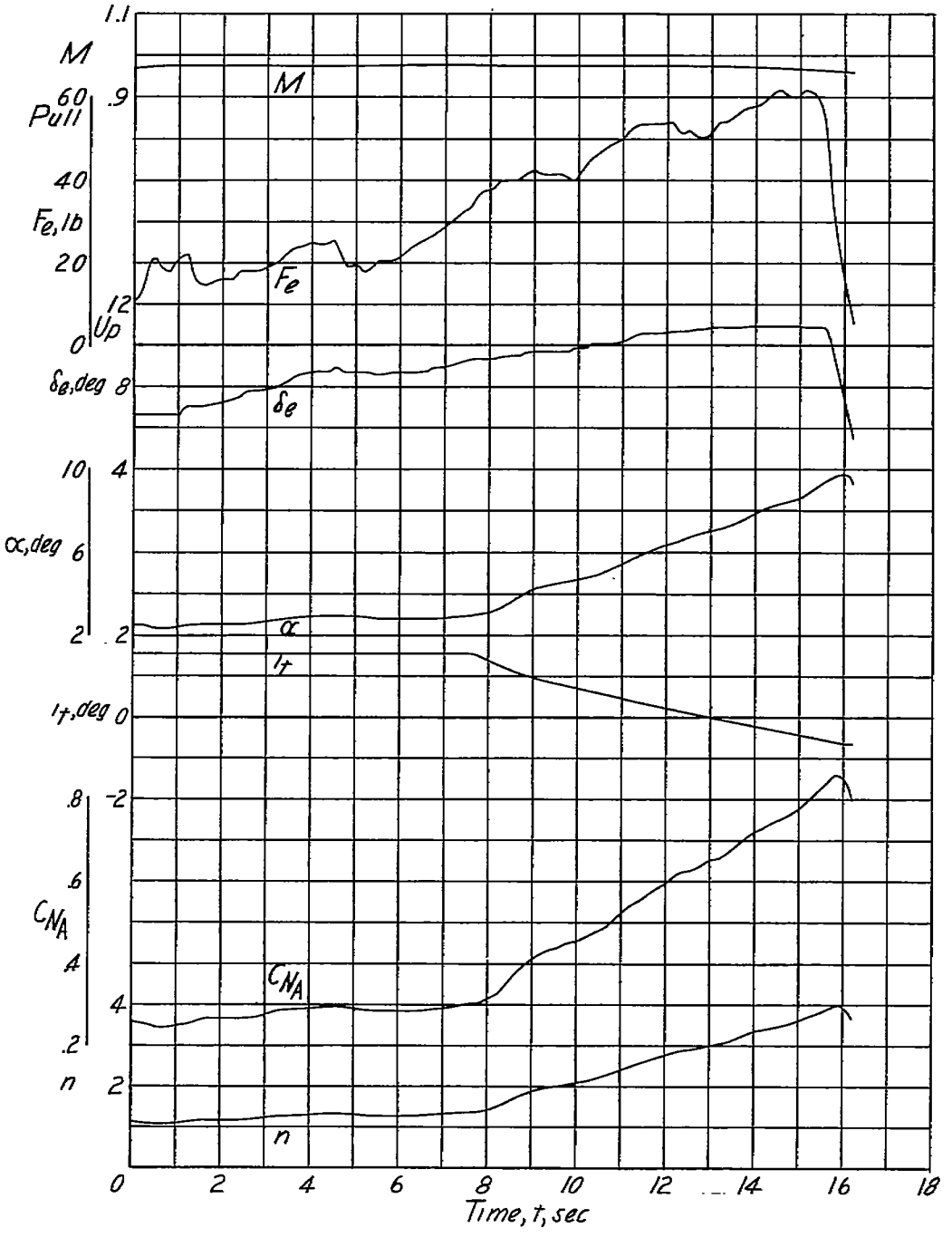

(o) $h_p \approx 35{,}100$ feet; center of gravity at 25.5 percent mean aerodynamic chord.

Figure 7.- Concluded.

[redacted]

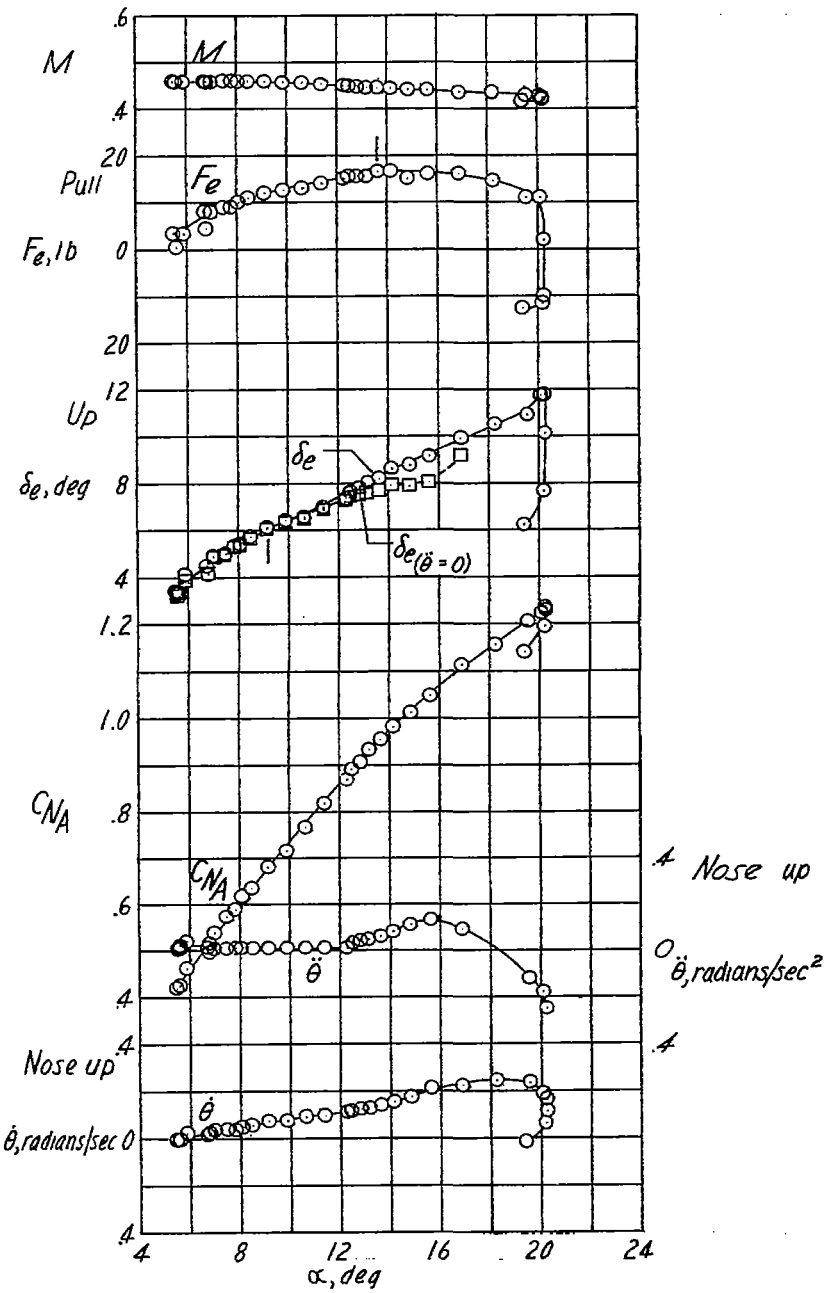

(a) $h_p \approx 18{,}300$ feet; $i_t = 1.6°$; center of gravity at 26.0 percent mean aerodynamic chord.

Figure 8.- Static longitudinal stability characteristics of the Douglas D-558-II research airplane, with slats fully extended and inboard fences on the wings, in turning flight.

[redacted]

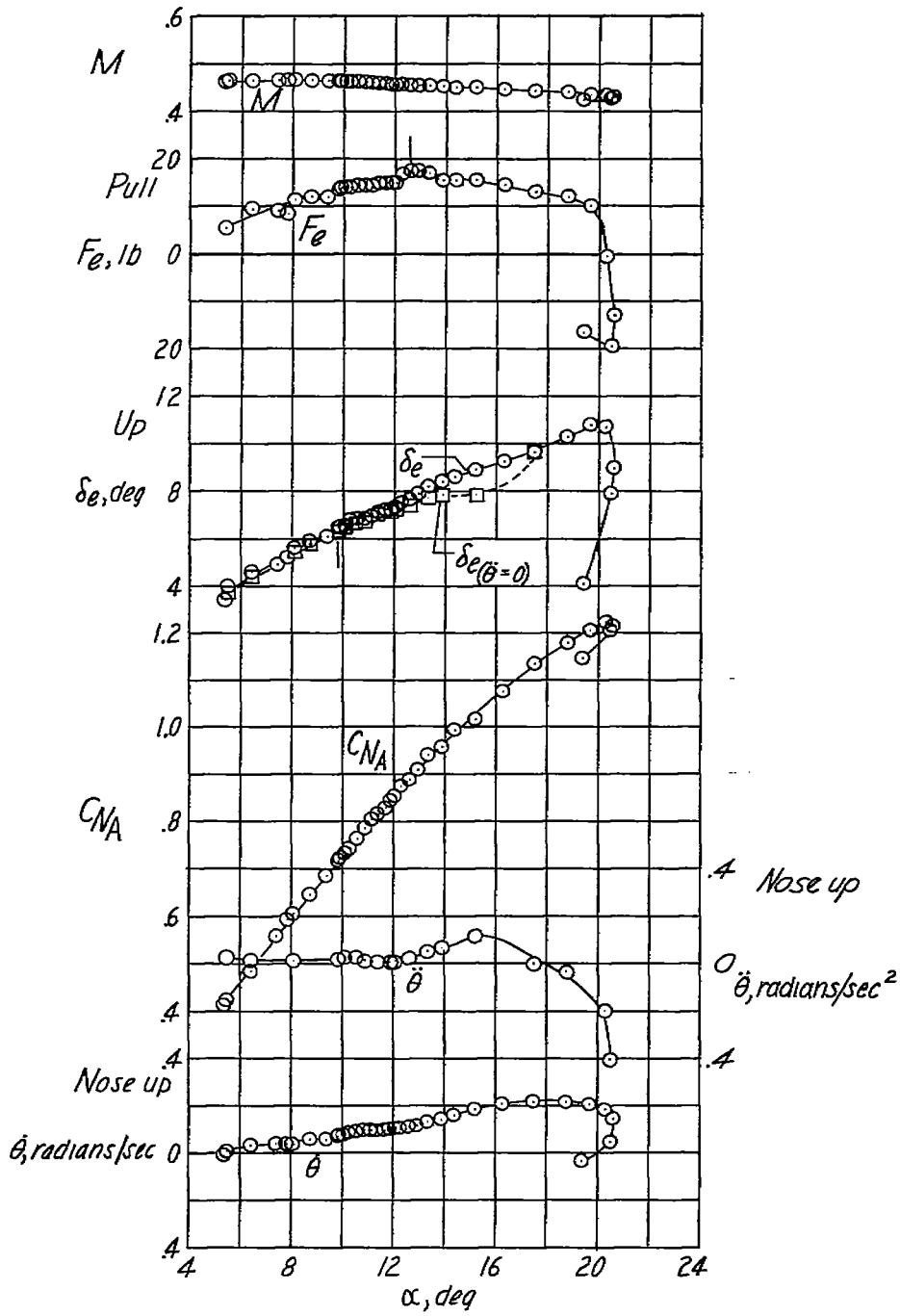

(b) $h_p \approx 19{,}200$ feet; $i_t = 1.6°$; center of gravity at 25.9 percent mean aerodynamic chord.

Figure 8.- Continued.

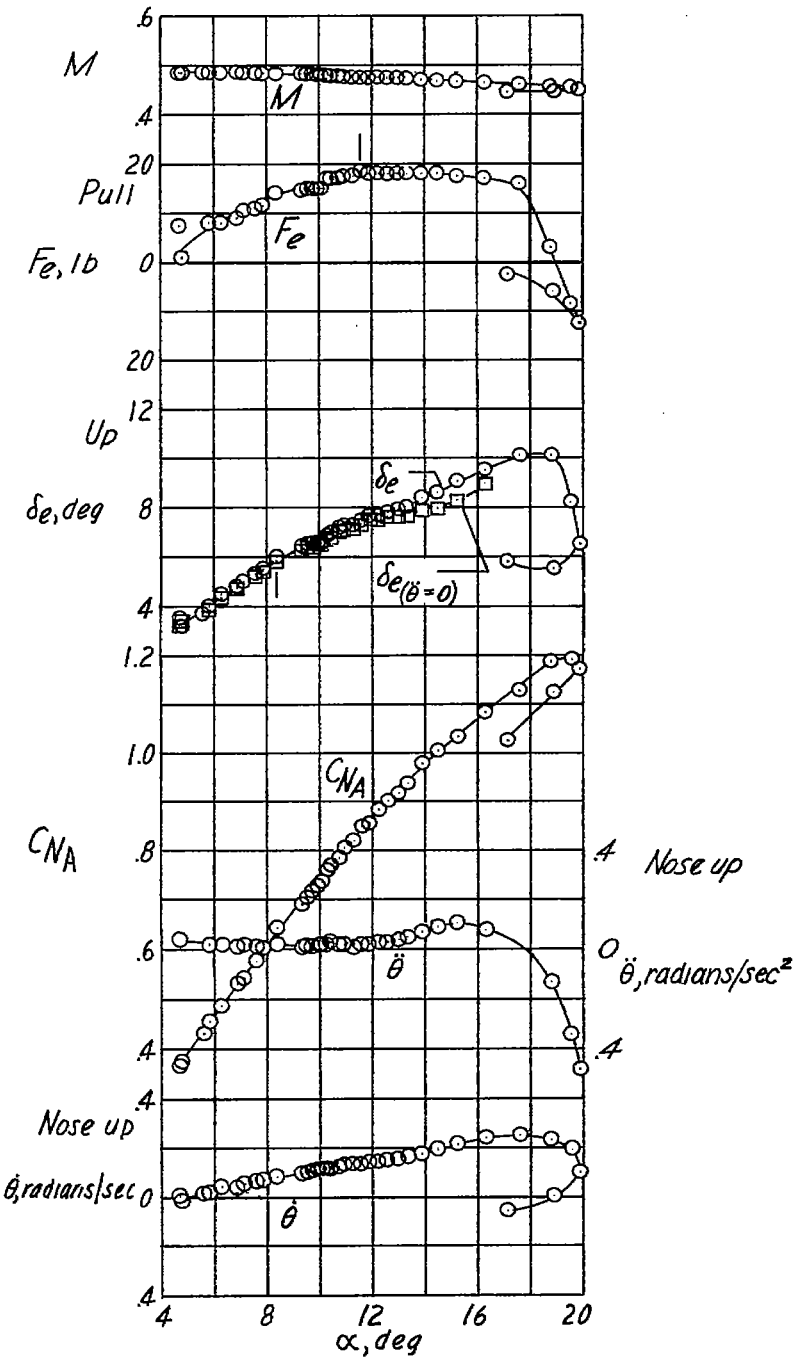

(c) $h_p \approx 17{,}000$ feet; $i_t = 1.6^\circ$; center of gravity at 26.1 percent mean aerodynamic chord.

Figure 8.- Continued.

[redacted]

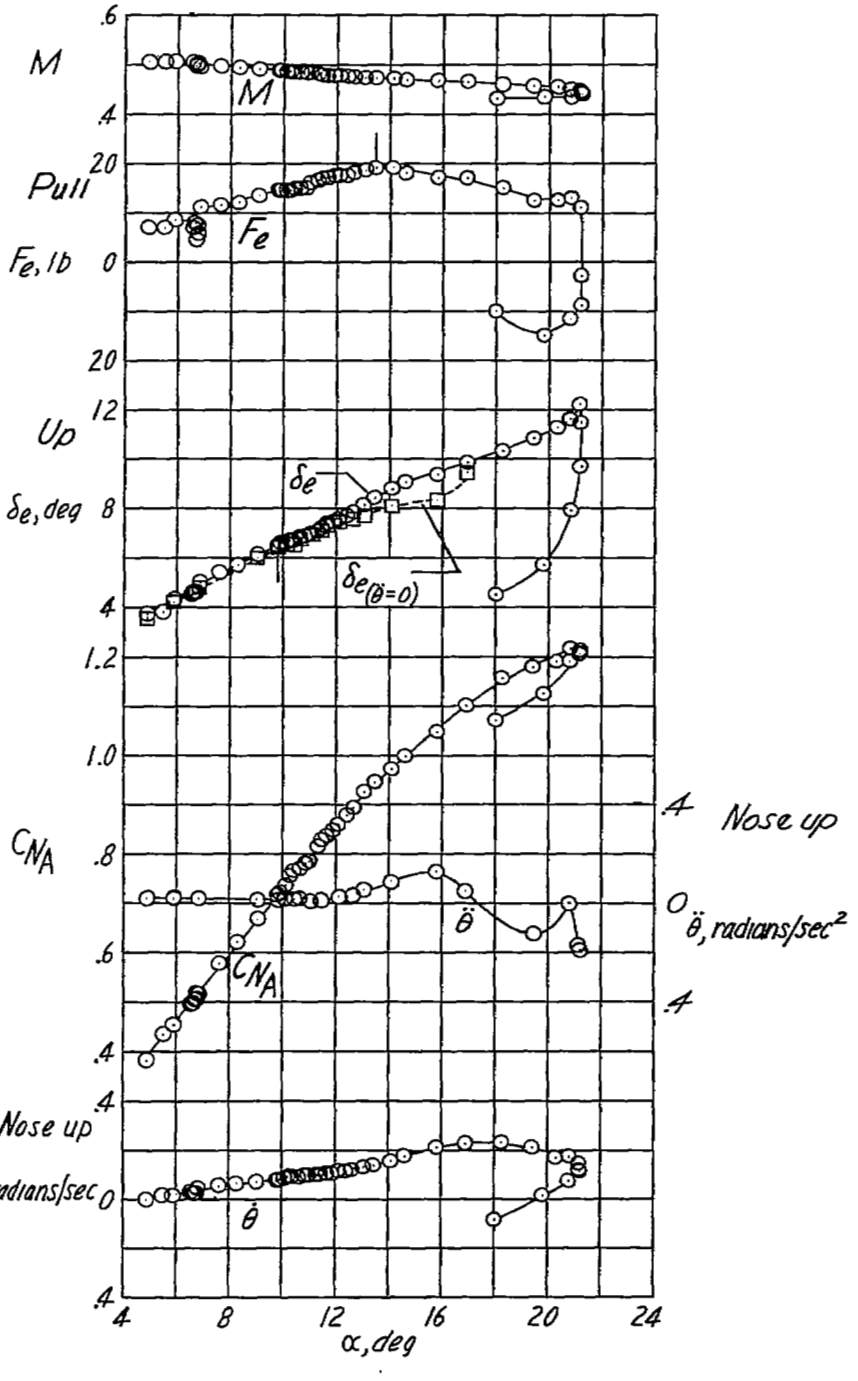

(d) $h_p \approx 19{,}700$ feet; $i_t = 1.6^\circ$; center of gravity at 25.8 percent mean aerodynamic chord.

Figure 8.- Continued.

[redacted]

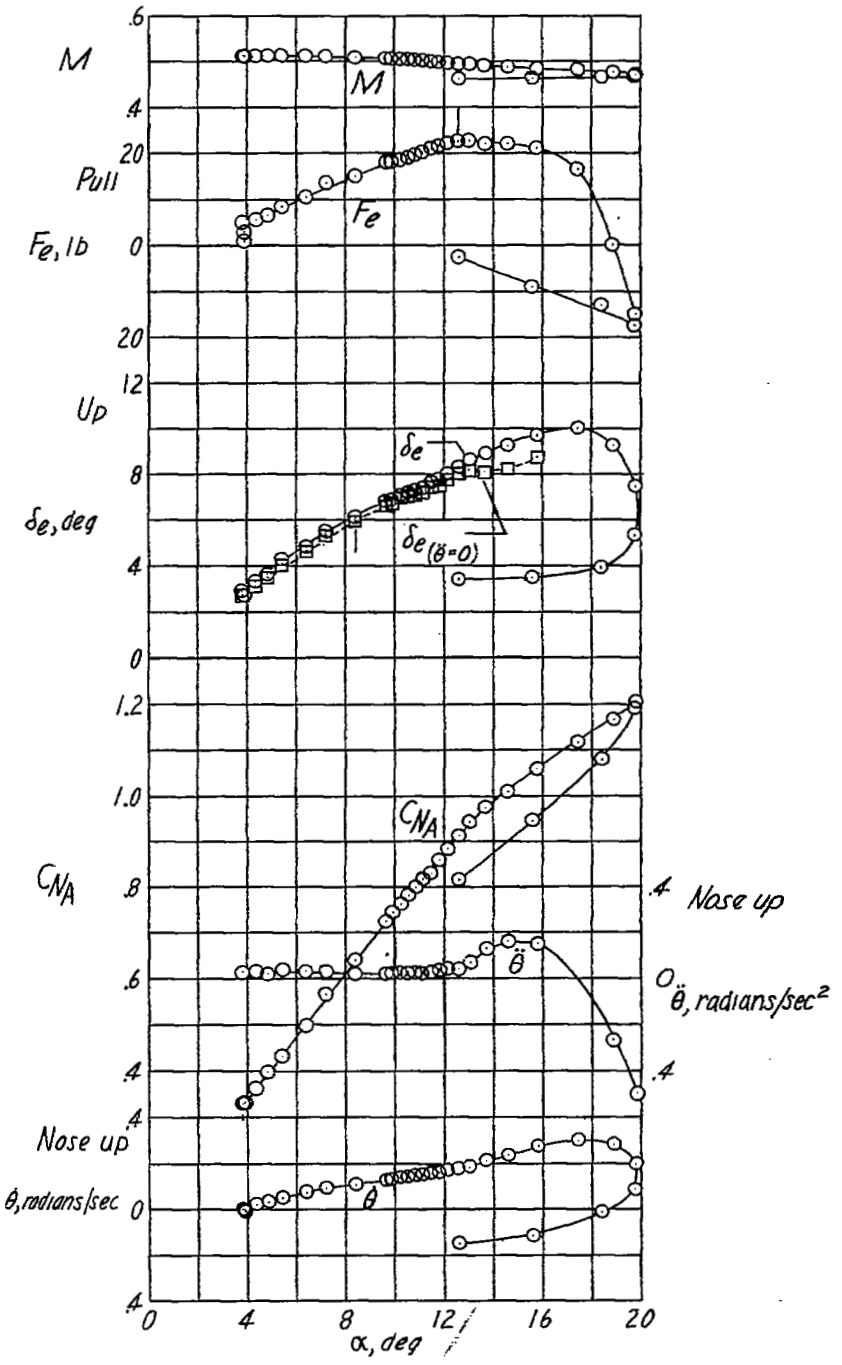

(e) $h_p \approx 15{,}700$ feet; $i_t = 1.6°$; center of gravity at 26.1 percent mean aerodynamic chord.

Figure 8.- Continued.

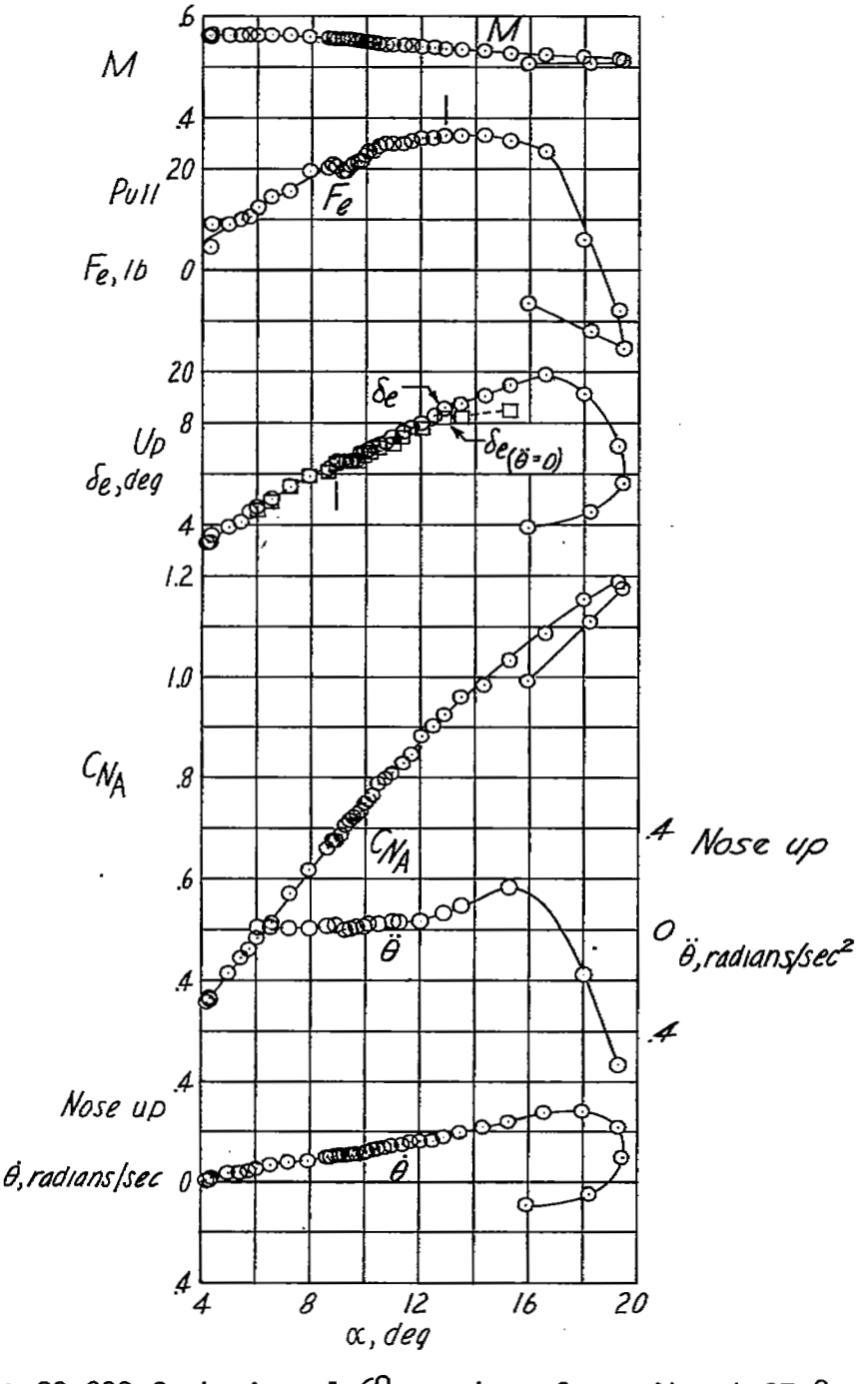

(f) $h_p \approx 20{,}000$ feet; $i_t = 1.6°$; center of gravity at 25.8 percent mean aerodynamic chord.

Figure 8.- Continued.

[redacted]

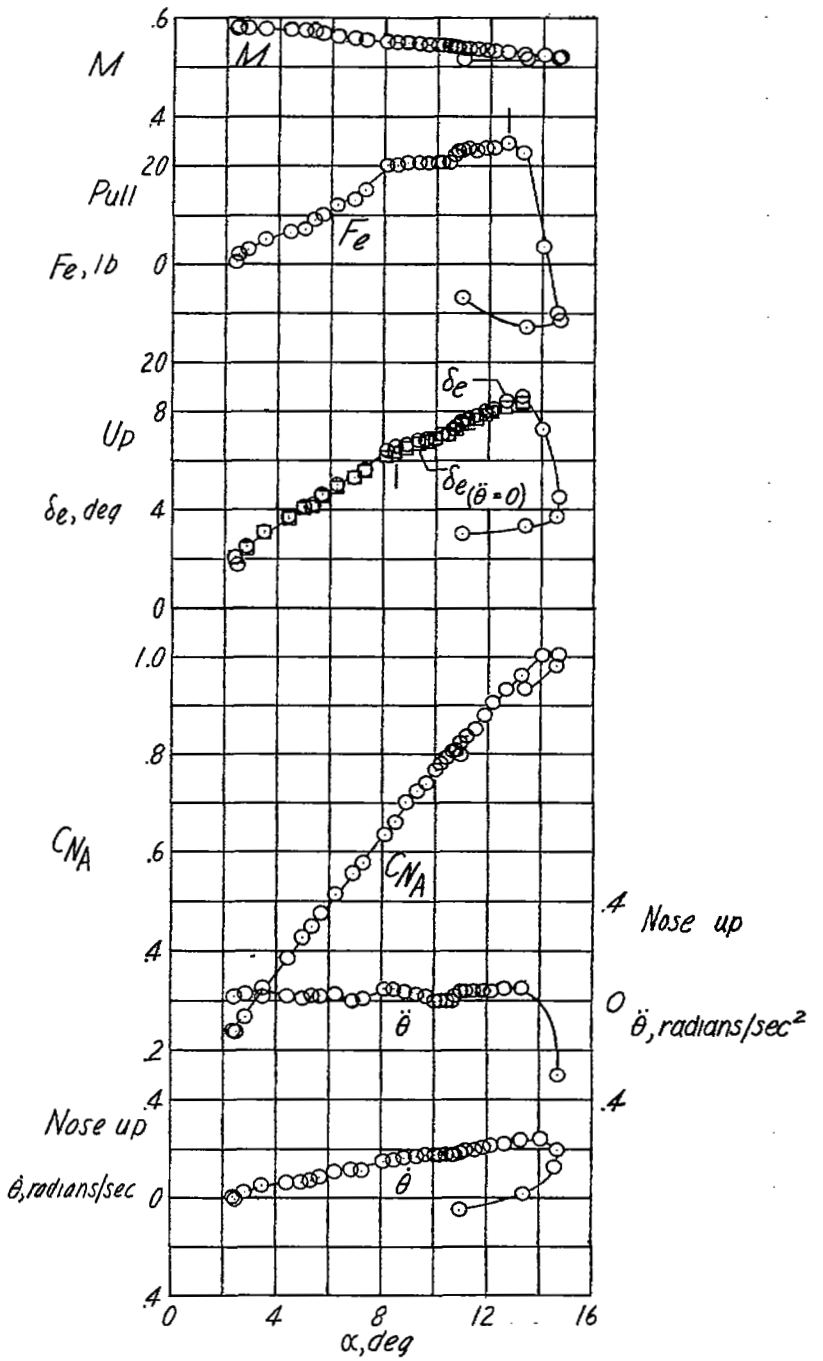

(g) $h_p \approx 14{,}000$ feet; $i_t = 1.6°$; center of gravity at 26.2 percent mean aerodynamic chord.

Figure 8.- Continued.

[redacted]

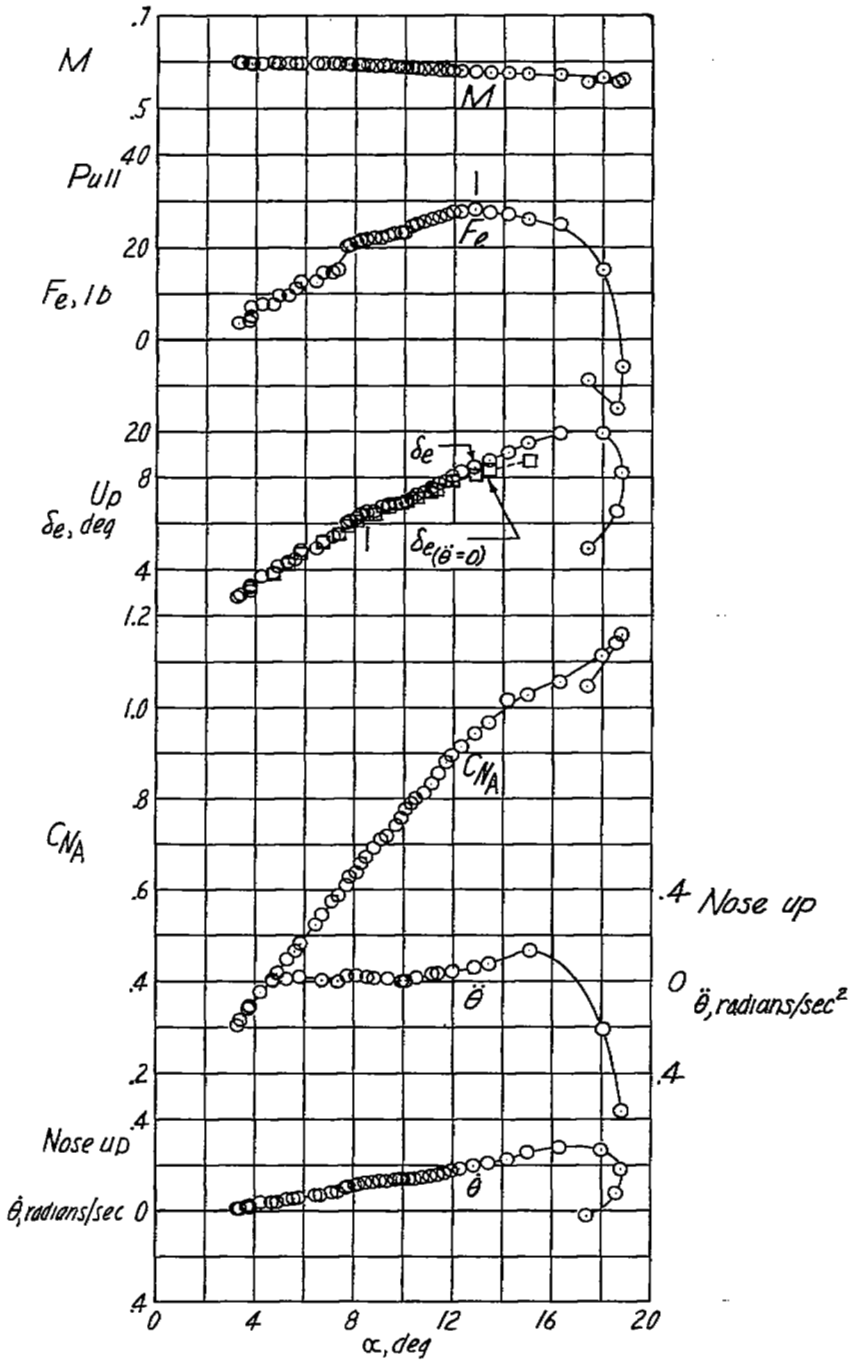

(h) $h_p \approx 21{,}000$ feet; $i_t = 1.6°$; center of gravity at 25.8 percent mean aerodynamic chord.

Figure 8.- Continued.

[redacted]

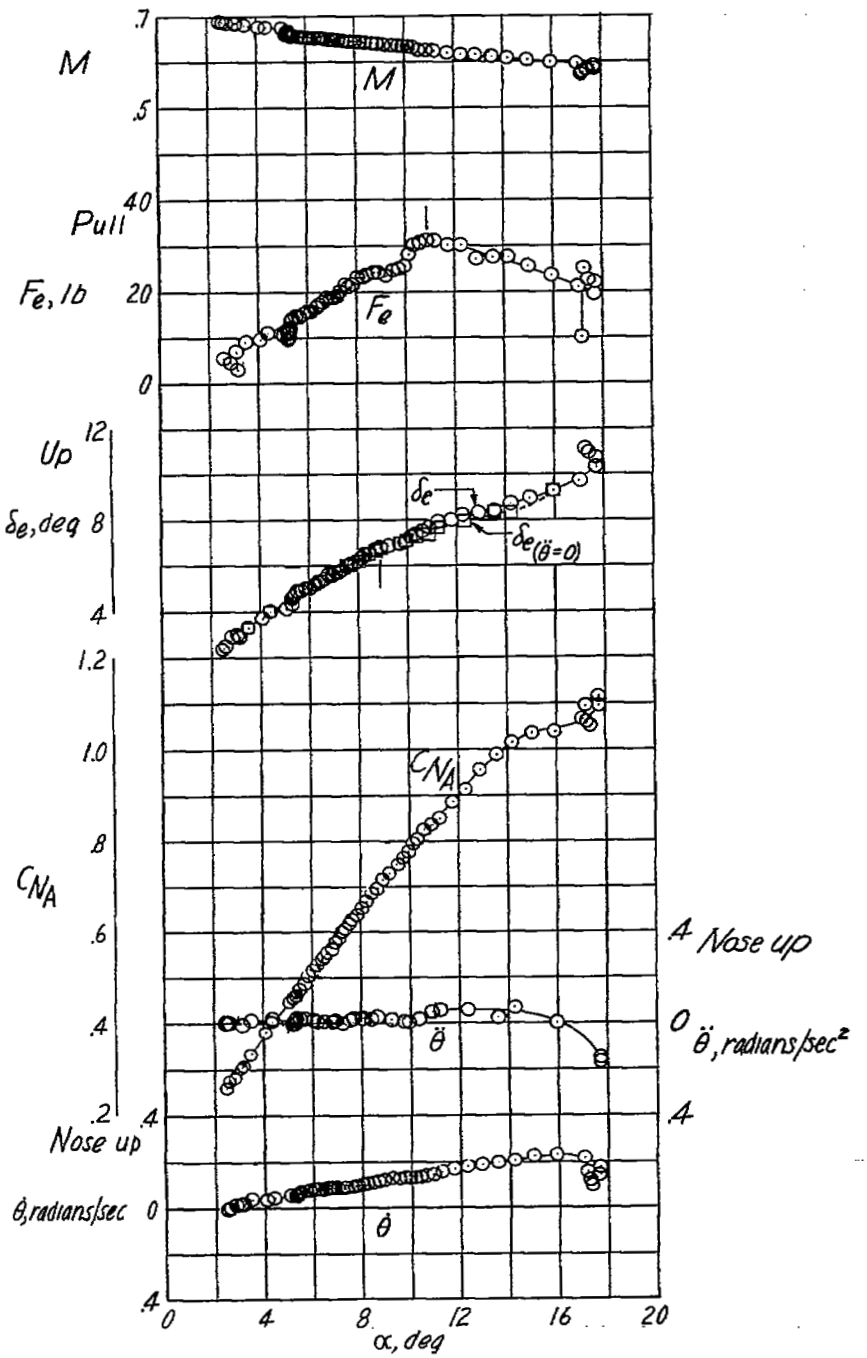

(i) $h_p \approx 23{,}000$ feet; $i_t = 1.6°$; center of gravity at 25.8 percent mean aerodynamic chord.

Figure 8.- Continued.

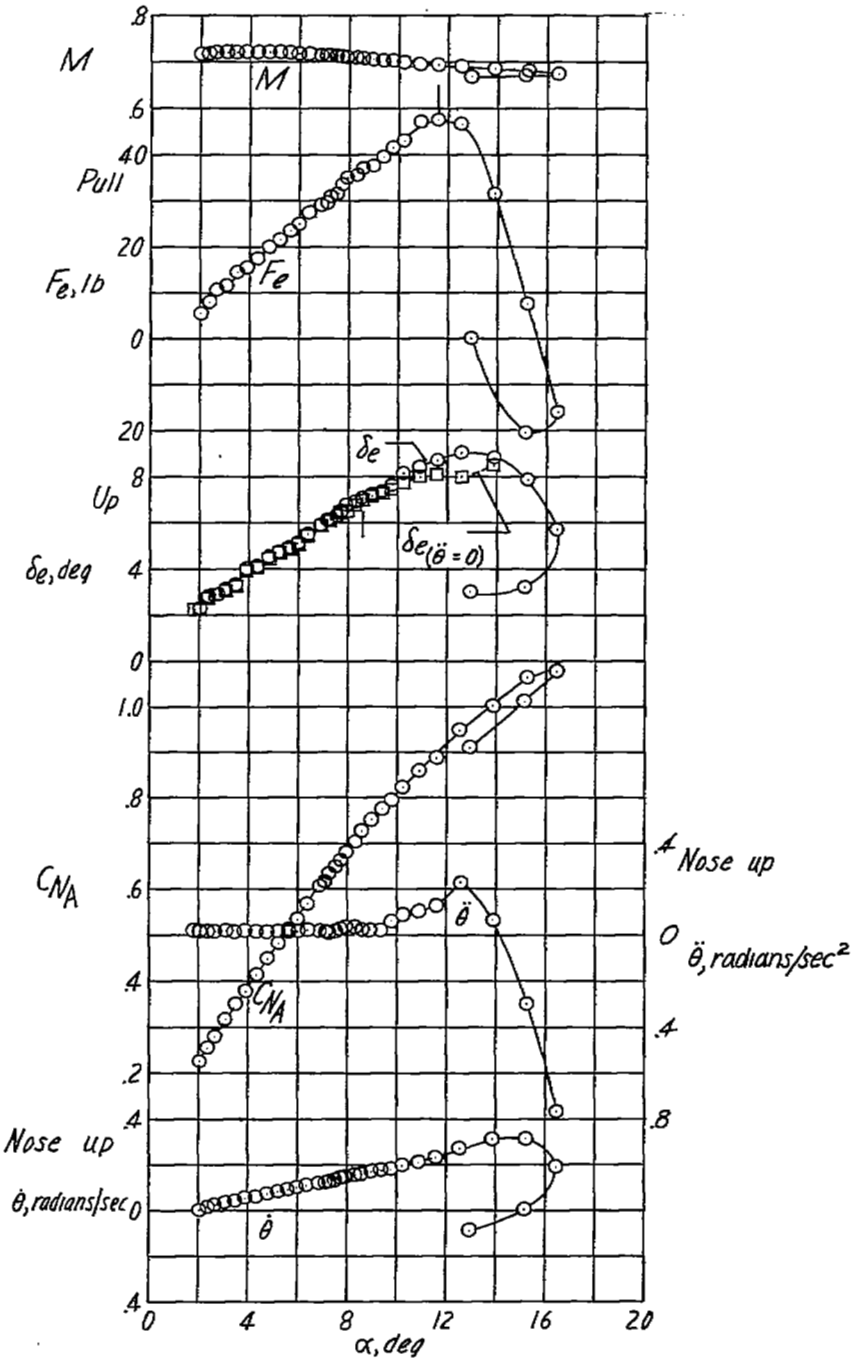

(j) $h_p \approx 21{,}500$ feet; $i_t = 1.6°$; center of gravity at 25.4 percent mean aerodynamic chord.

Figure 8.- Continued.

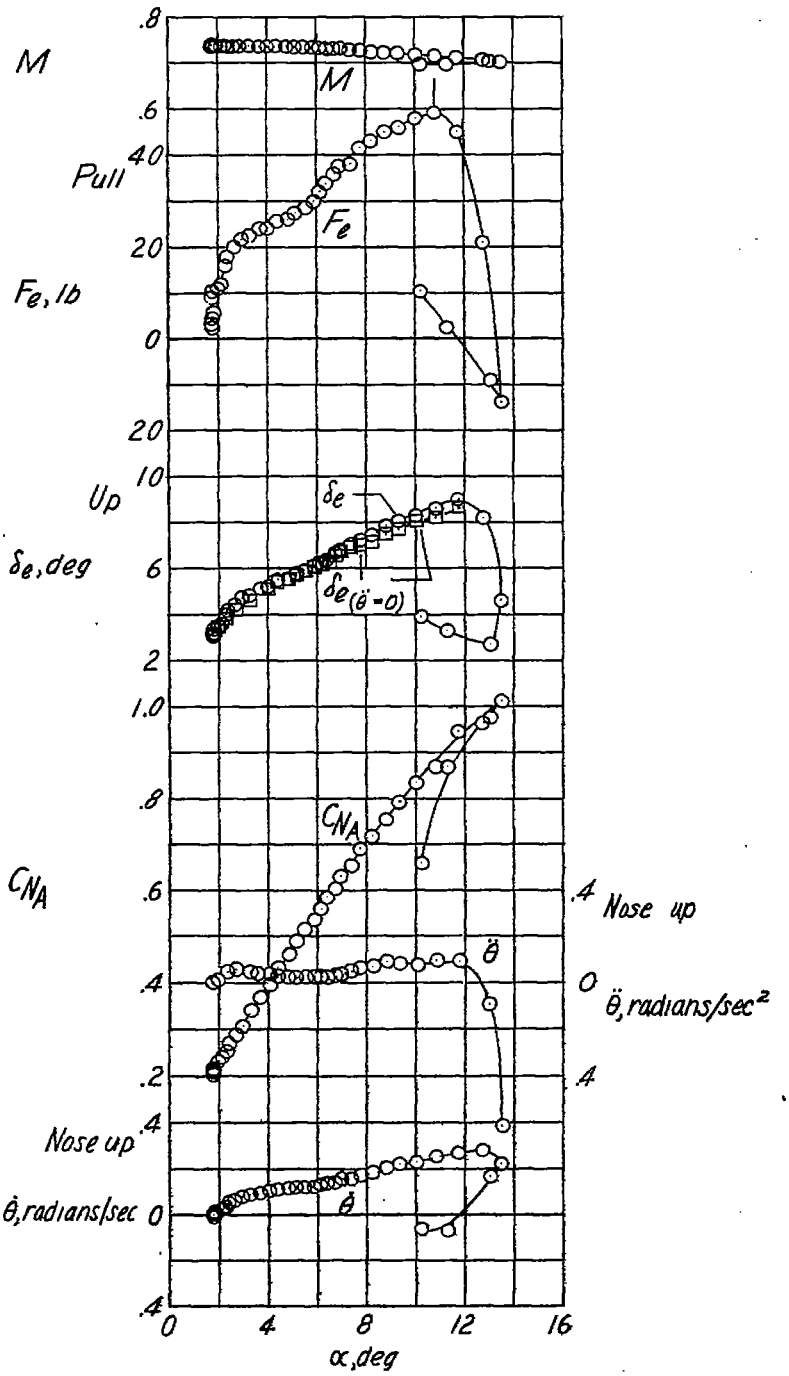

(k) $h_p \approx 19{,}600$ feet; $i_t = 2.2^\circ$; center of gravity at 25.9 percent mean aerodynamic chord.

Figure 8.- Continued.

[redacted]

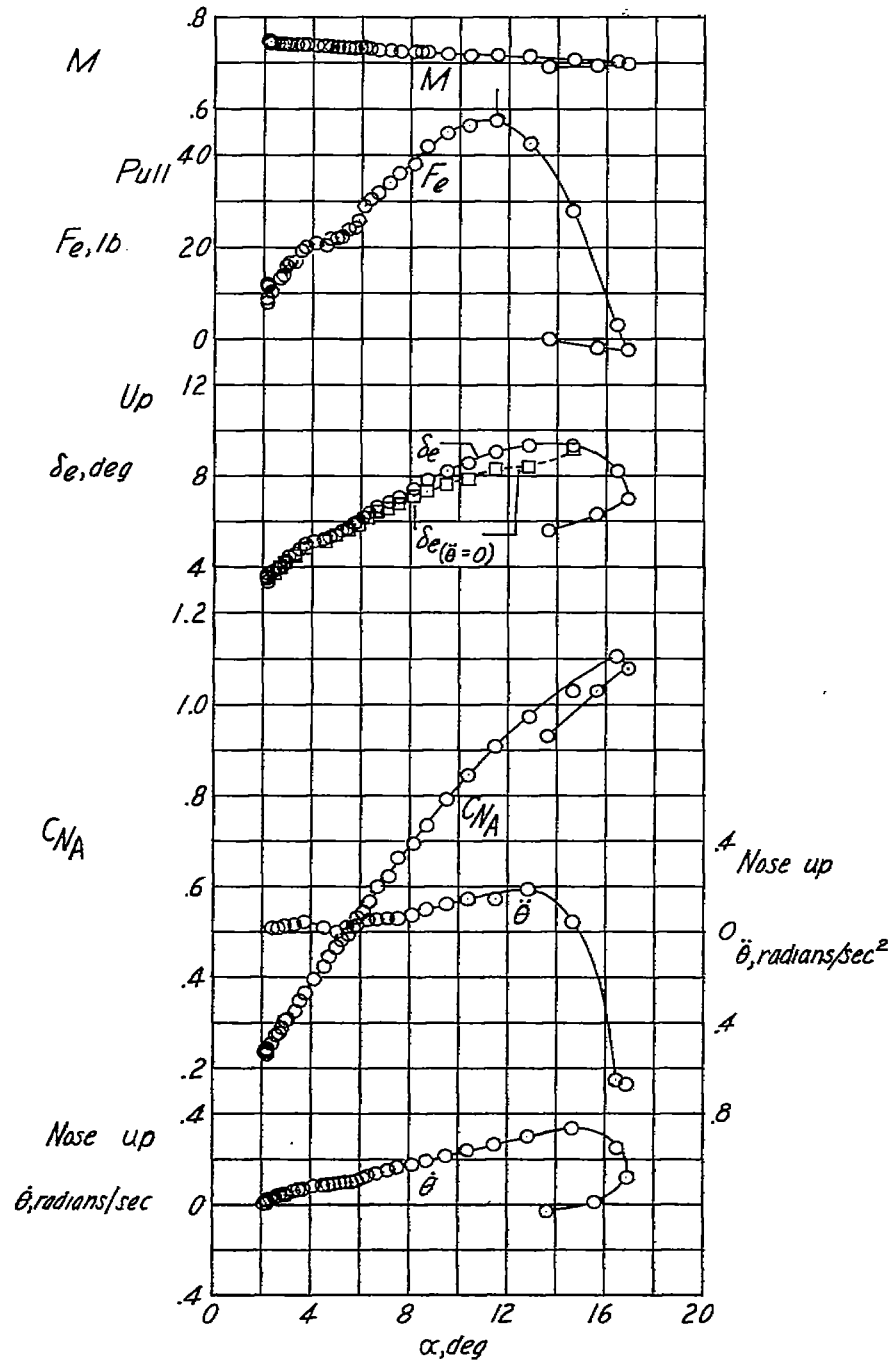

(l) $h_p \approx 23{,}800$ feet; $i_t = 2.3°$; center of gravity at 25.8 percent mean aerodynamic chord.

Figure 8.- Continued.

[redacted]

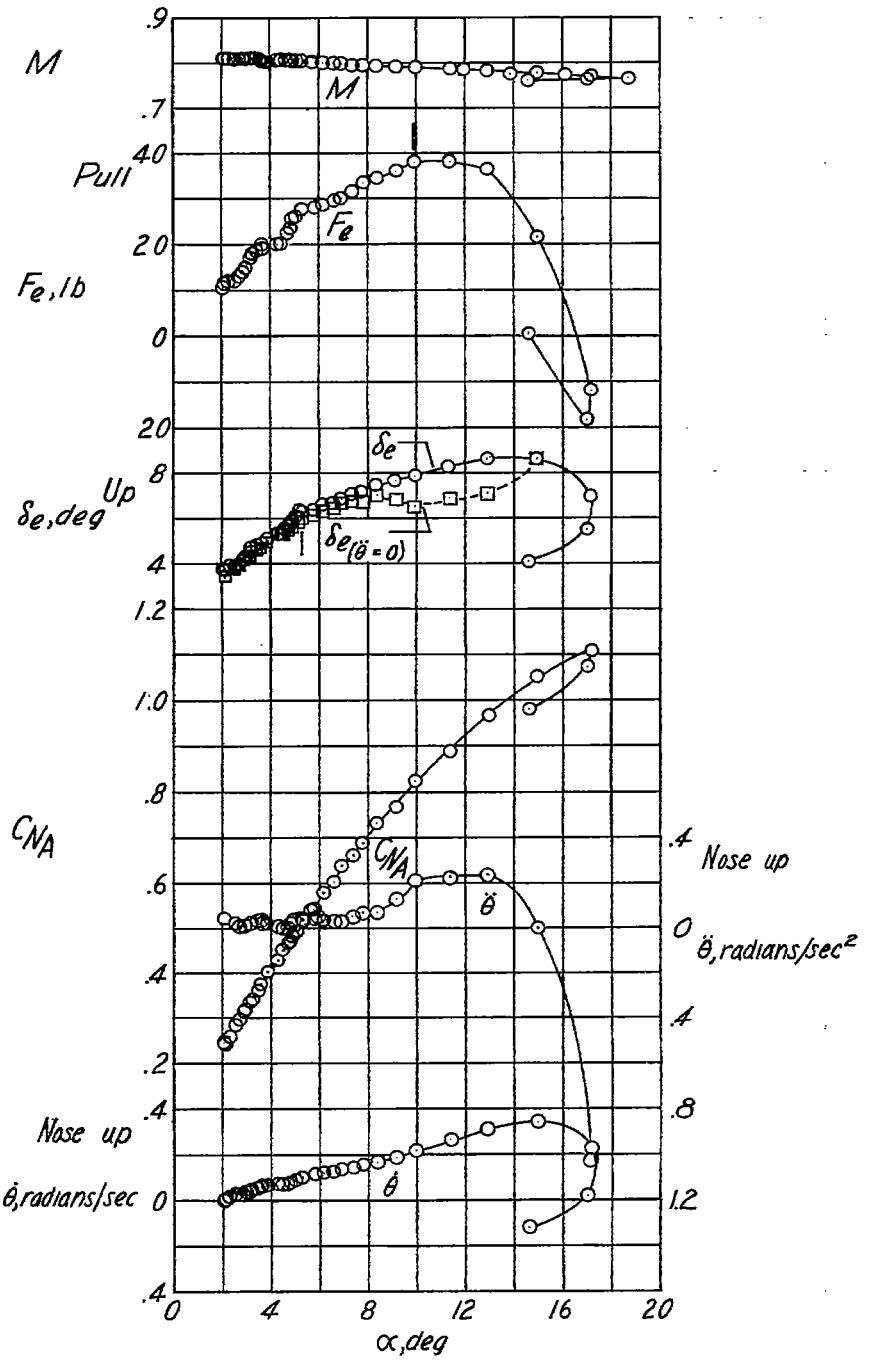

(m) $h_p \approx 28{,}500$ feet; $i_t = 2.3°$; center of gravity at 25.8 percent mean aerodynamic chord.

Figure 8.- Continued.

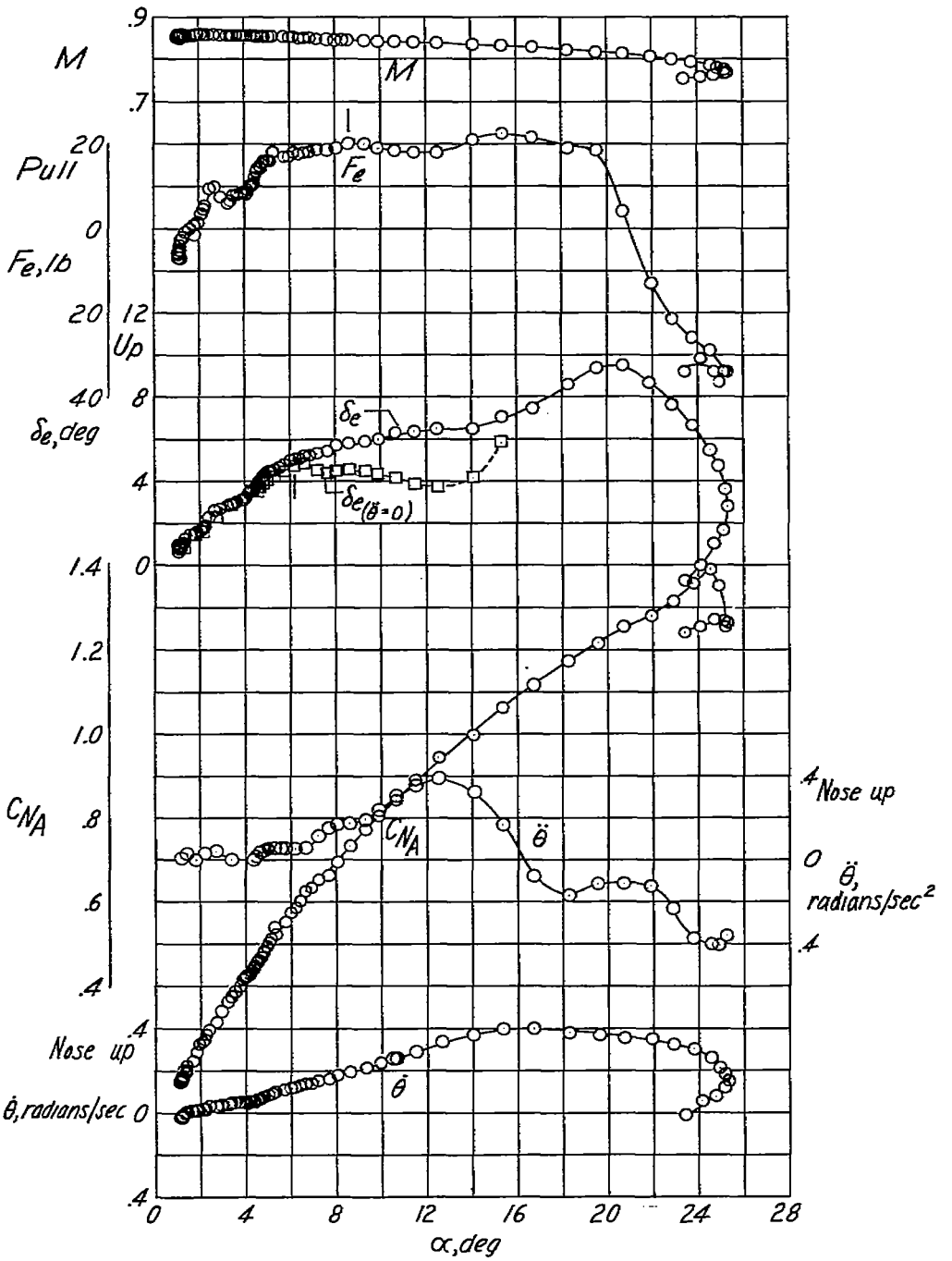

(n) $h_p \approx 33{,}000$ feet; $i_t = 1.6°$; center of gravity at 25.8 percent mean aerodynamic chord.

Figure 8.- Continued.

[redacted]

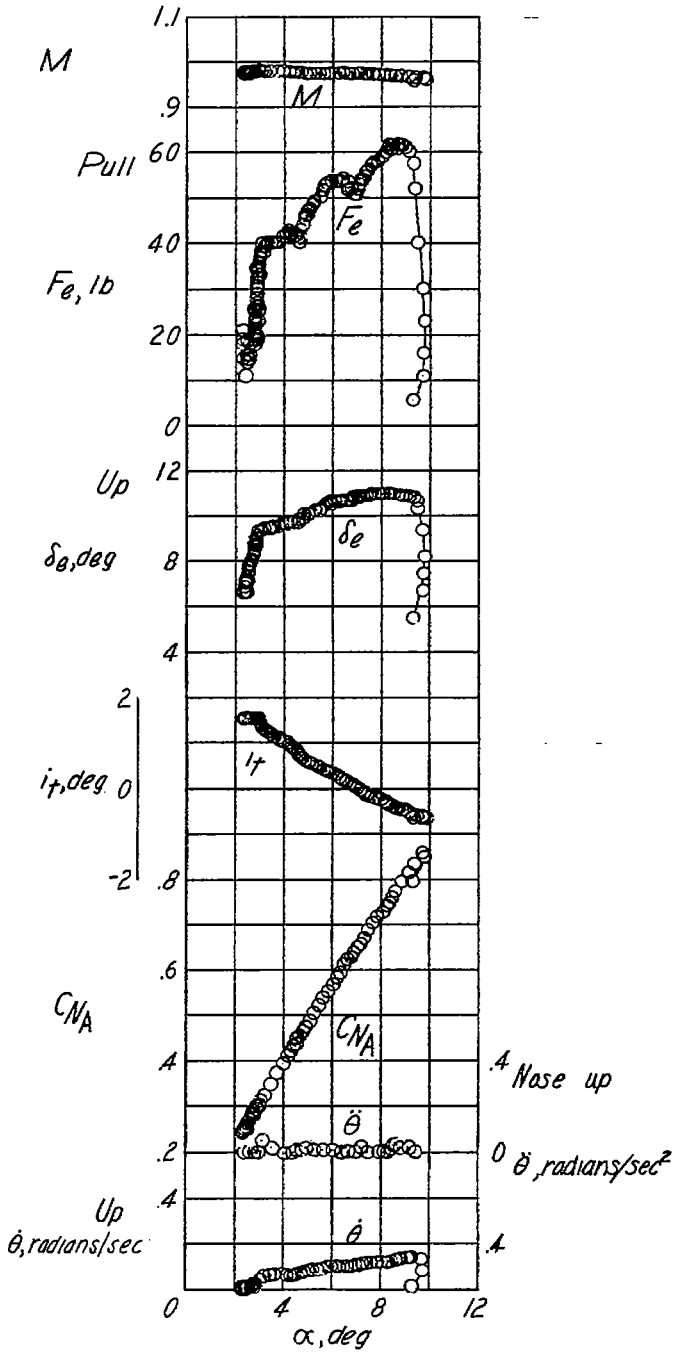

(o) $h_p \approx 35{,}100$ feet; center of gravity at 25.5 percent mean aerodynamic chord.

Figure 8.- Concluded.

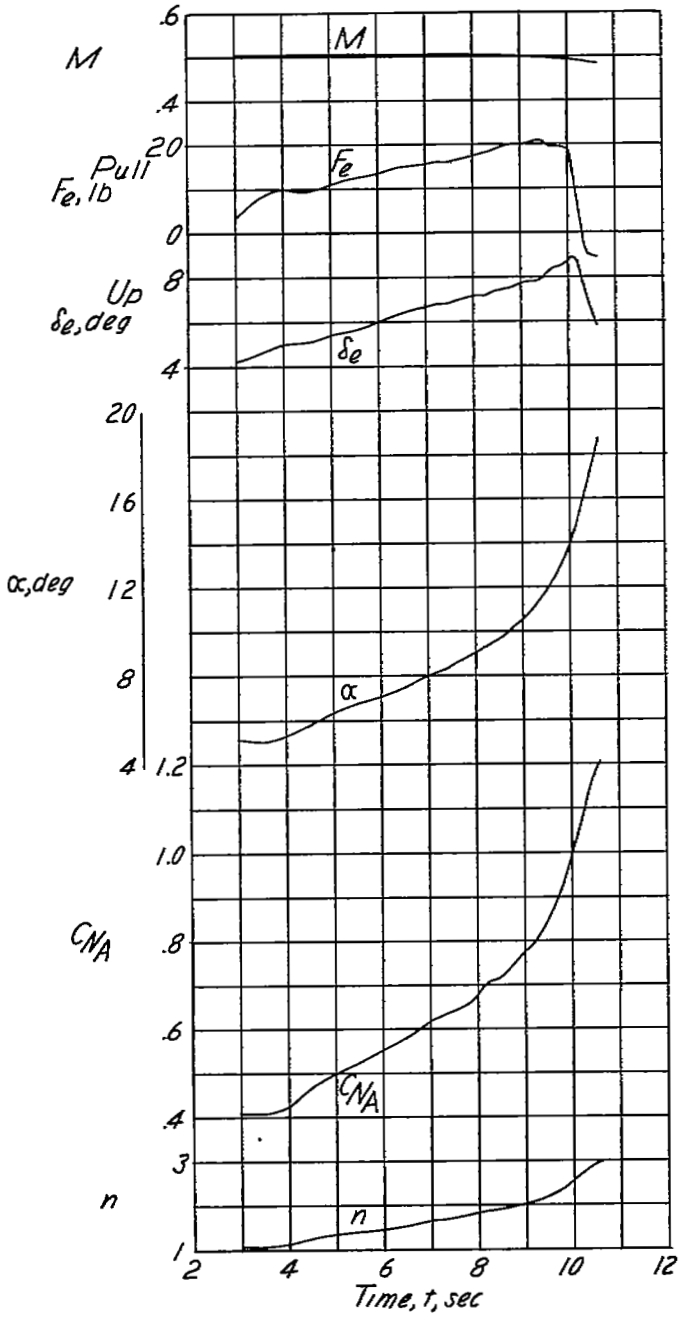

(a) $h_p \approx 19{,}700$ feet; $i_t = 1.6°$; center of gravity at 25.3 percent mean aerodynamic chord.

Figure 9.- Time histories of wind-up turns with the Douglas D-558-II research airplane with slats fully extended and inboard wing fences removed.

[redacted]

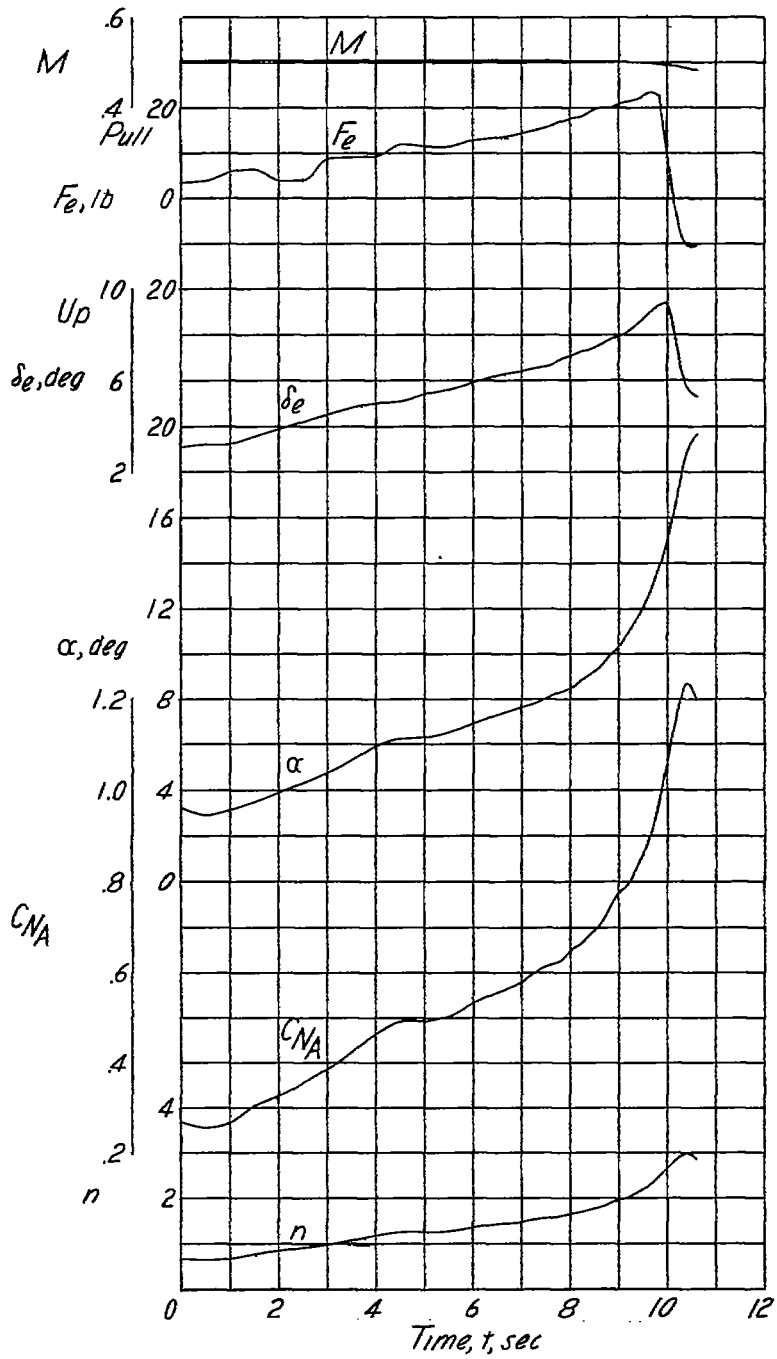

(b) $h_p \approx 20{,}700$ feet; $i_t = 1.6°$; center of gravity at 25.3 percent mean aerodynamic chord.

Figure 9.- Continued.

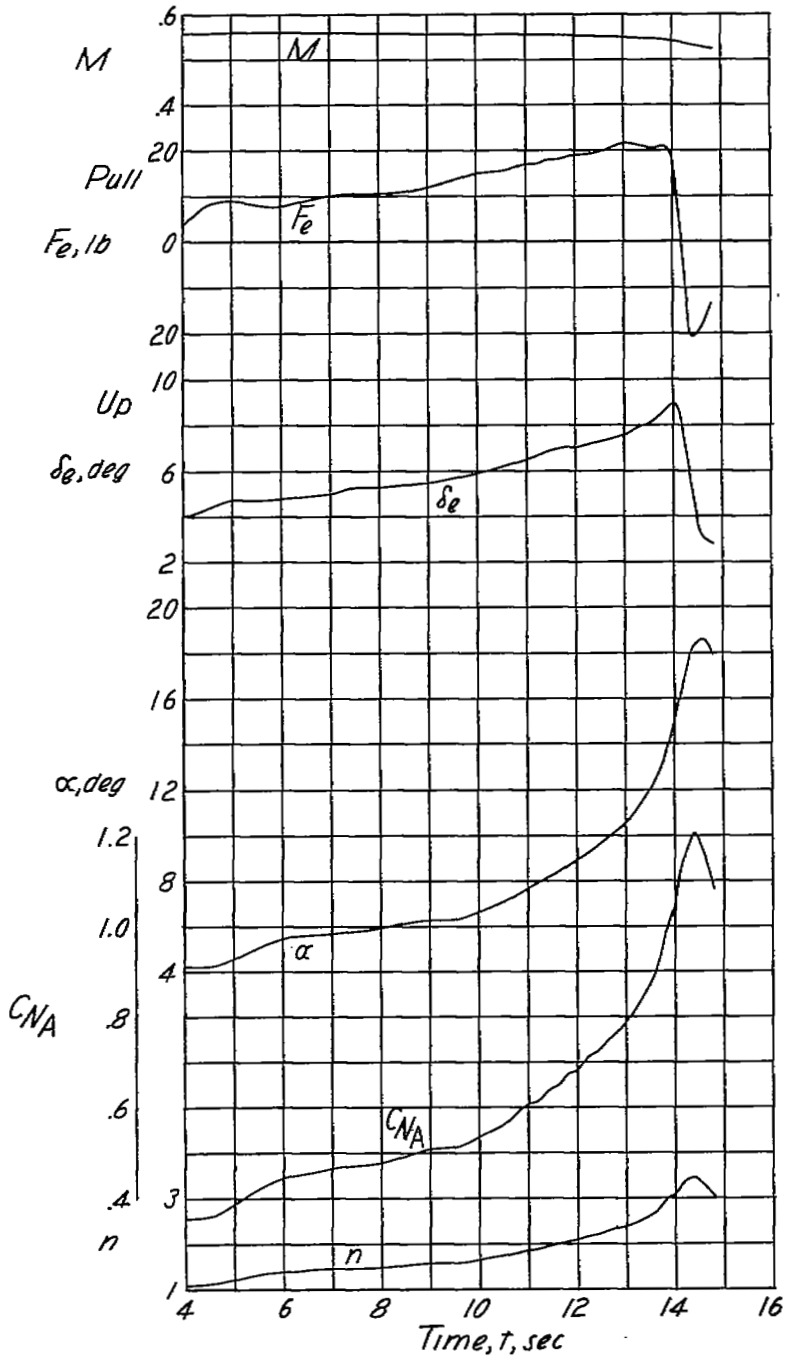

(c) $h_p \approx 20{,}700$ feet; $i_t = 1.6°$; center of gravity at 25.3 percent mean aerodynamic chord.

Figure 9.- Continued.

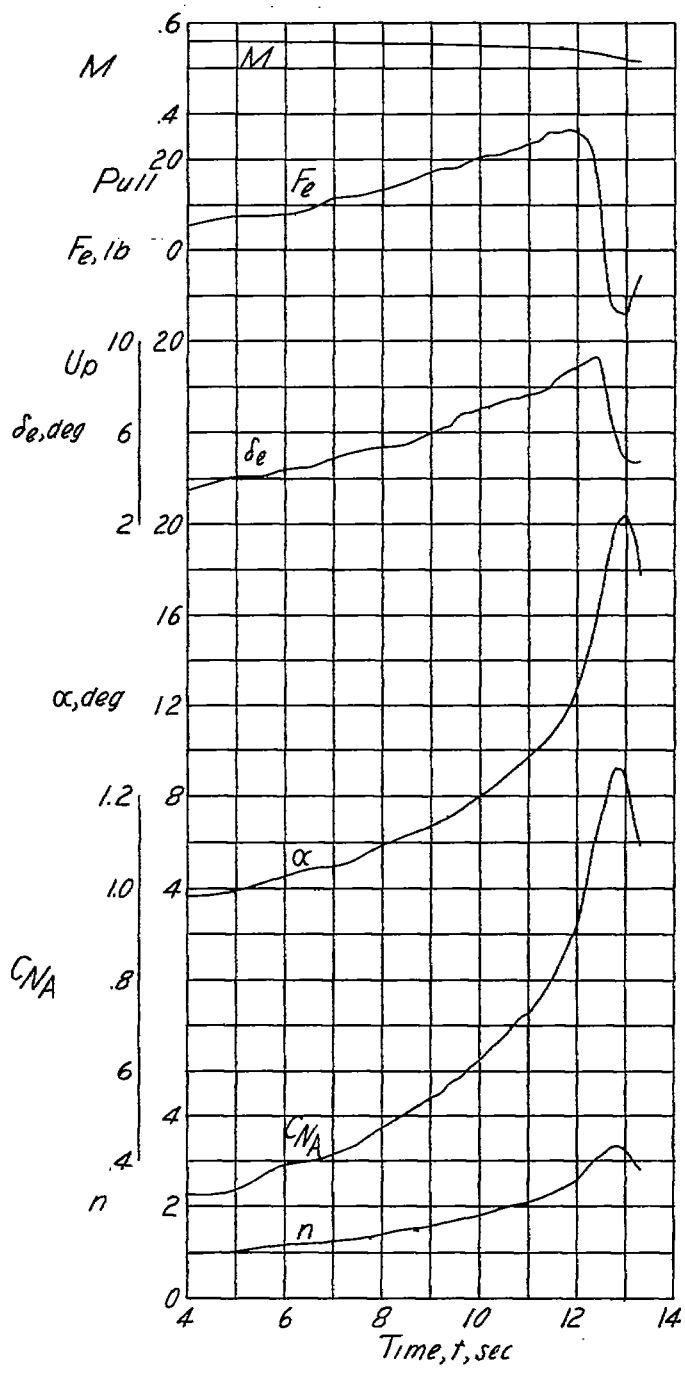

(d) $h_p \approx 21{,}800$ feet; $i_t = 1.6°$; center of gravity at 25.2 percent mean aerodynamic chord.

Figure 9.- Continued.

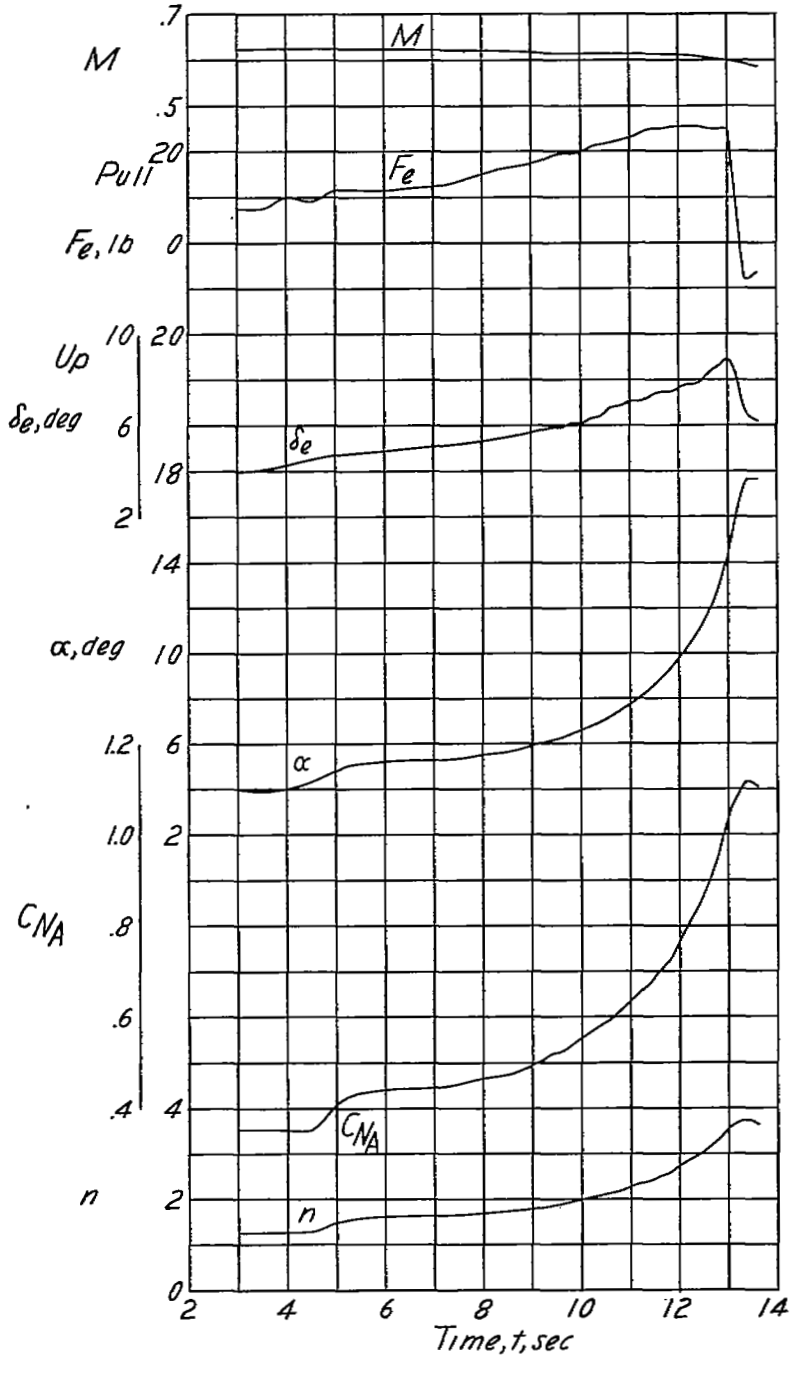

(e) $h_p \approx 22{,}100$ feet; $i_t = 1.6°$; center of gravity at 25.2 percent mean aerodynamic chord.

Figure 9.- Continued.

[redacted]

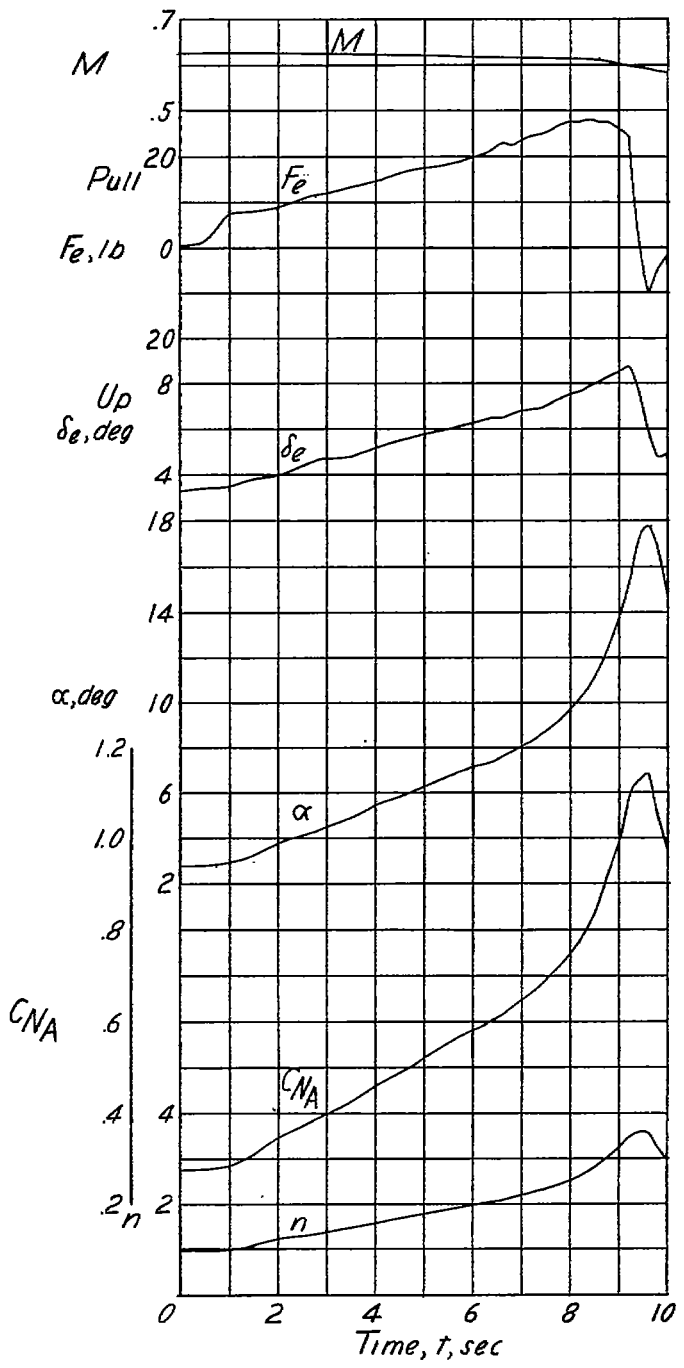

(f) $h_p \approx 23{,}400$ feet; $i_t = 1.6^\circ$; center of gravity at 25.2 percent mean aerodynamic chord.

Figure 9.- Continued.

[redacted]

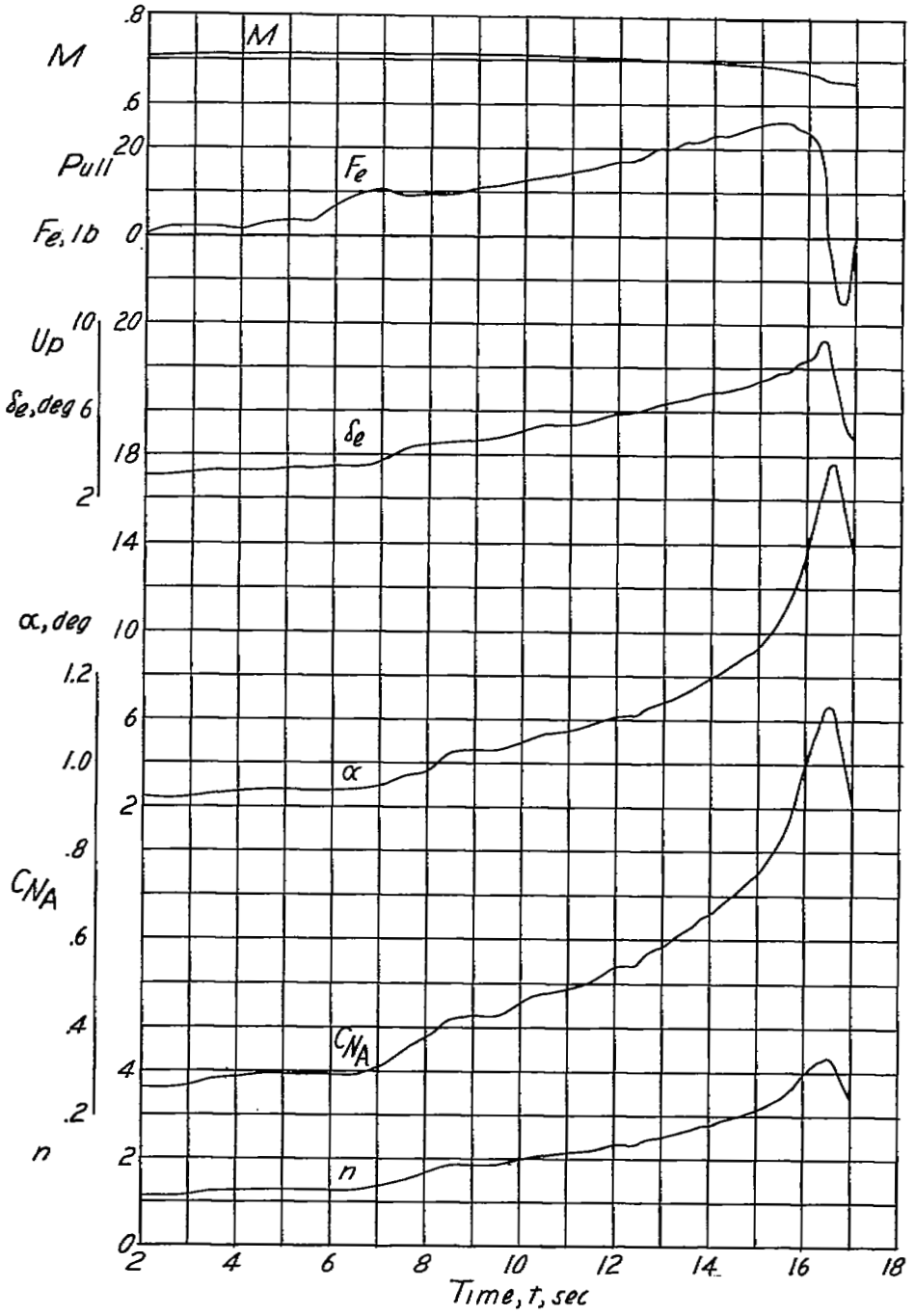

(g) $h_p \approx 24{,}000$ feet; $i_t = 1.6^\circ$; center of gravity at 25.2 percent mean aerodynamic chord.

Figure 9.- Continued.

[redacted]

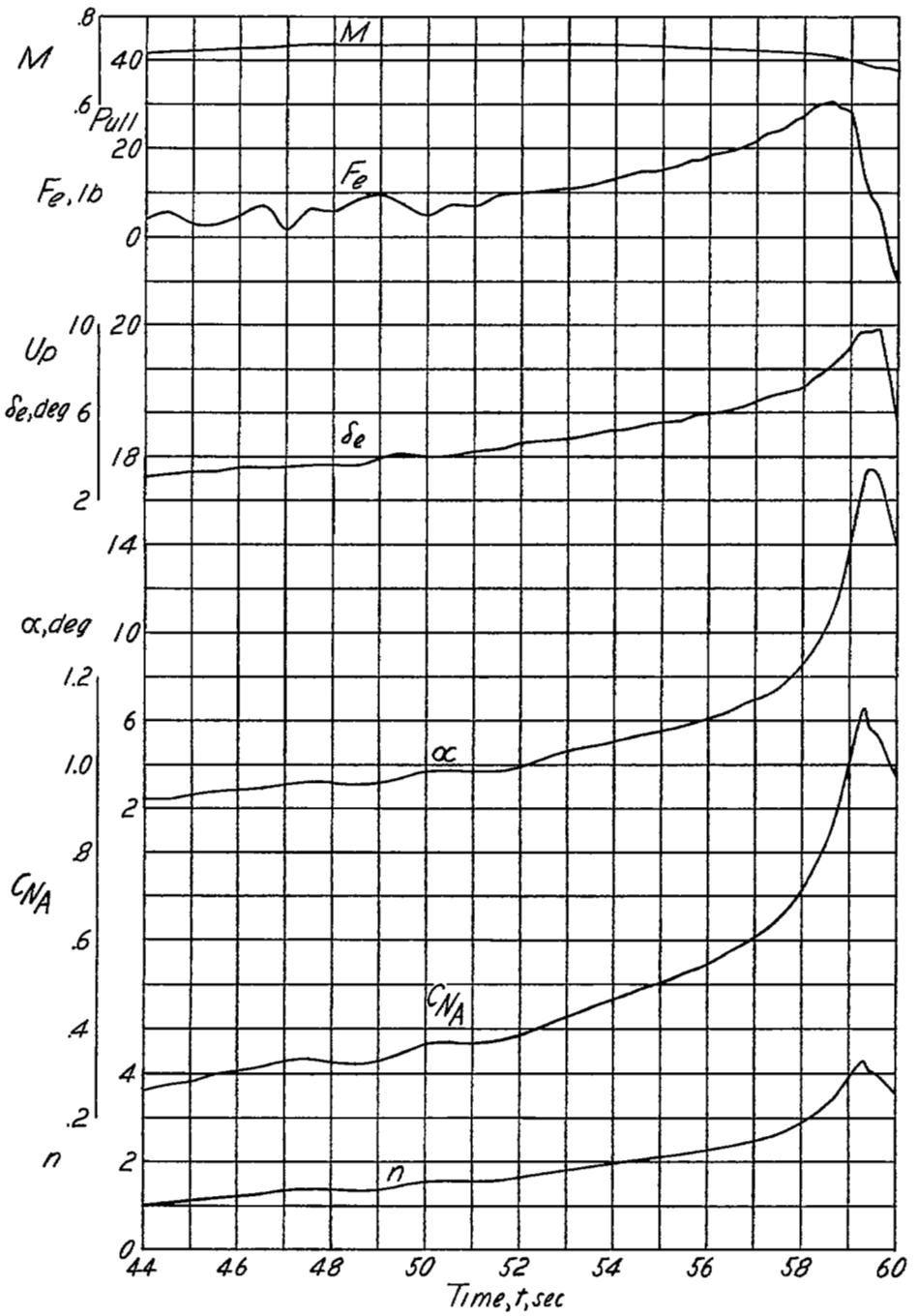

(h) $h_p \approx 26{,}500$ feet; $i_t = 1.6°$; center of gravity at 25.2 percent mean aerodynamic chord.

Figure 9.- Concluded.

[redacted]

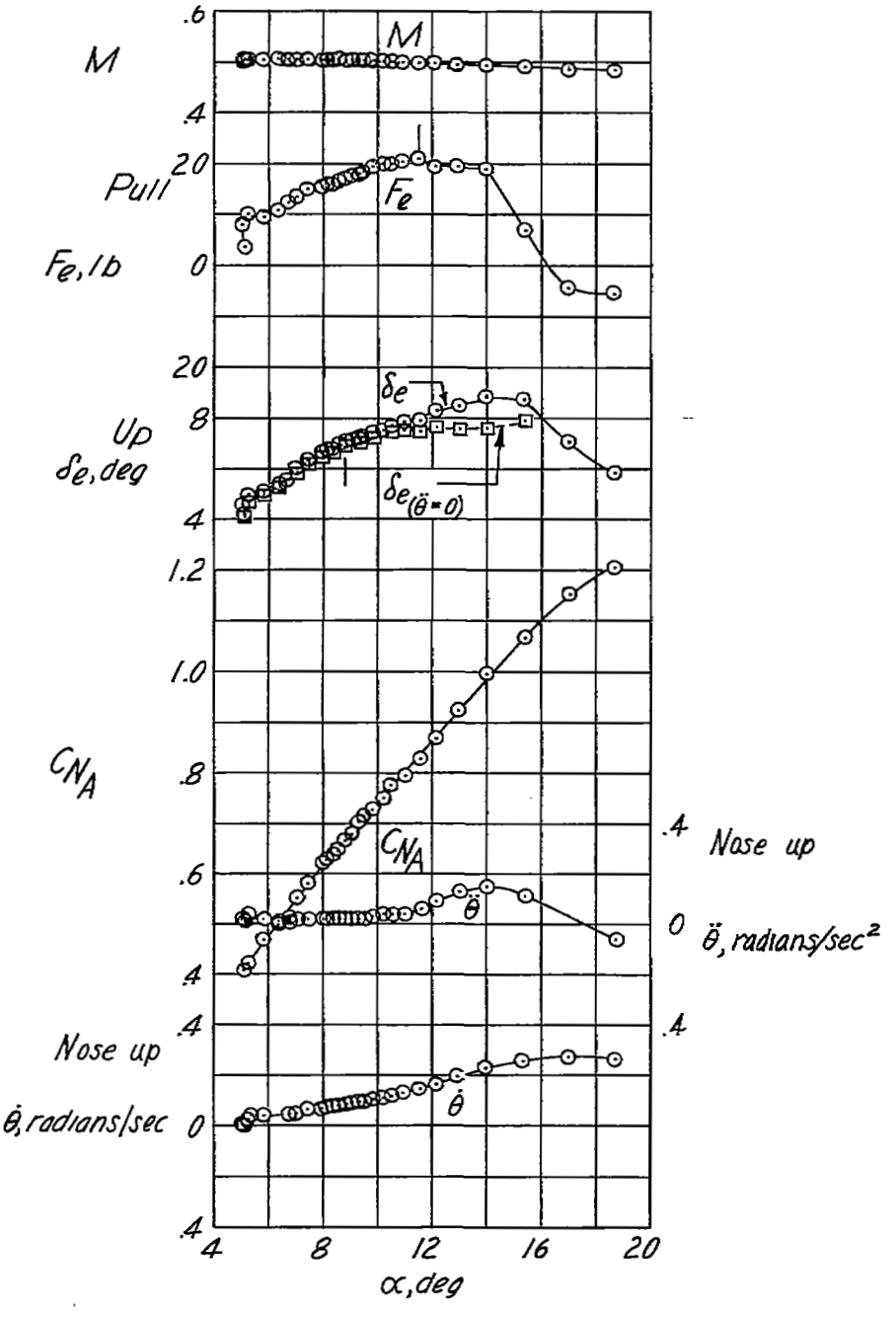

(a) $h_p \approx 19{,}700$ feet; $i_t = 1.6°$; center of gravity at 25.3 percent mean aerodynamic chord.

Figure 10.- Static longitudinal stability characteristics of the Douglas D-558-II research airplane in turning flight with slats fully extended and inboard wing fences removed.

[redacted]

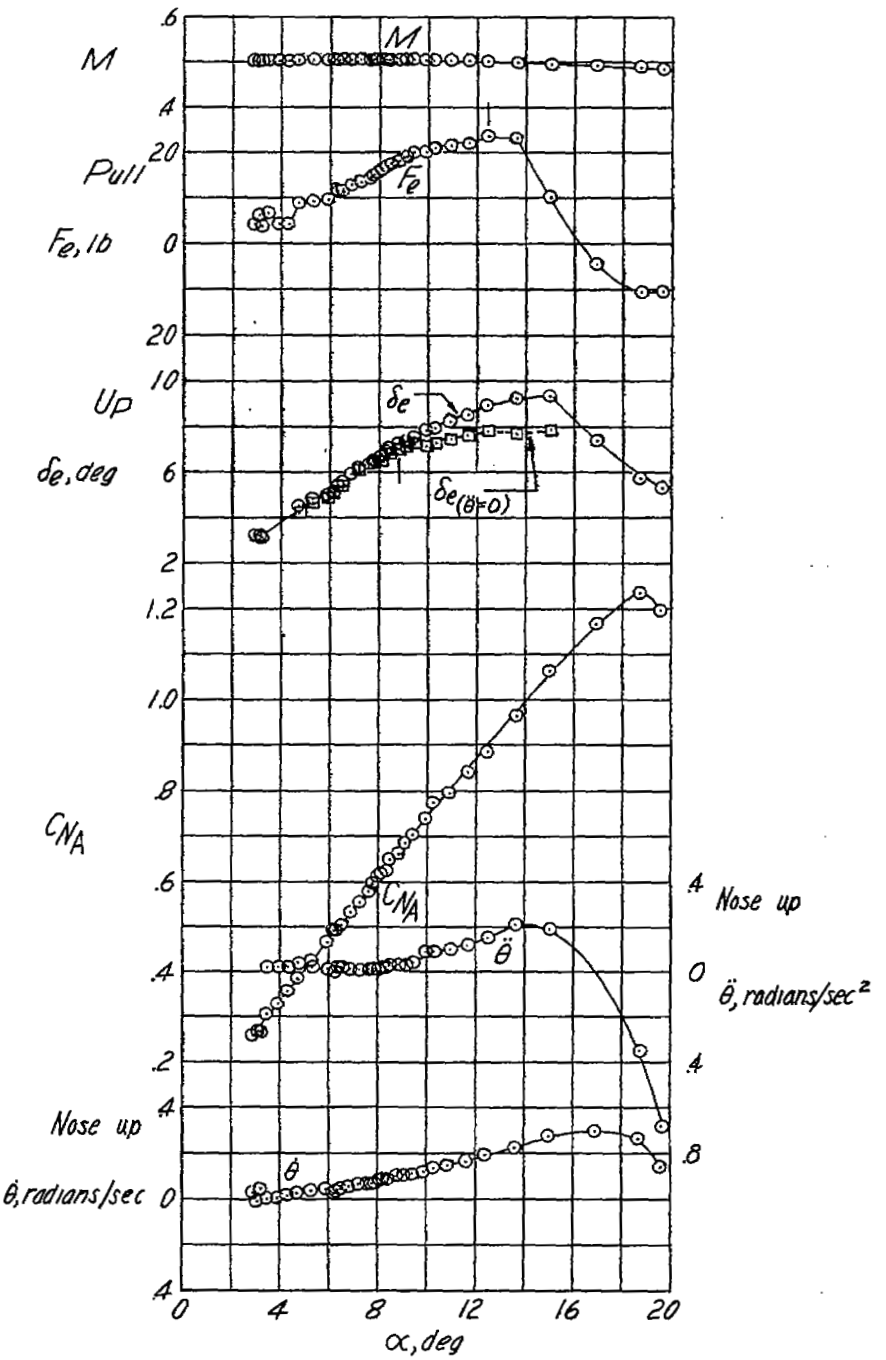

(b) $h_p \approx 20{,}700$ feet; $i_t = 1.6°$; center of gravity at 25.3 percent mean aerodynamic chord.

Figure 10.- Continued.

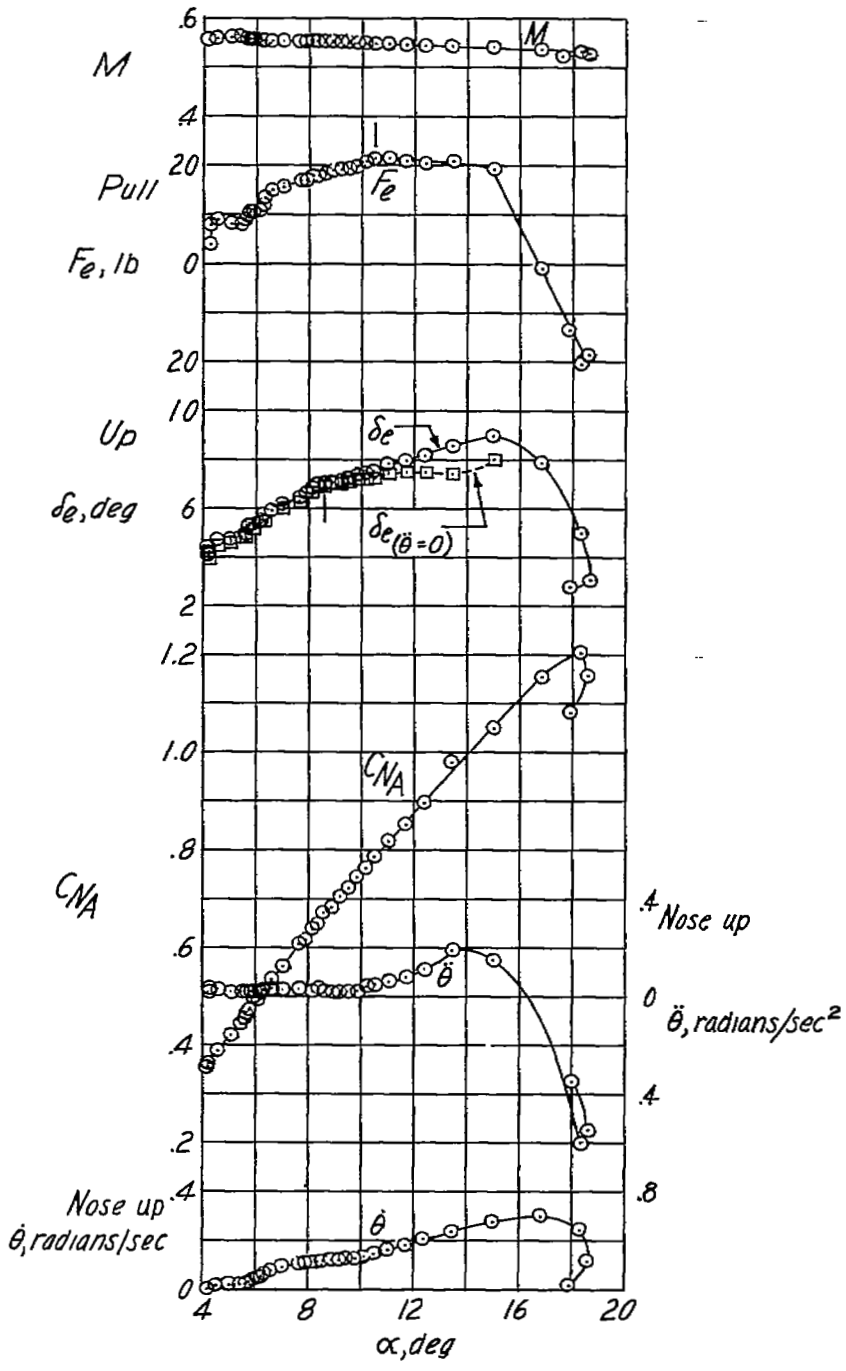

(c) $h_p \approx 20{,}700$ feet; $i_t = 1.6°$; center of gravity at 25.3 percent mean aerodynamic chord.

Figure 10.- Continued.

[redacted]

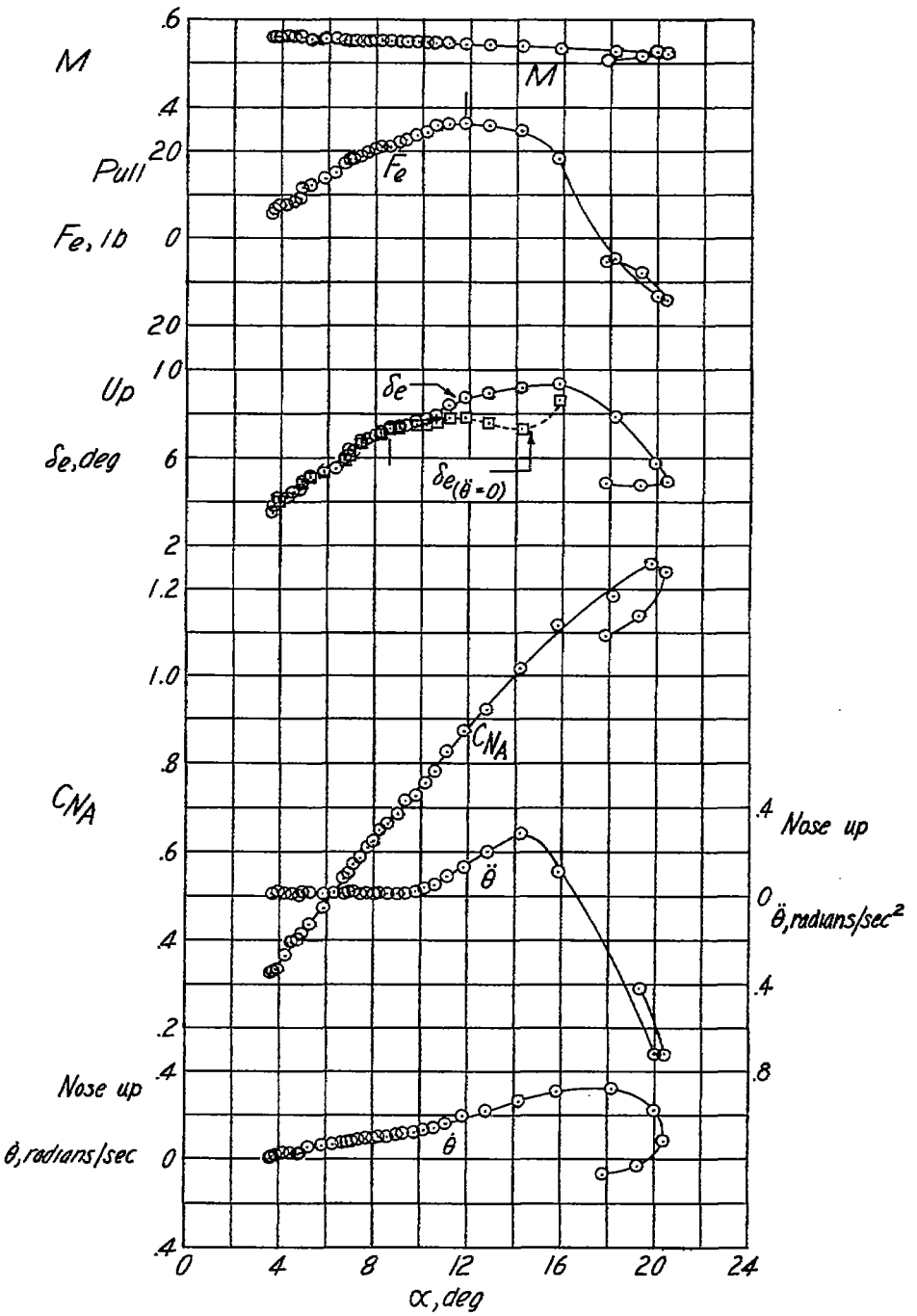

(d) $h_p \approx 21{,}800$ feet; $i_t = 1.6°$; center of gravity at 25.2 percent mean aerodynamic chord.

Figure 10.- Continued.

[redacted]

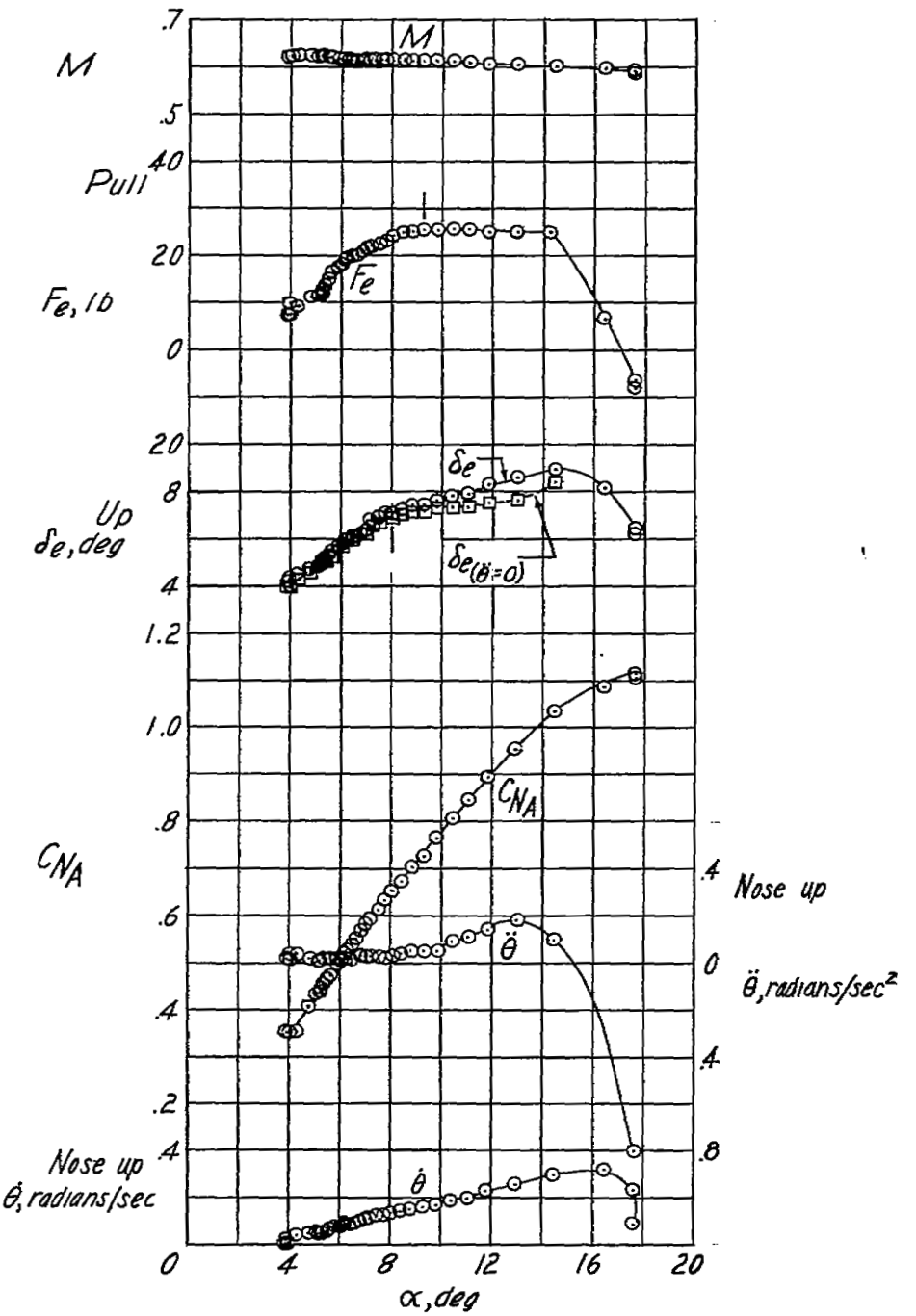

(e) $h_p \approx 22{,}100$ feet; $i_t = 1.6^\circ$; center of gravity at 25.2 percent mean aerodynamic chord.

Figure 10.- Continued.

[redacted]

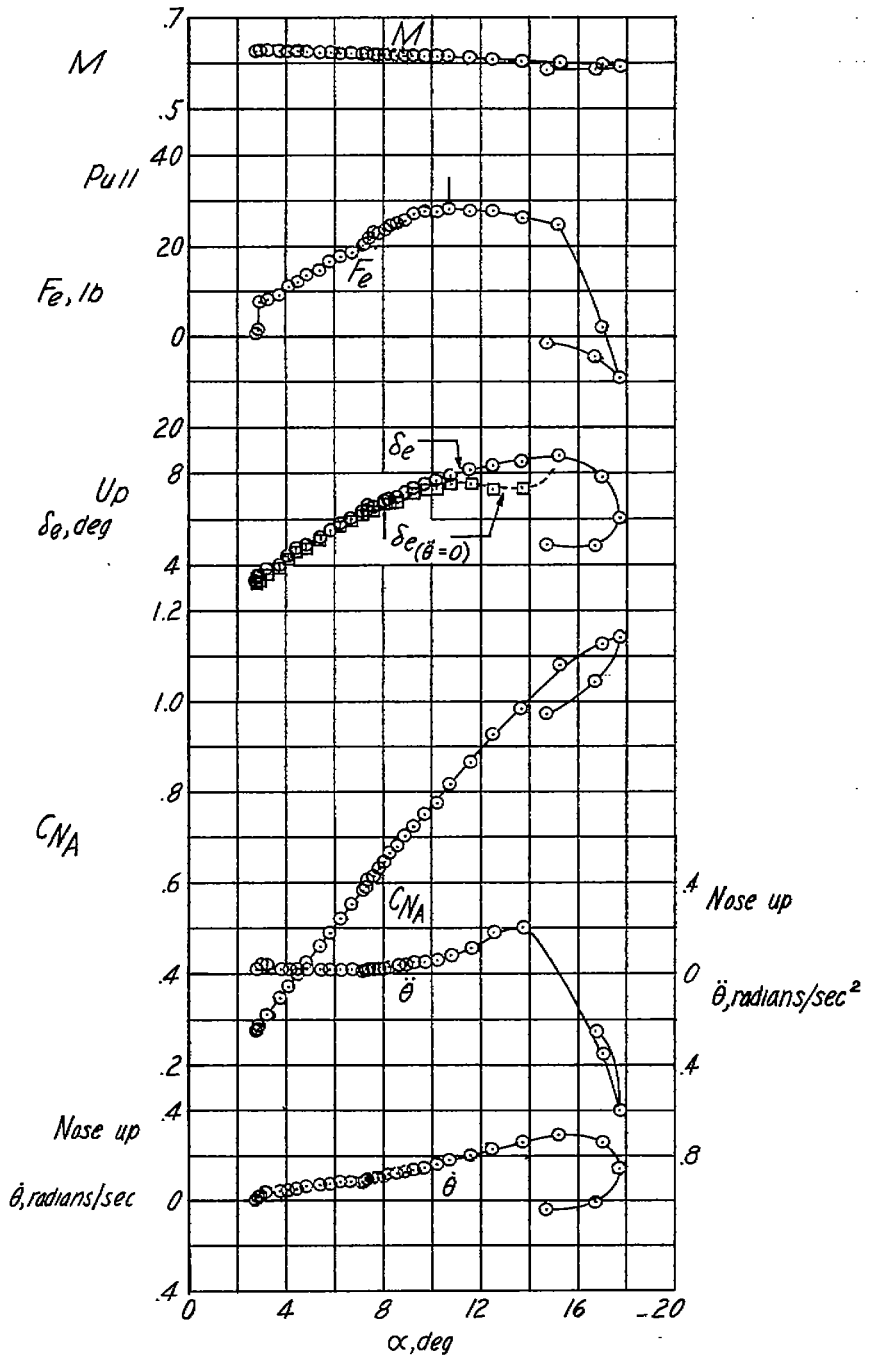

(f) $h_p \approx 23{,}400$ feet; $i_t = 1.6^\circ$; center of gravity at 25.2 percent mean aerodynamic chord.

Figure 10.- Continued.

[redacted]

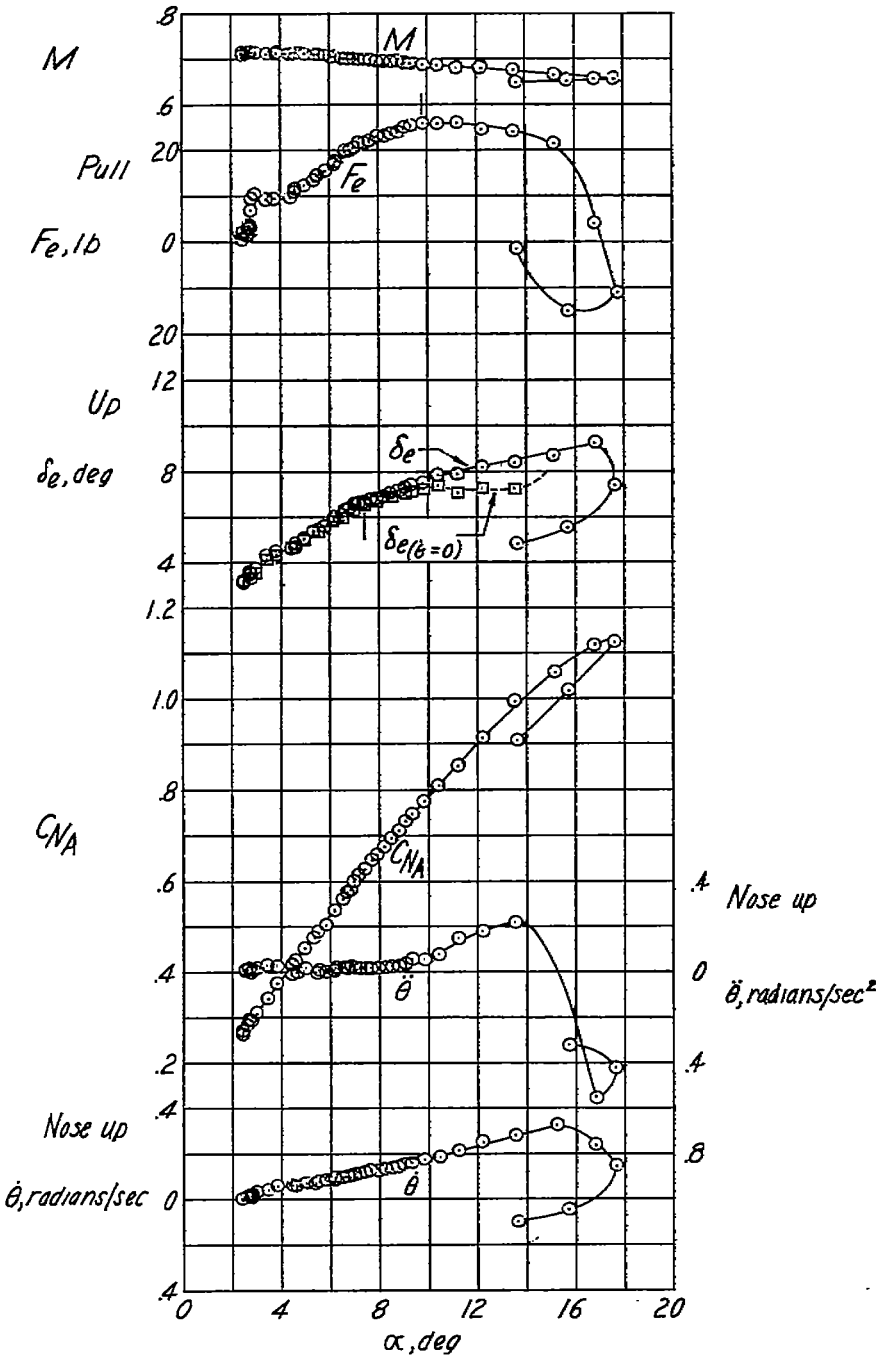

(g) $h_p \approx 24{,}000$ feet; $i_t = 1.6°$; center of gravity at 25.2 percent mean aerodynamic chord.

Figure 10.- Continued.

[redacted]

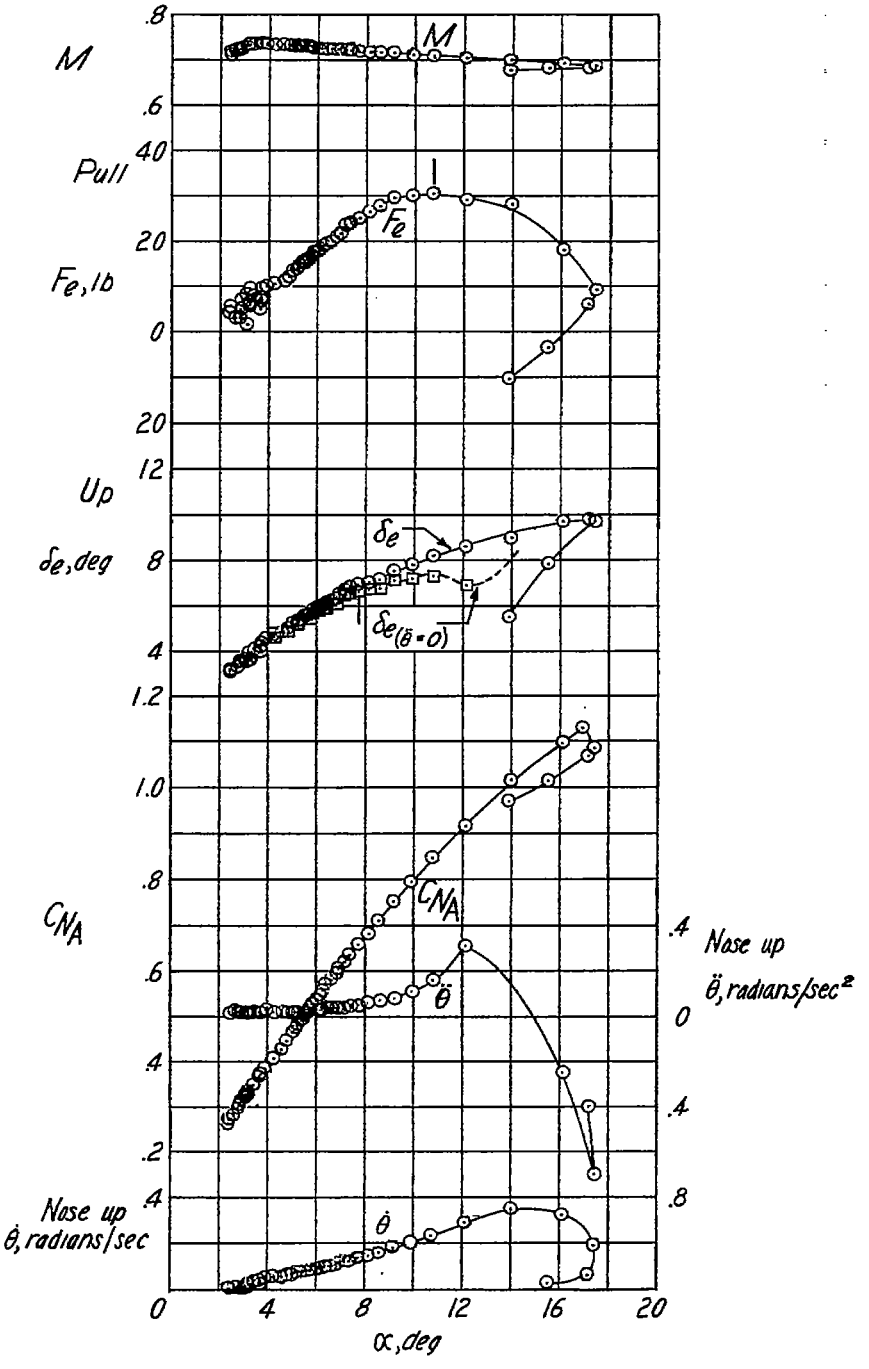

(h) $h_p \approx 26{,}500$ feet; $i_t = 1.6°$; center of gravity at 25.2 percent mean aerodynamic chord.

Figure 10.- Concluded.

[redacted]

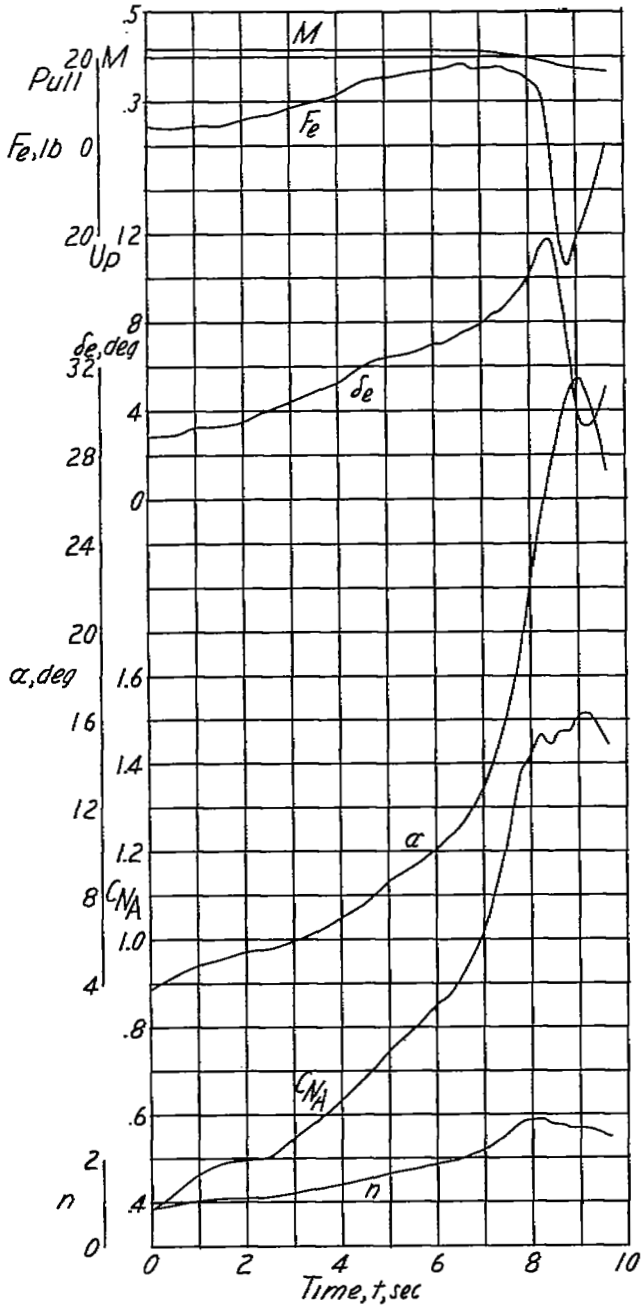

(a) $h_p \approx 14{,}900$ feet; $i_t = 1.3°$; center of gravity at 26.4 percent mean aerodynamic chord.

Figure 11.- Time histories of wind-up turns with the Douglas D-558-II research airplane with slats fully extended, inboard wing fences removed, and a soft bungee installed on the control column.

[redacted]

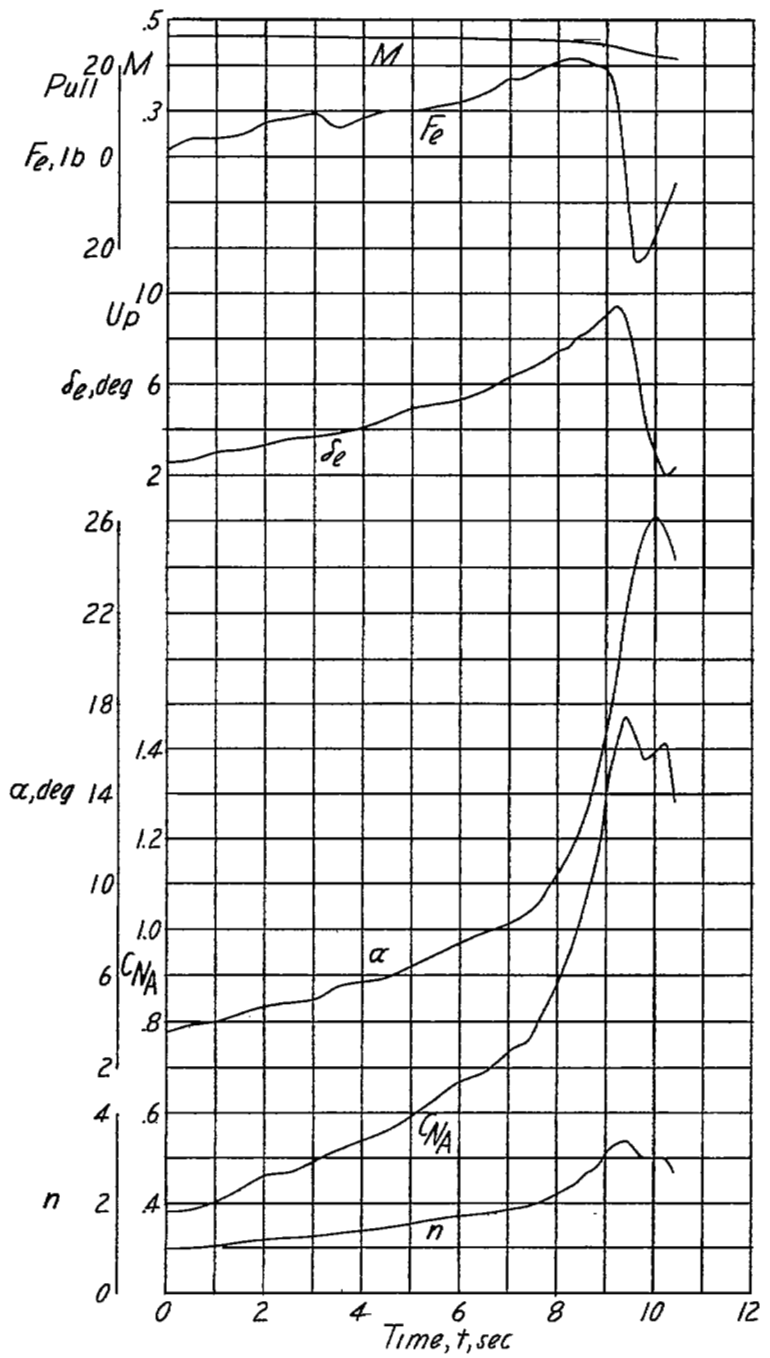

(b) $h_p \approx 15{,}900$ feet; $i_t = 1.3°$; center of gravity at 26.4 percent mean aerodynamic chord.

Figure 11.- Continued.

[redacted]

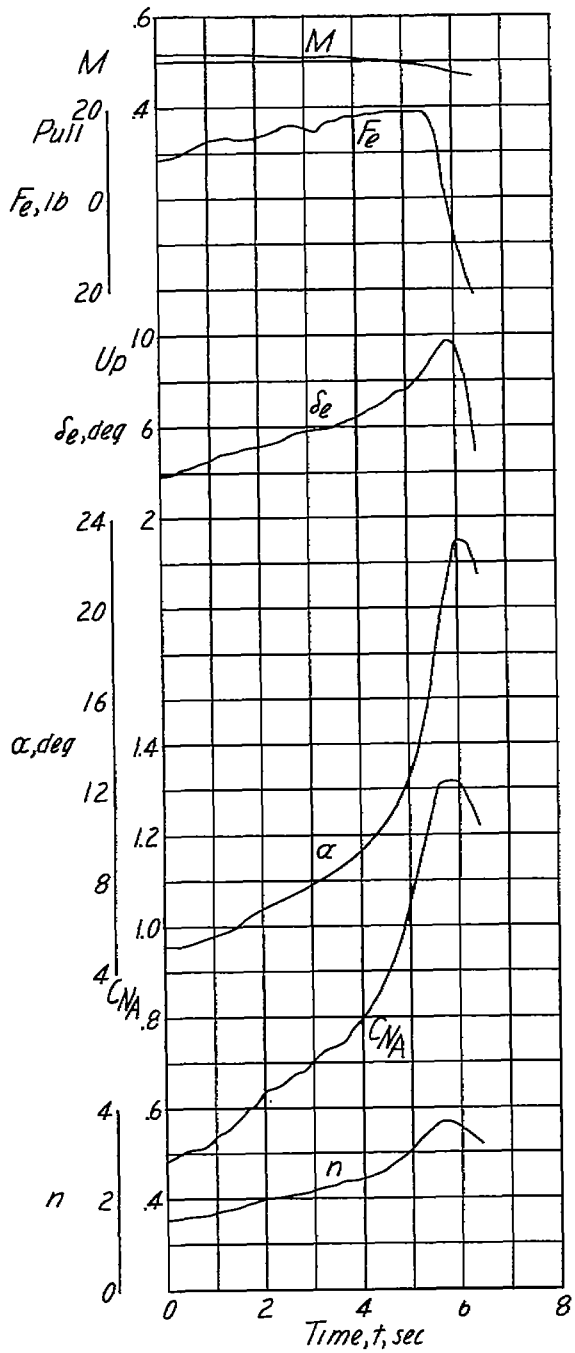

(c) $h_p \approx 16{,}500$ feet; $i_t = 1.3°$; center of gravity at 26.4 percent mean aerodynamic chord.

Figure 11.- Continued.

[redacted]

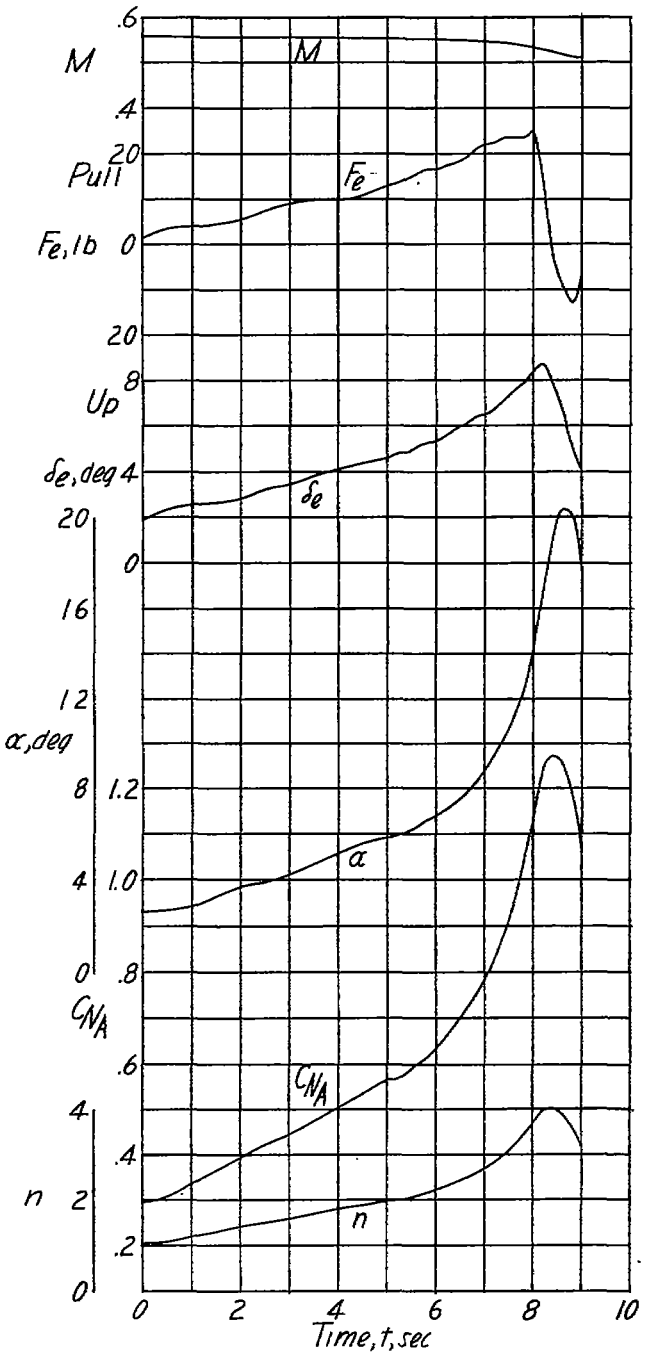

(d) $h_p \approx 17{,}200$ feet; $i_t = 1.3°$; center of gravity at 26.4 percent mean aerodynamic chord.

Figure 11.- Continued.

[redacted]

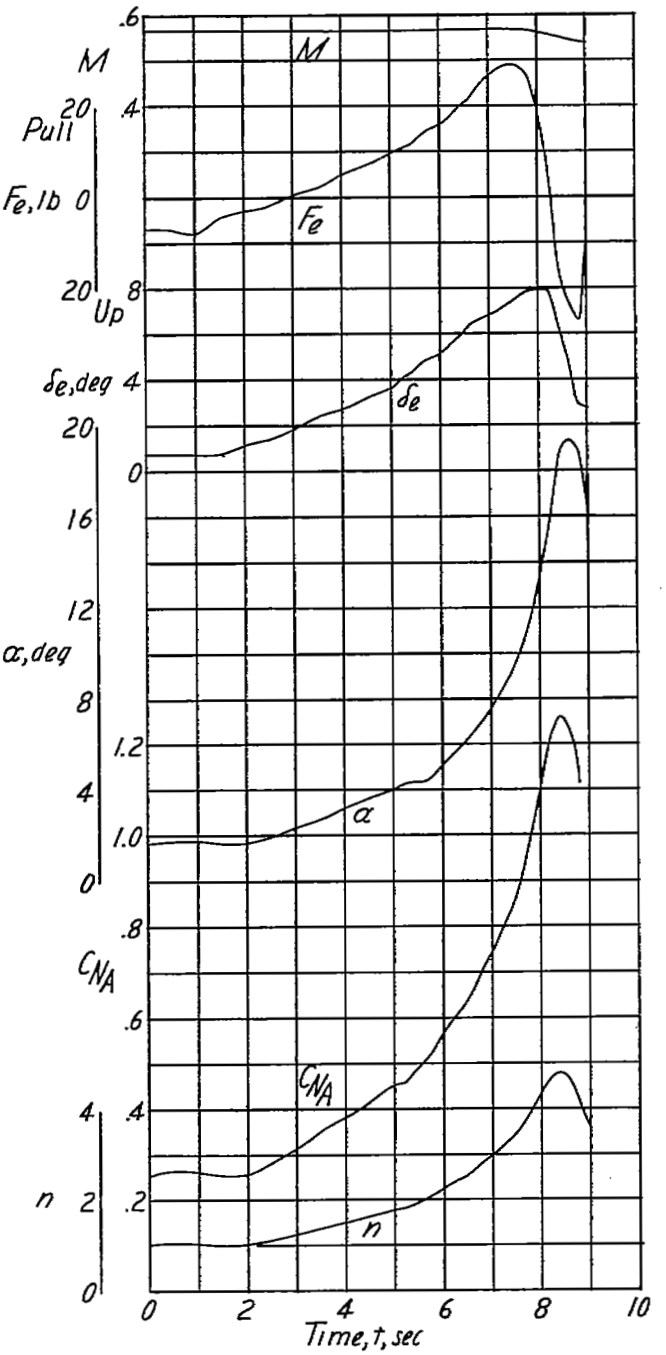

(e) $h_p \approx 16{,}000$ feet; $i_t = 1.3^\circ$; center of gravity at 26.7 percent mean aerodynamic chord.

Figure 11.- Continued.

[redacted]

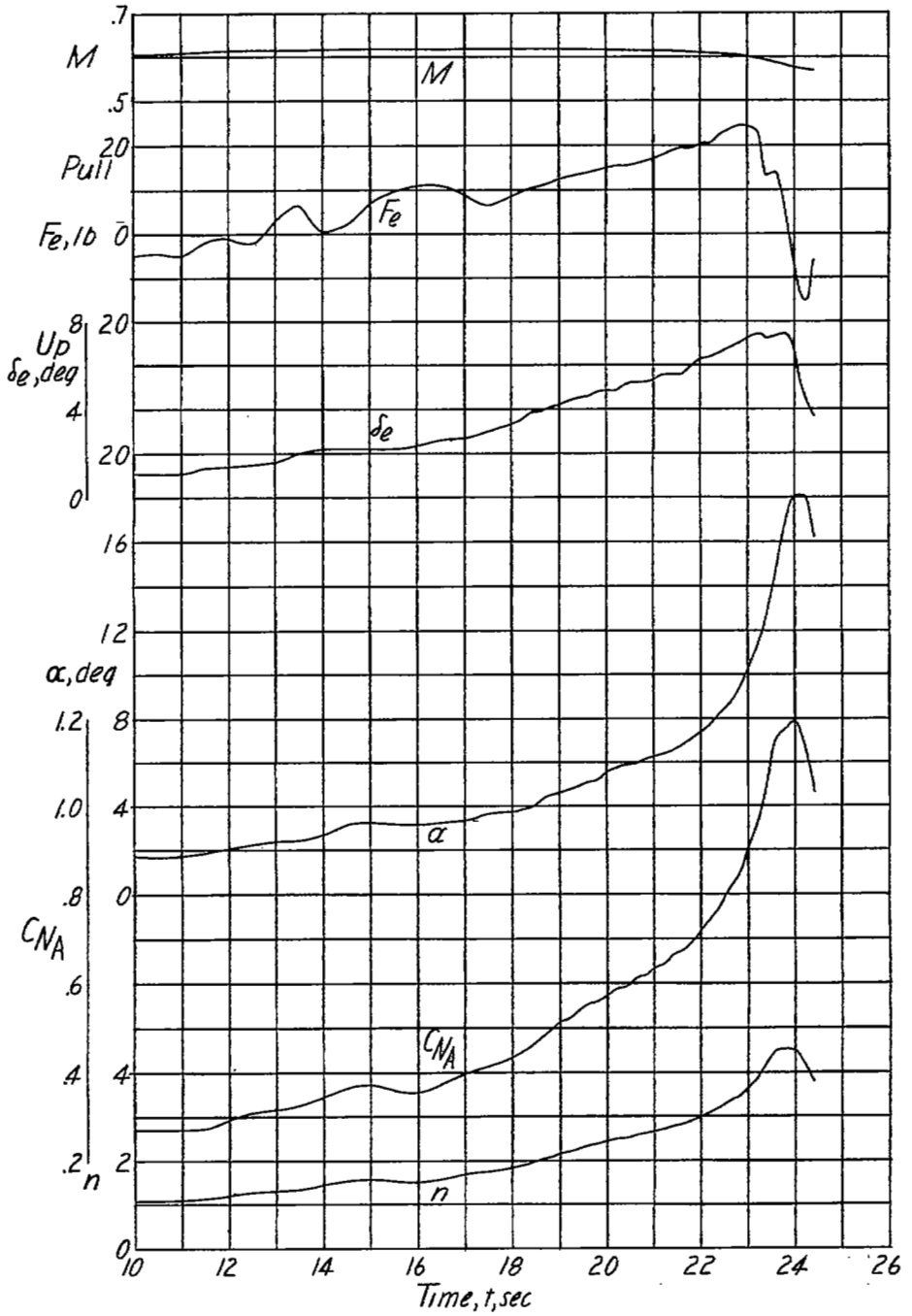

(f) $h_p \approx 18{,}000$ feet; $i_t = 1.3^\circ$; center of gravity at 26.4 percent mean aerodynamic chord.

Figure 11.- Continued.

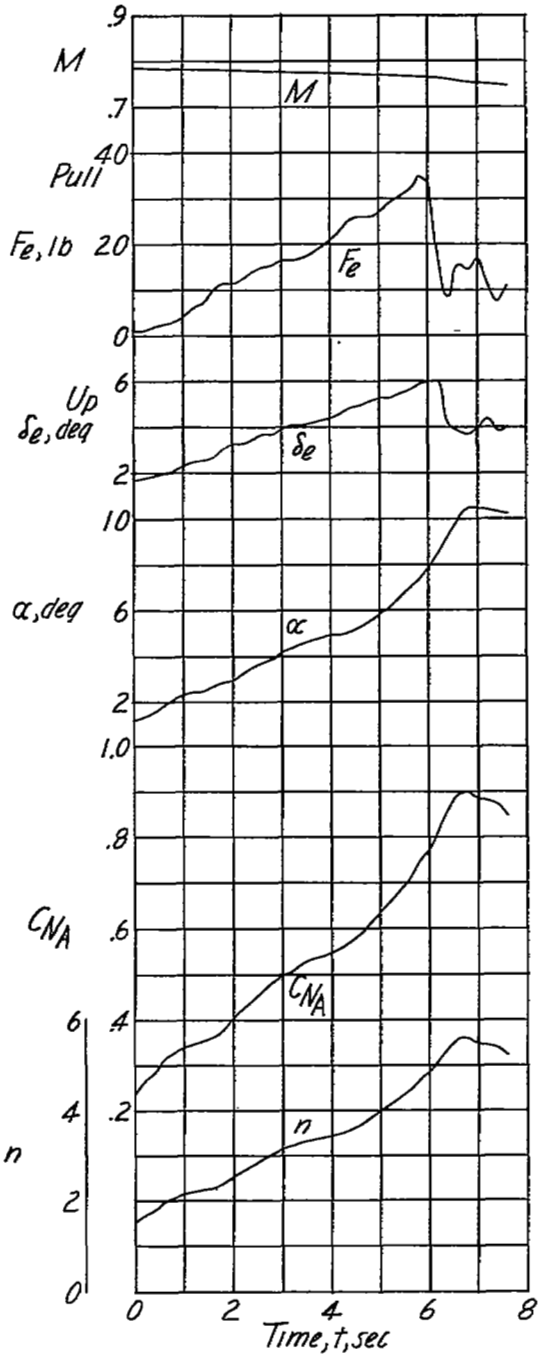

(g) $h_p \approx 19{,}000$ feet; $i_t = 1.3°$; center of gravity at 26.2 percent mean aerodynamic chord.

Figure 11.- Continued.

[redacted]

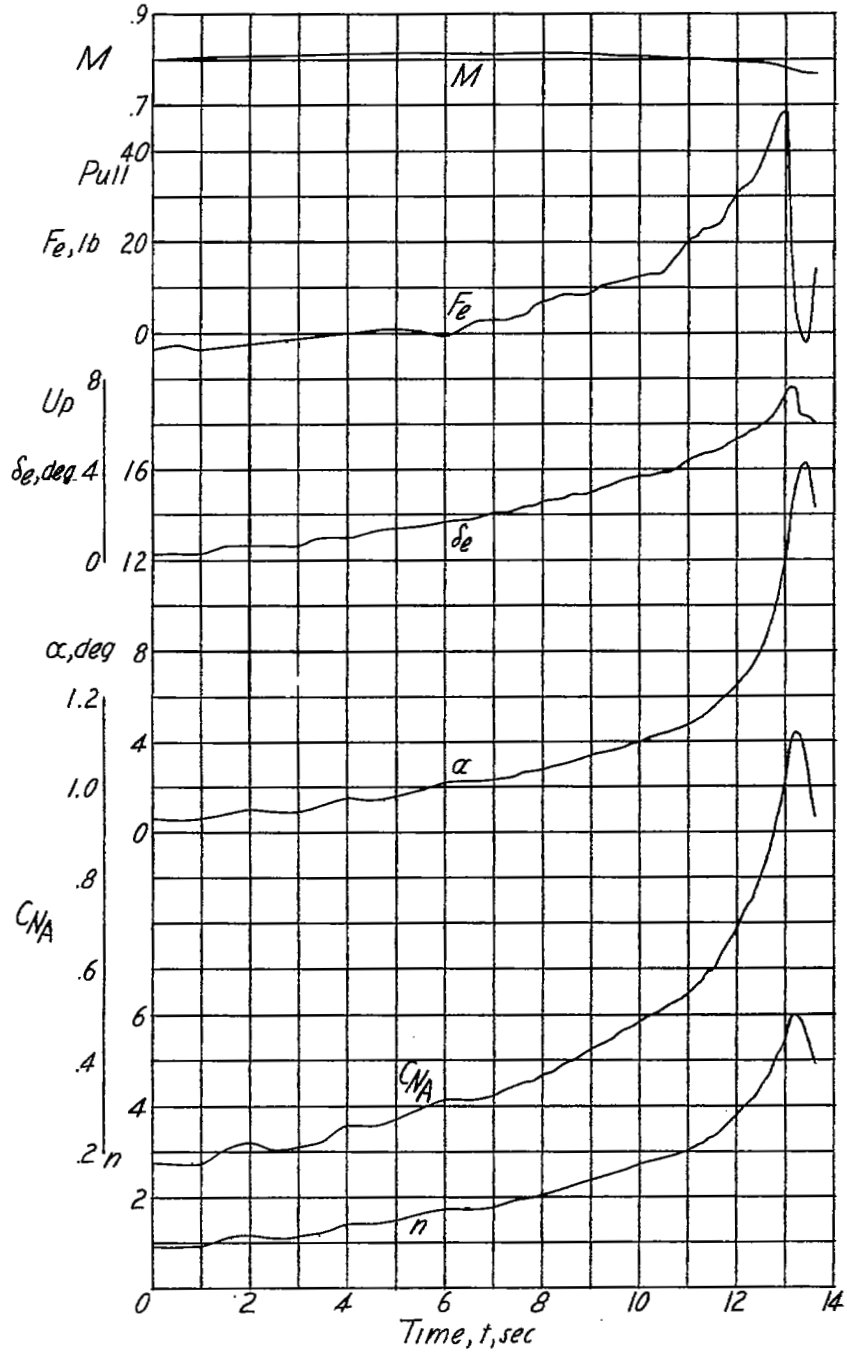

(h) $h_p \approx 23{,}000$ feet; $i_t = 1.3°$; center of gravity at 26.2 percent mean aerodynamic chord.

Figure 11.- Continued.

[redacted]

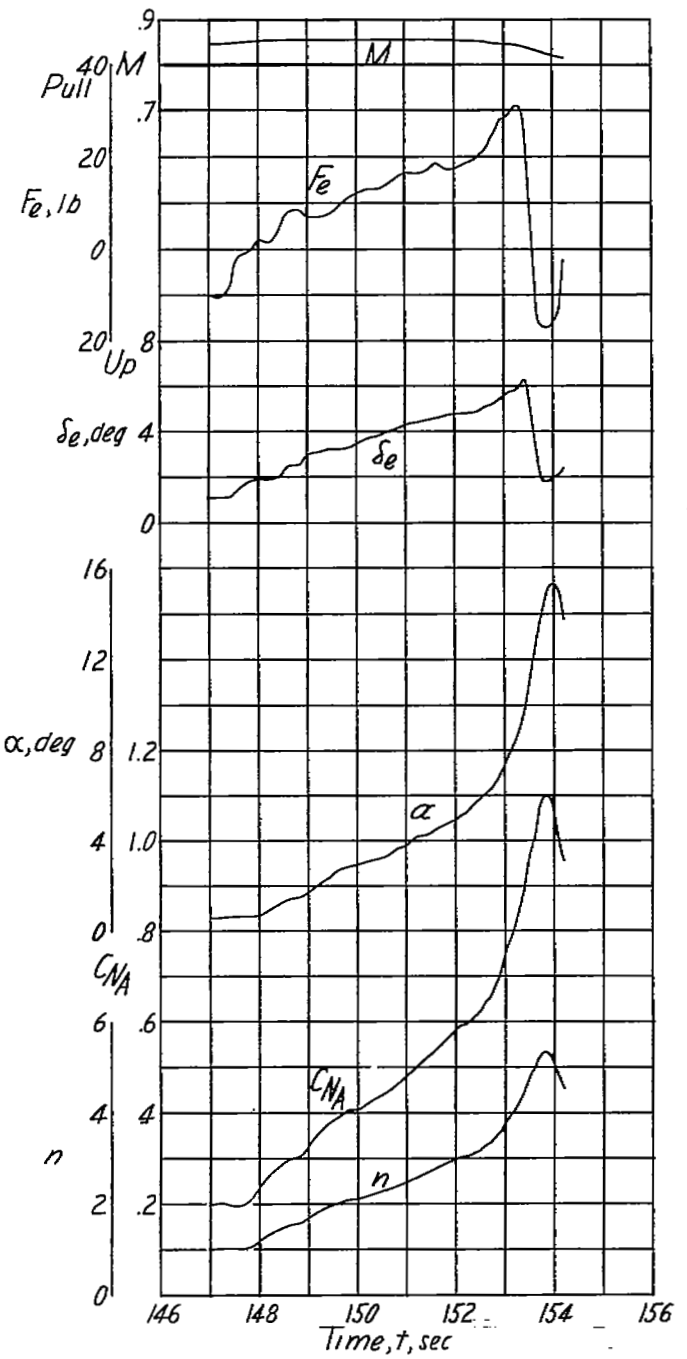

(i) $h_p \approx 27{,}300$ feet; $i_t = 1.3°$; center of gravity at 26.6 percent mean aerodynamic chord.

Figure 11.- Continued.

[redacted]

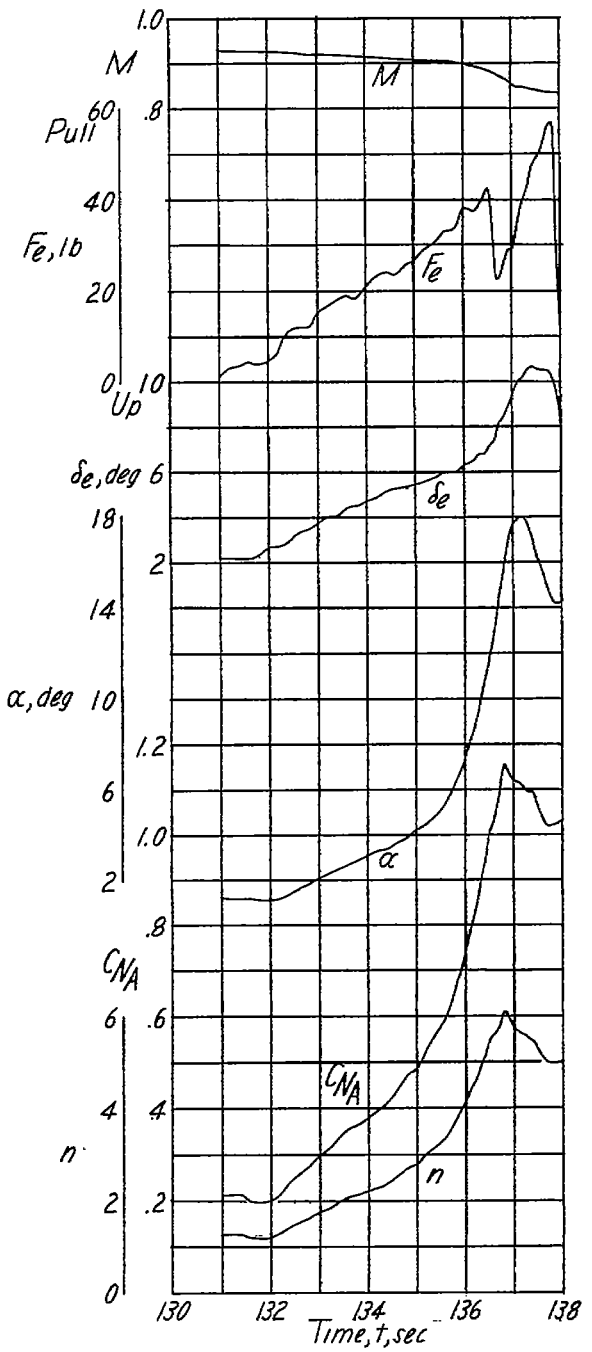

(j) $h_p \approx 27{,}000$ feet; $i_t = 1.3^\circ$; center of gravity at 26.5 percent mean aerodynamic chord.

Figure 11.- Continued.

[redacted]

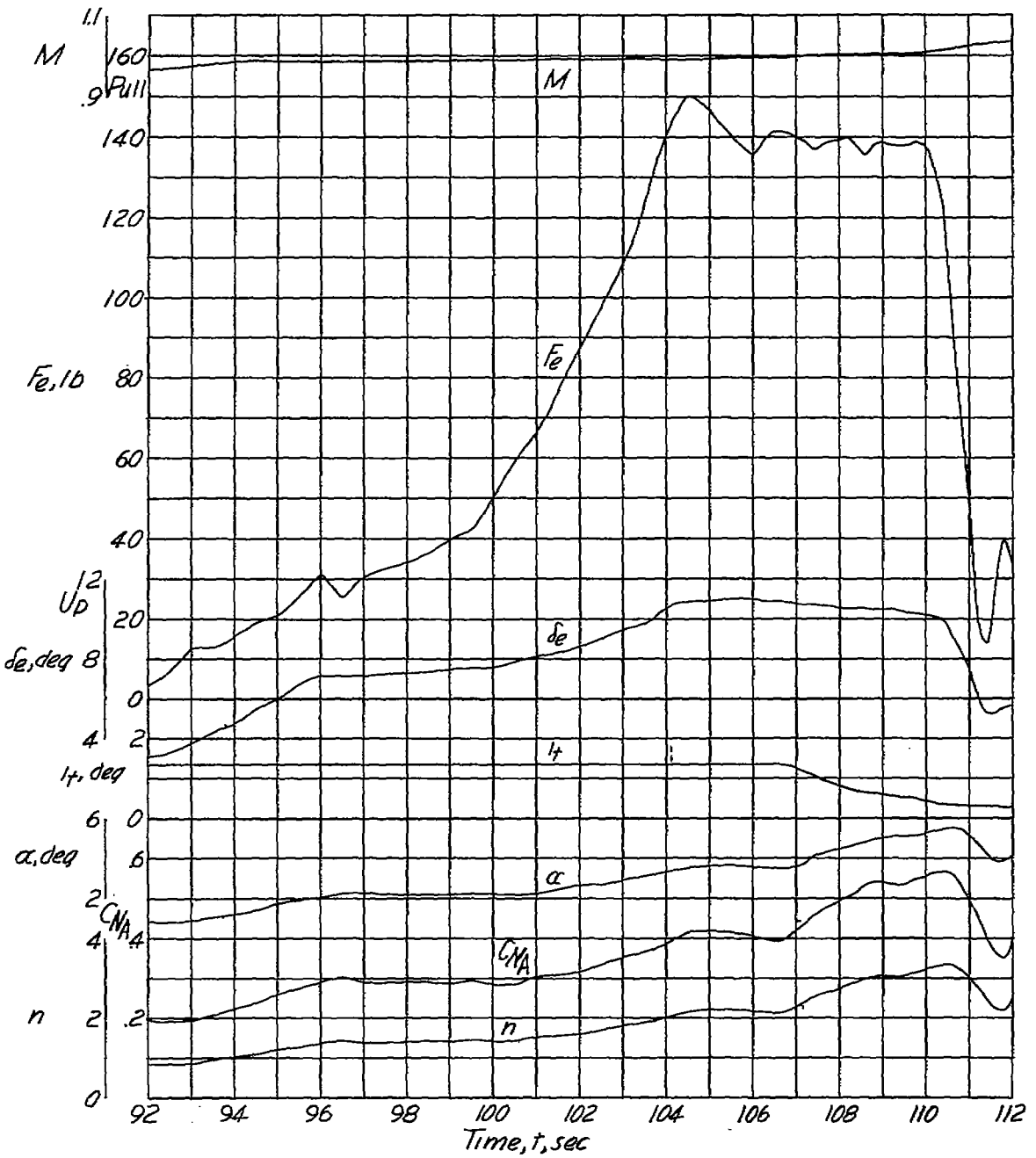

(k) $h_p \approx 33{,}000$ feet; center of gravity at 26.3 percent mean aerodynamic chord.

Figure 11.- Concluded.

[redacted]

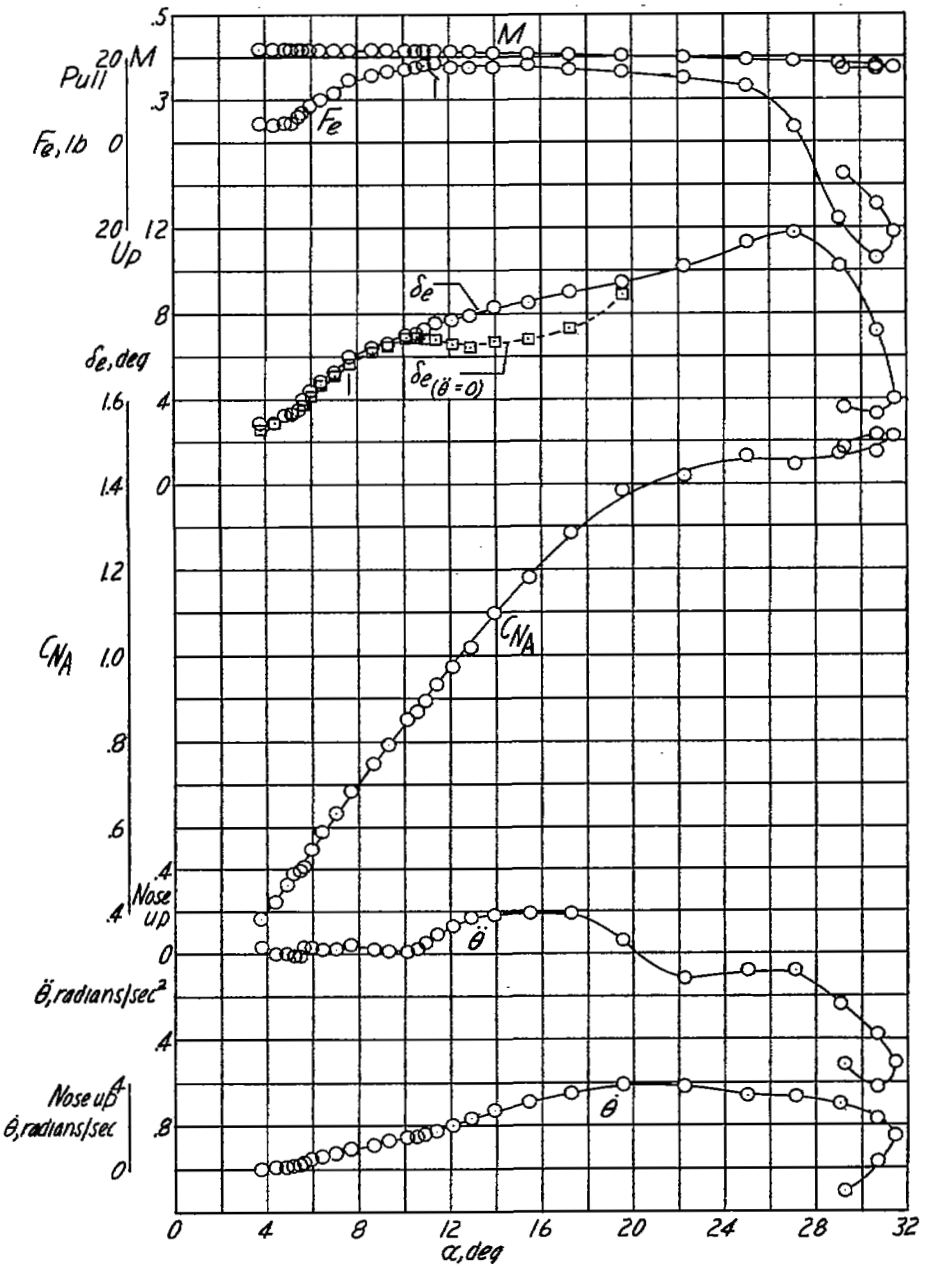

(a) $h_p \approx 14{,}900$ feet; $i_t = 1.3^\circ$; center of gravity at 26.4 percent mean aerodynamic chord.

Figure 12.- Static longitudinal stability characteristics of the Douglas D-558-II research airplane with slats fully extended, inboard wing fences removed, and a soft bungee installed on the control column.

[redacted]

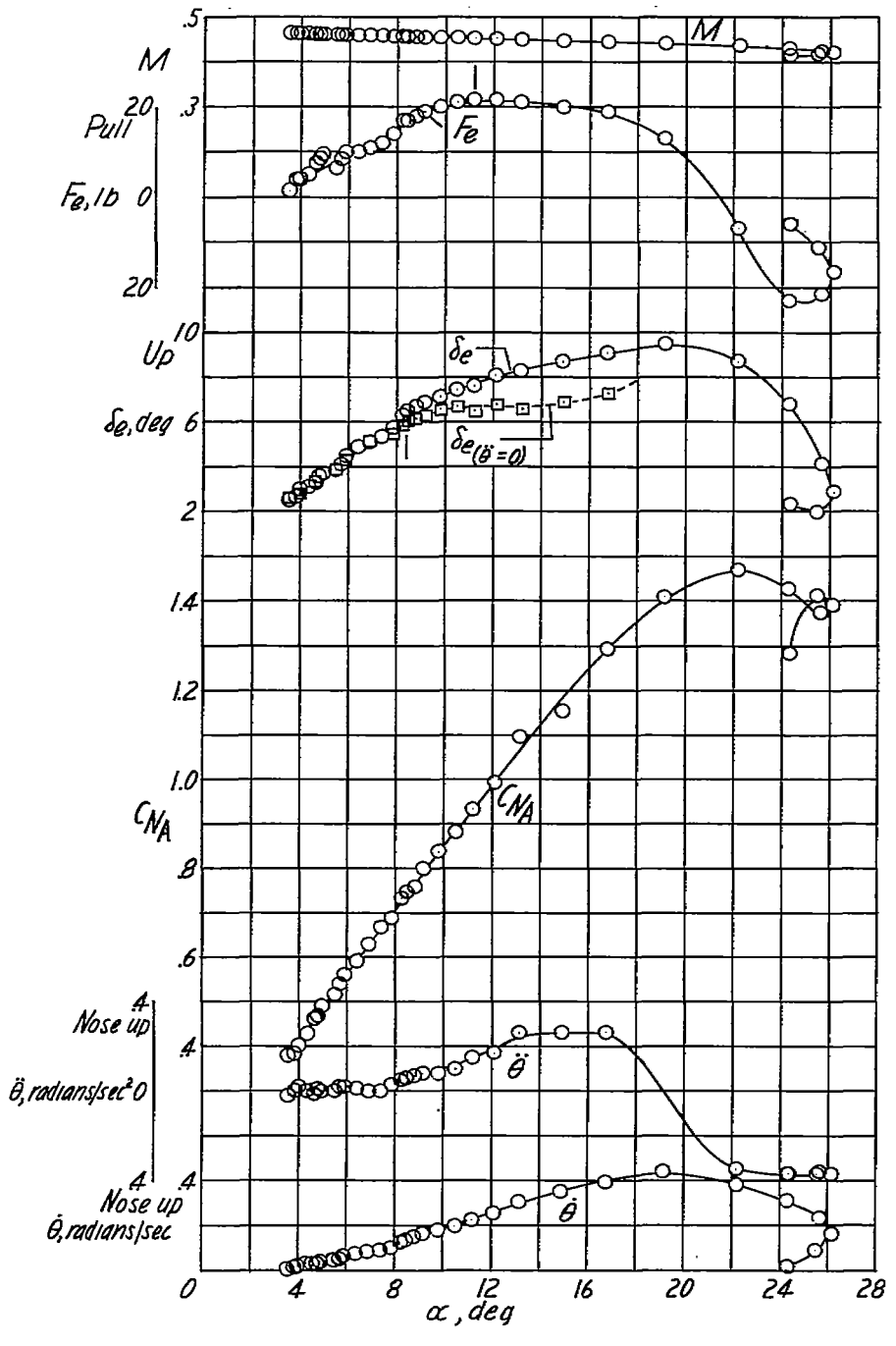

(b) $h_p \approx 15{,}900$ feet; $i_t = 1.3°$; center of gravity at 26.4 percent mean aerodynamic chord.

Figure 12.- Continued.

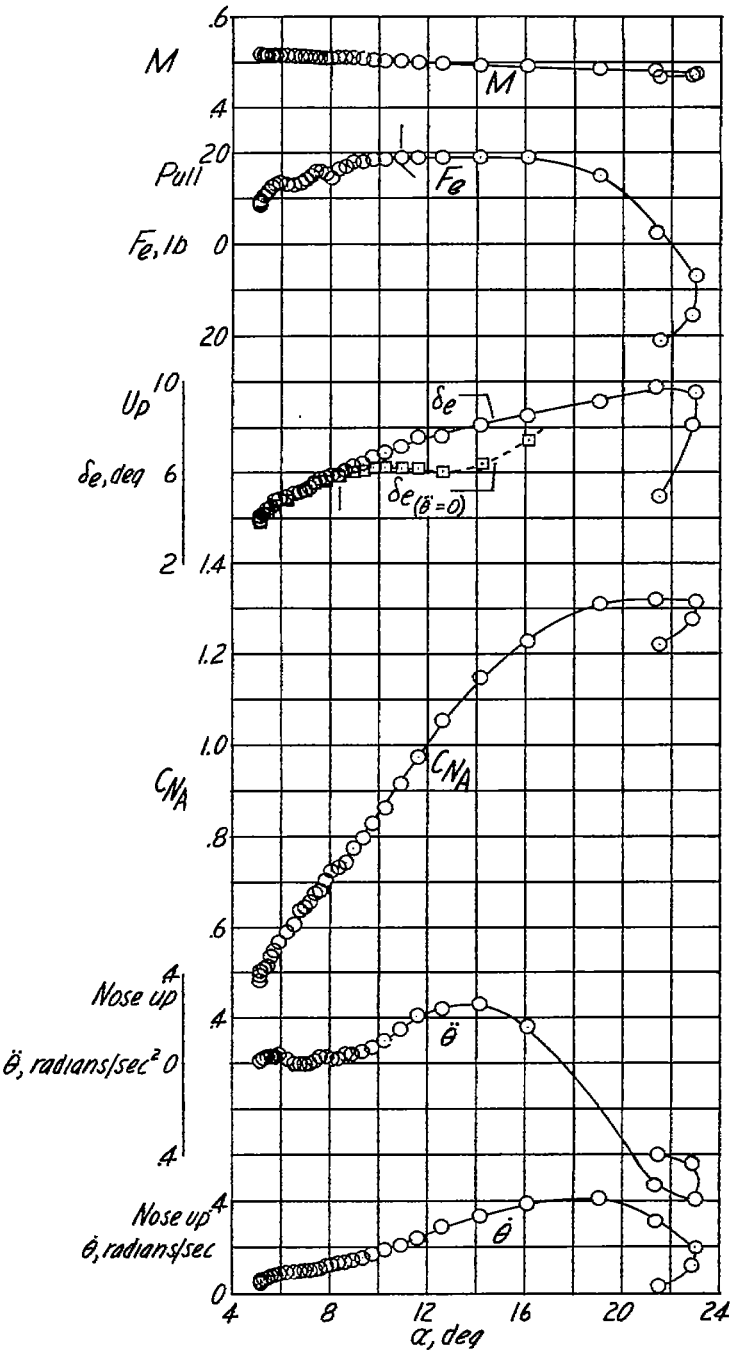

(c) $h_p \approx 16{,}500$ feet; $i_t = 1.3°$; center of gravity at 26.4 percent mean aerodynamic chord.

Figure 12.- Continued.

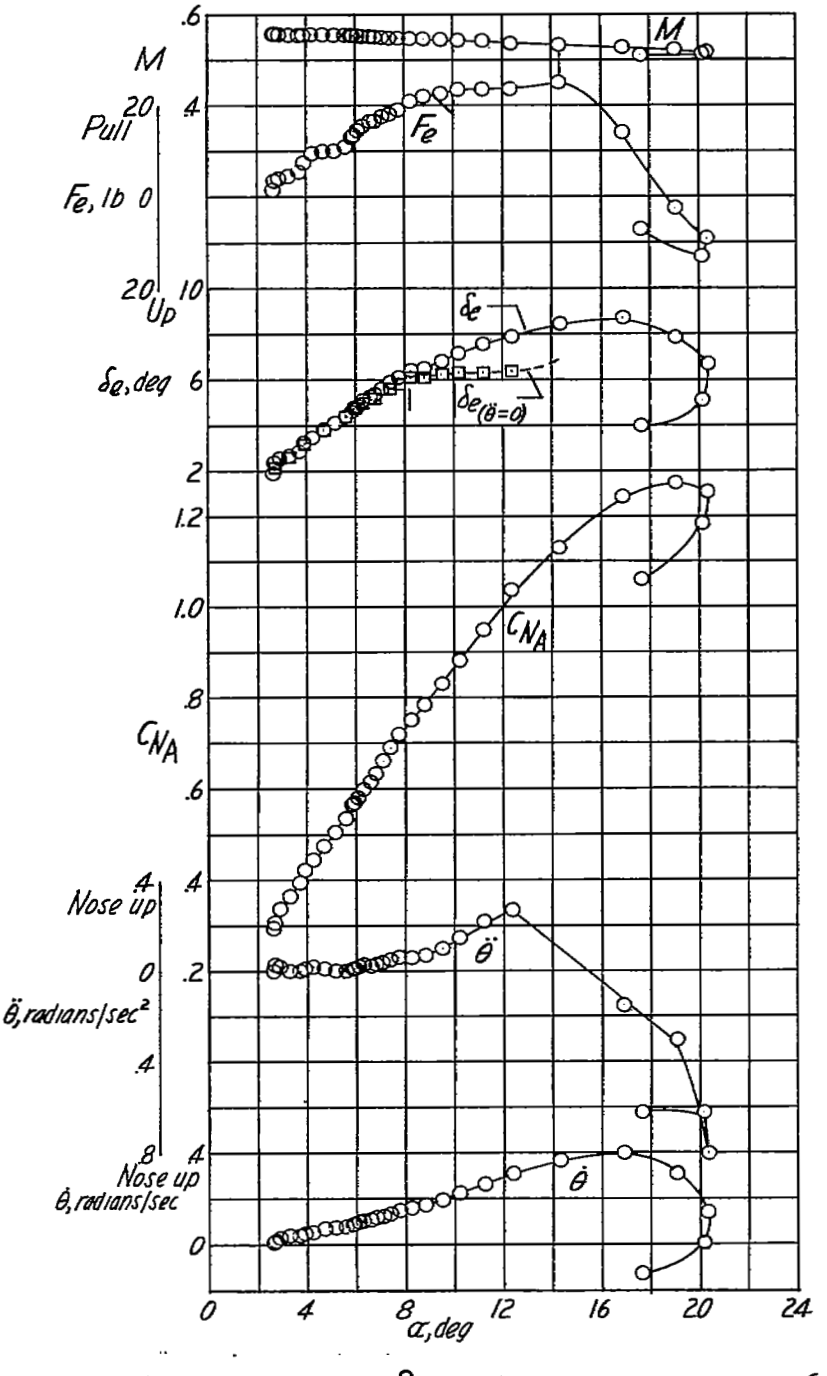

(d) $h_p \approx 17{,}200$ feet; $i_t = 1.3°$; center of gravity at 26.4 percent mean aerodynamic chord.

Figure 12.- Continued.

[redacted]

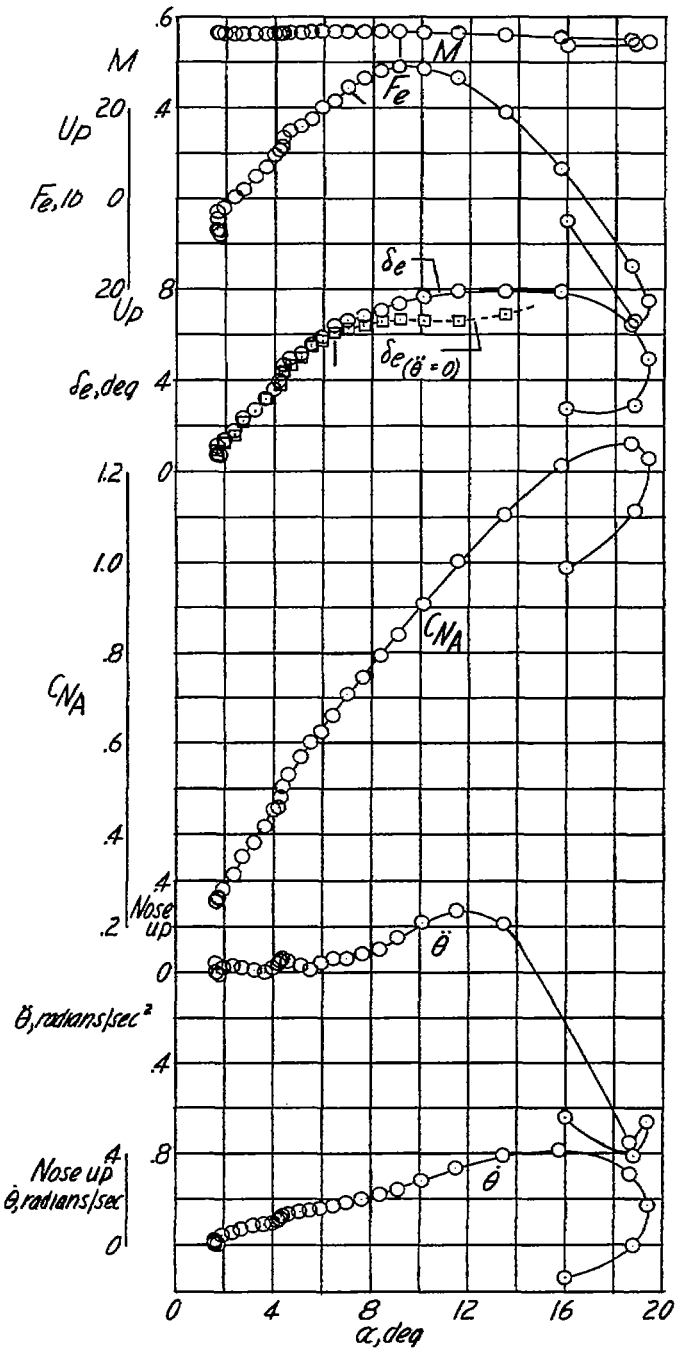

(e) $h_p \approx 16{,}000$ feet; $i_t = 1.3°$; center of gravity at 26.7 percent mean aerodynamic chord.

Figure 12.- Continued.

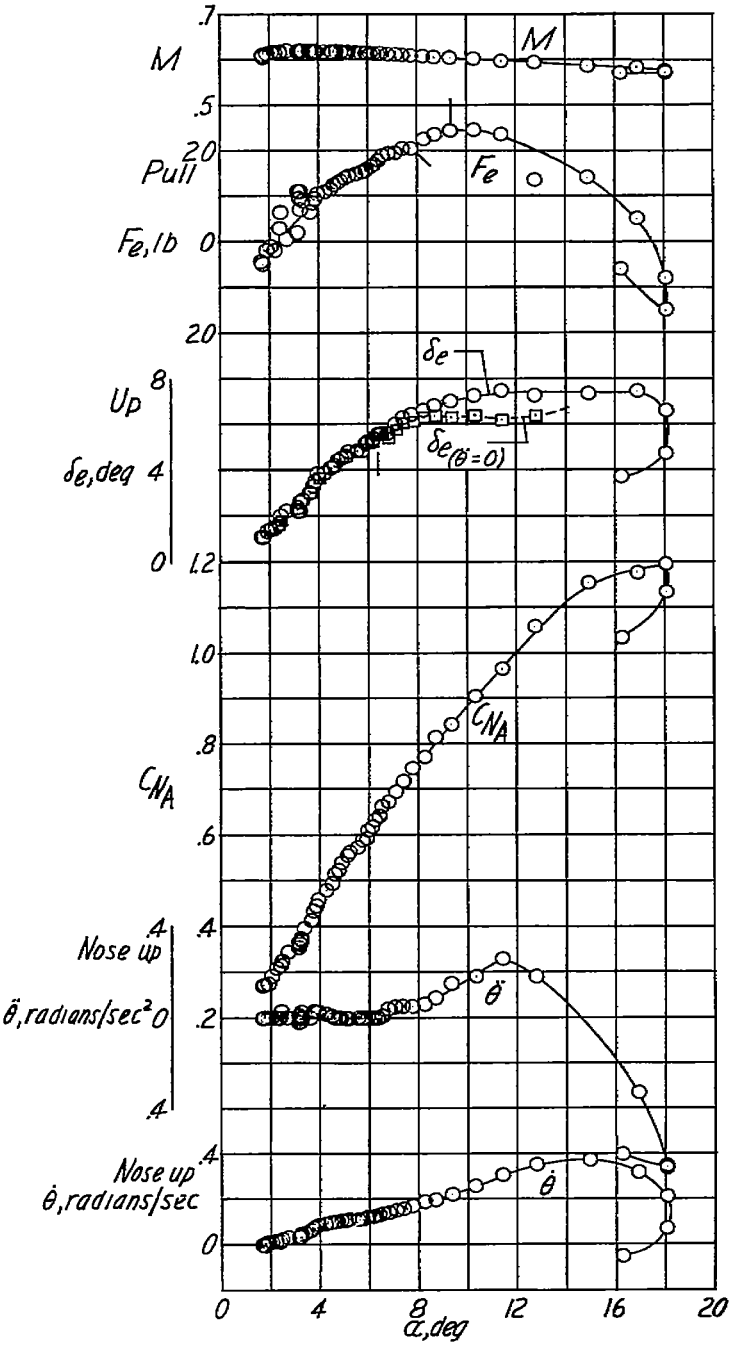

(f) $h_p \approx 18{,}000$ feet; $i_t = 1.3°$; center of gravity at 26.4 percent mean aerodynamic chord.

Figure 12.- Continued.

[redacted]

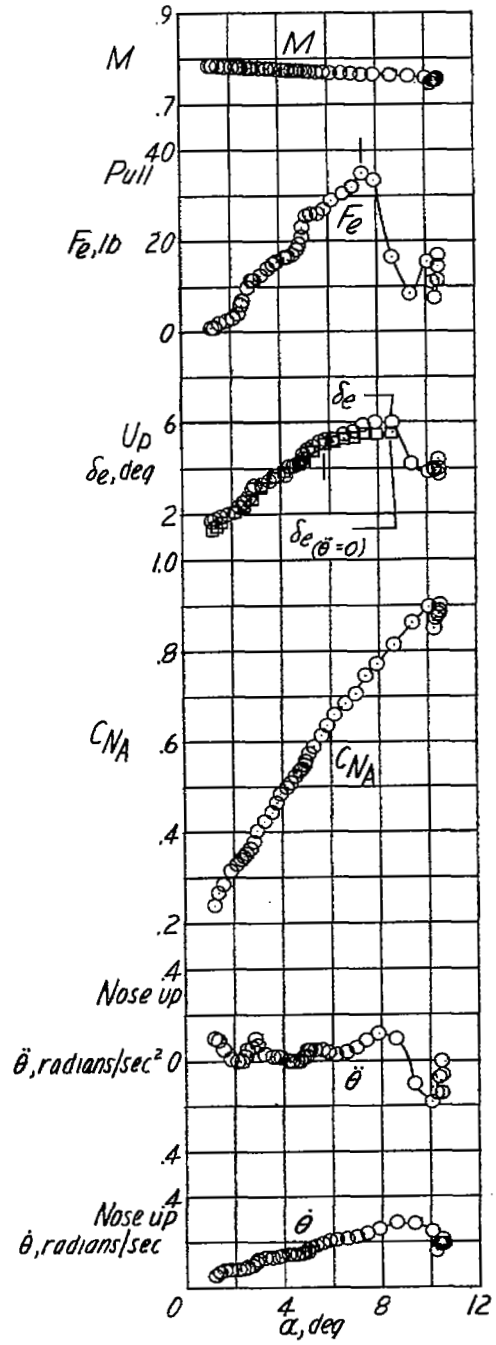

(g) $h_p \approx 19{,}000$ feet; $i_t = 1.3°$; center of gravity at 26.2 percent mean aerodynamic chord.

Figure 12.- Continued.

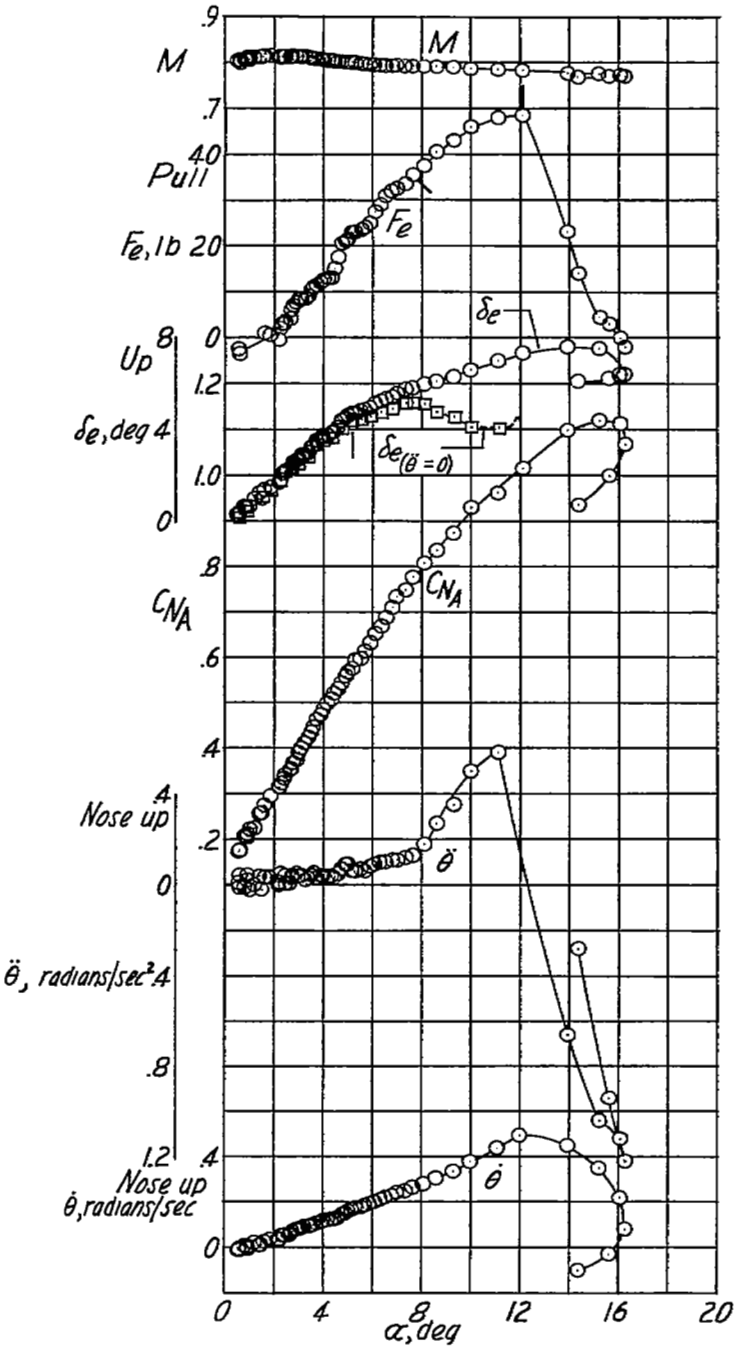

(h) $h_p \approx 23{,}000$ feet; $i_t = 1.3^\circ$; center of gravity at 26.2 percent mean aerodynamic chord.

Figure 12.- Continued.

[redacted]

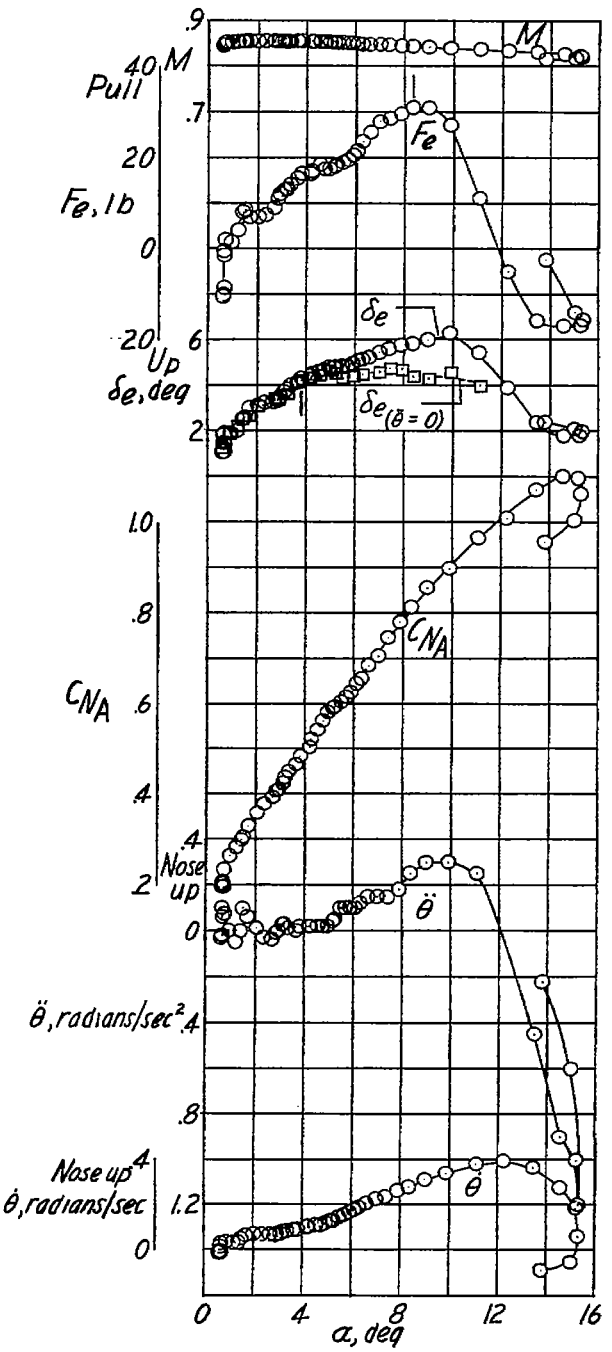

(i) $h_p \approx 27{,}300$ feet; $i_t = 1.3°$; center of gravity at 26.6 percent mean aerodynamic chord.

Figure 12.- Continued.

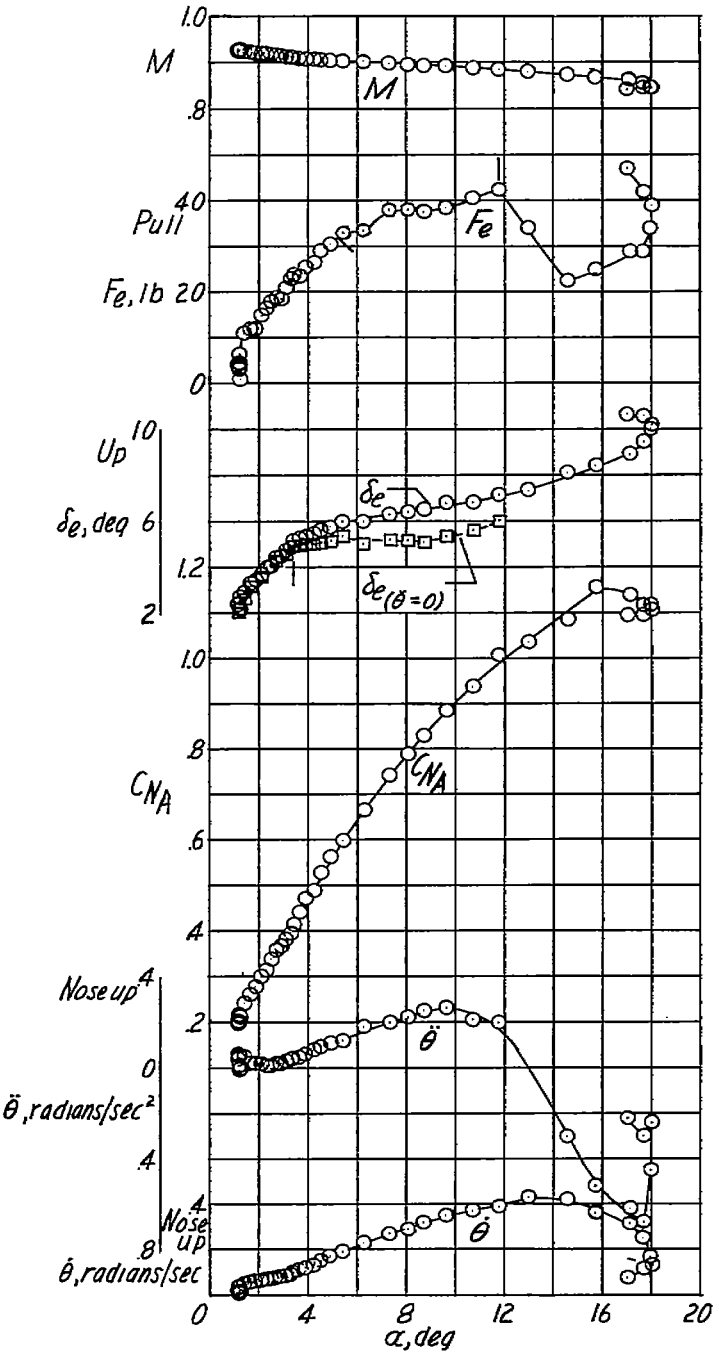

(j) $h_p \approx 27{,}000$ feet; $i_t = 1.3°$; center of gravity at 26.5 percent mean aerodynamic chord.

Figure 12.- Continued.

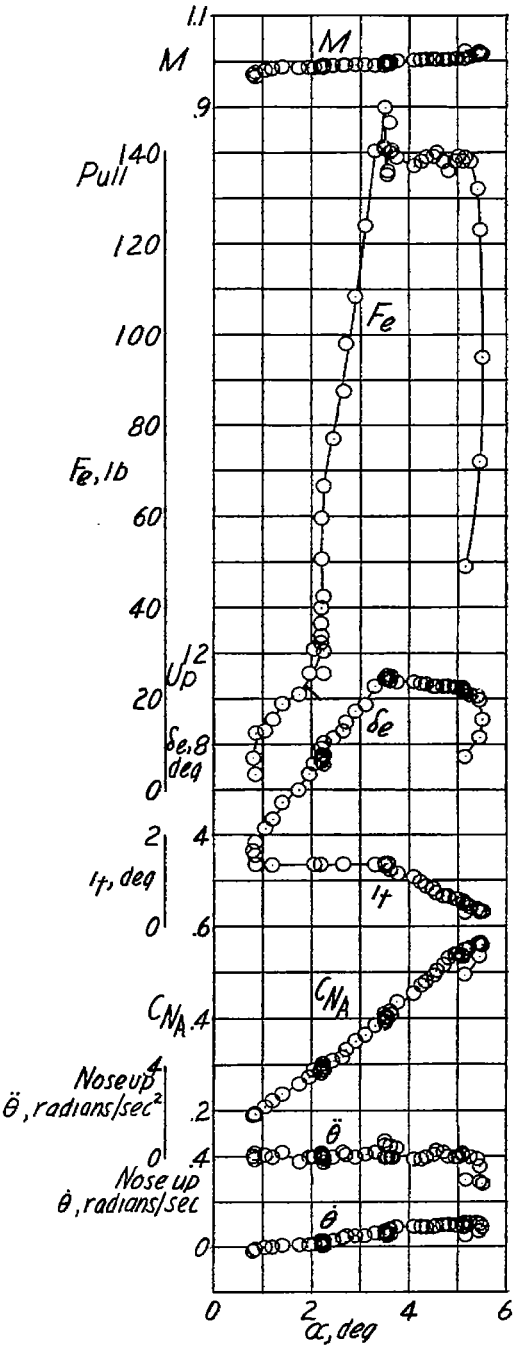

(k) $h_p \approx 33{,}000$ feet; center of gravity at 26.3 percent mean aerodynamic chord.

Figure 12.- Concluded.

[redacted]

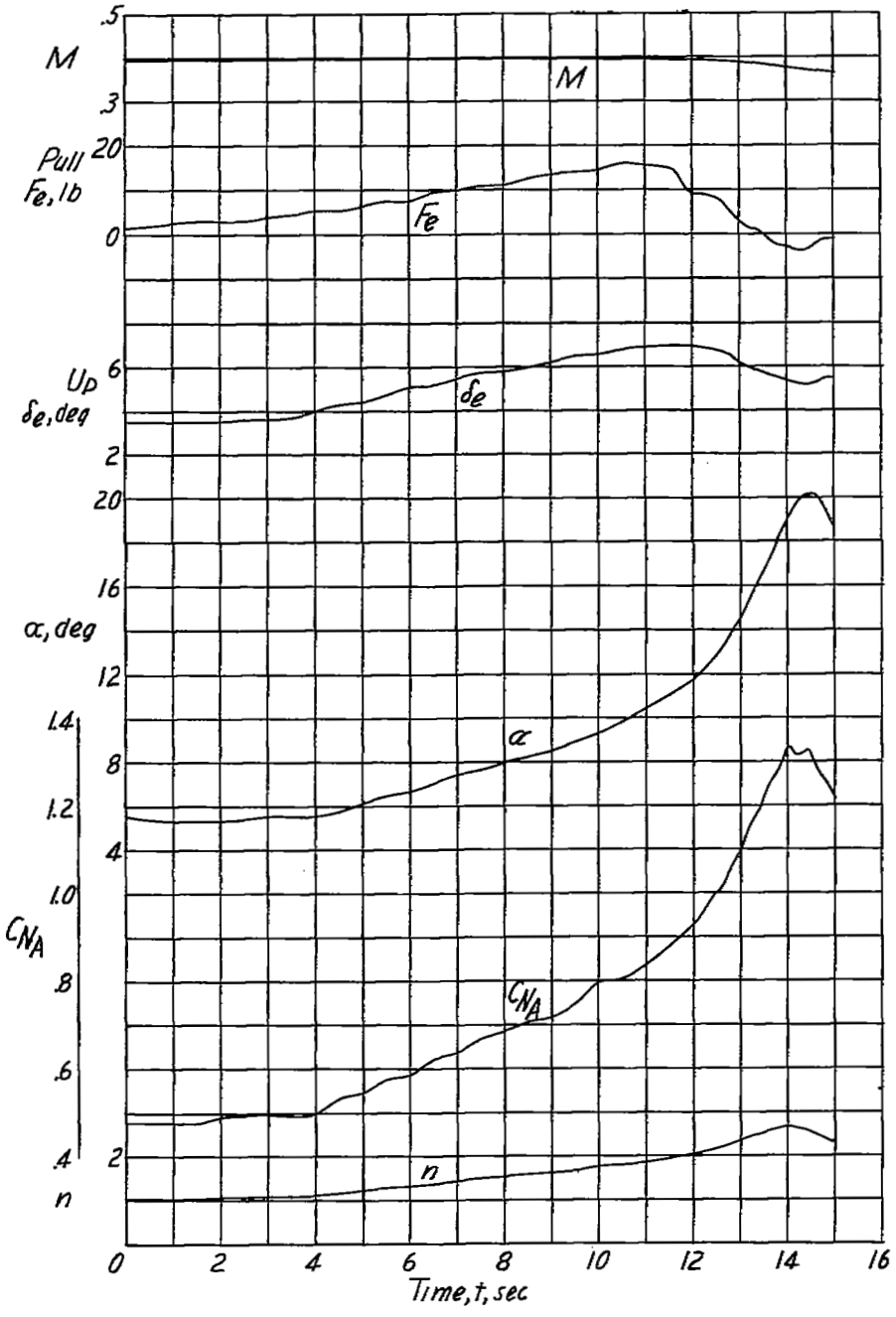

(a) $h_p \approx 12{,}700$ feet; $i_t = 1.5°$; center of gravity at 26.6 percent mean aerodynamic chord.

Figure 13.- Time histories of wind-up turns with the Douglas D-558-II research airplane with slats fully extended, inboard wing fences removed, and a stiff bungee installed on the control column.

[redacted]

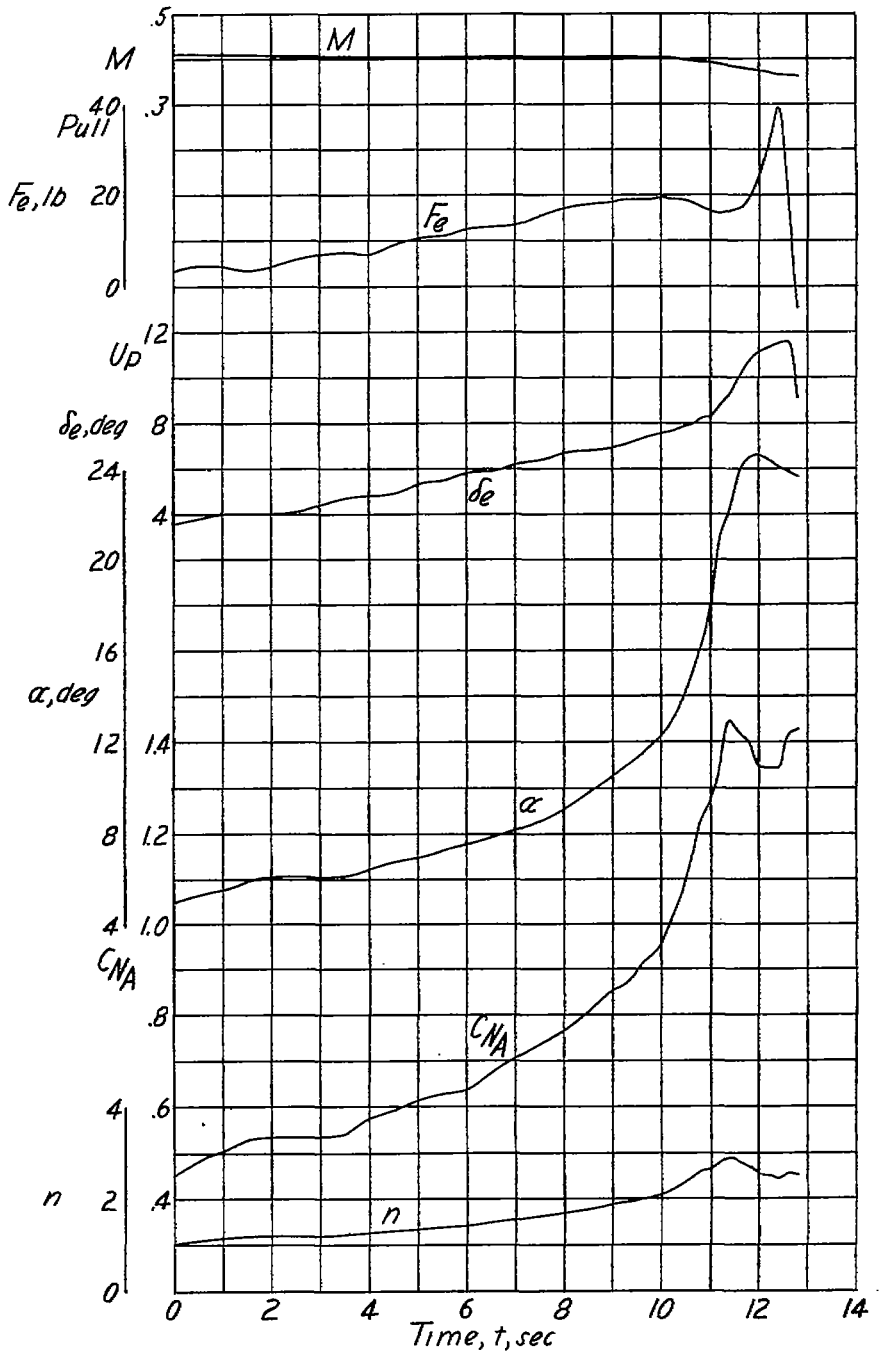

(b) $h_p \approx 13{,}600$ feet; $i_t = 1.5^\circ$; center of gravity at 26.6 percent mean aerodynamic chord.

Figure 13.- Continued.

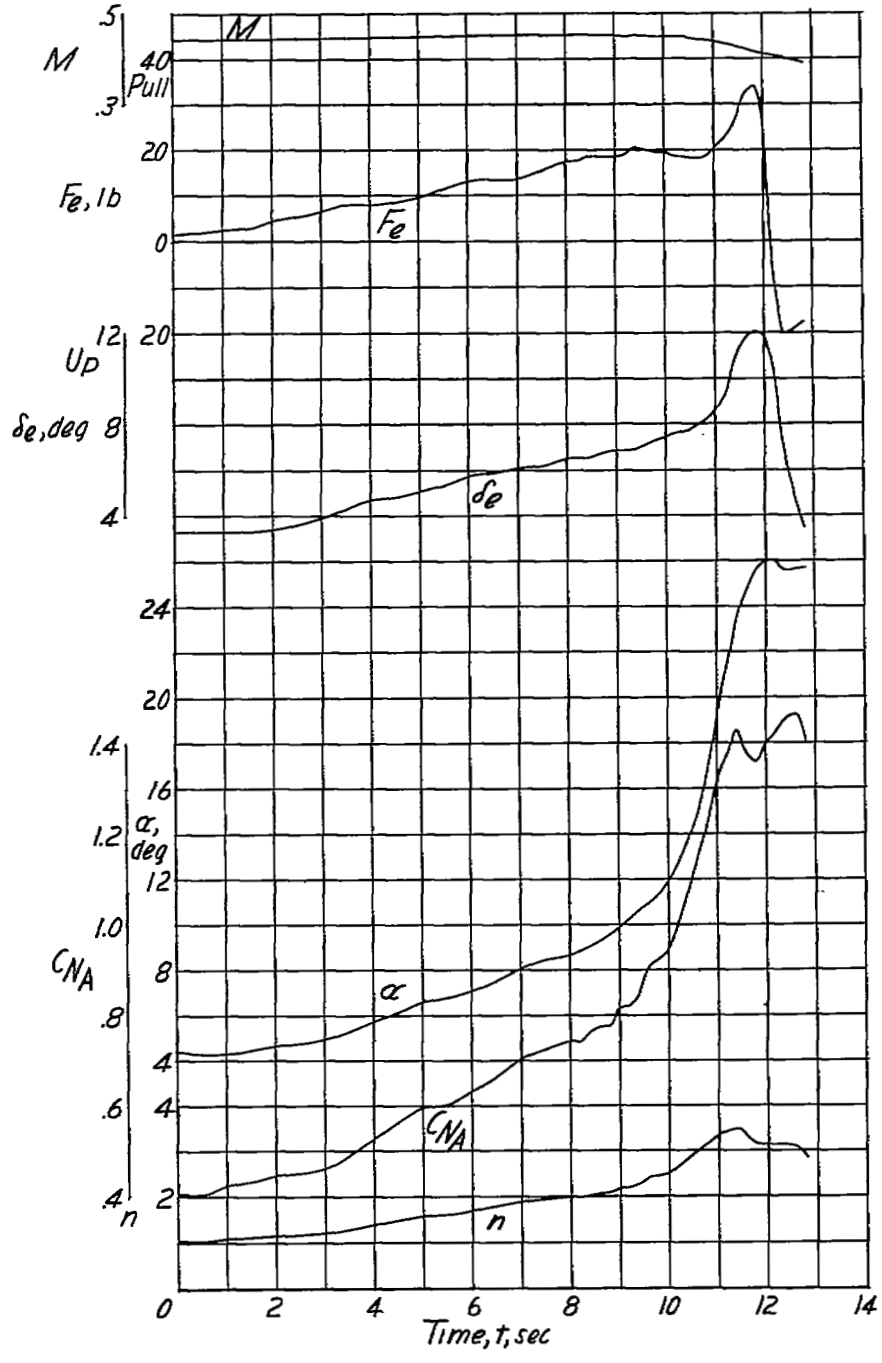

(c) $h_p \approx 14{,}200$ feet; $i_t = 1.5°$; center of gravity at 26.5 percent mean aerodynamic chord.

Figure 13.- Continued.

[redacted]

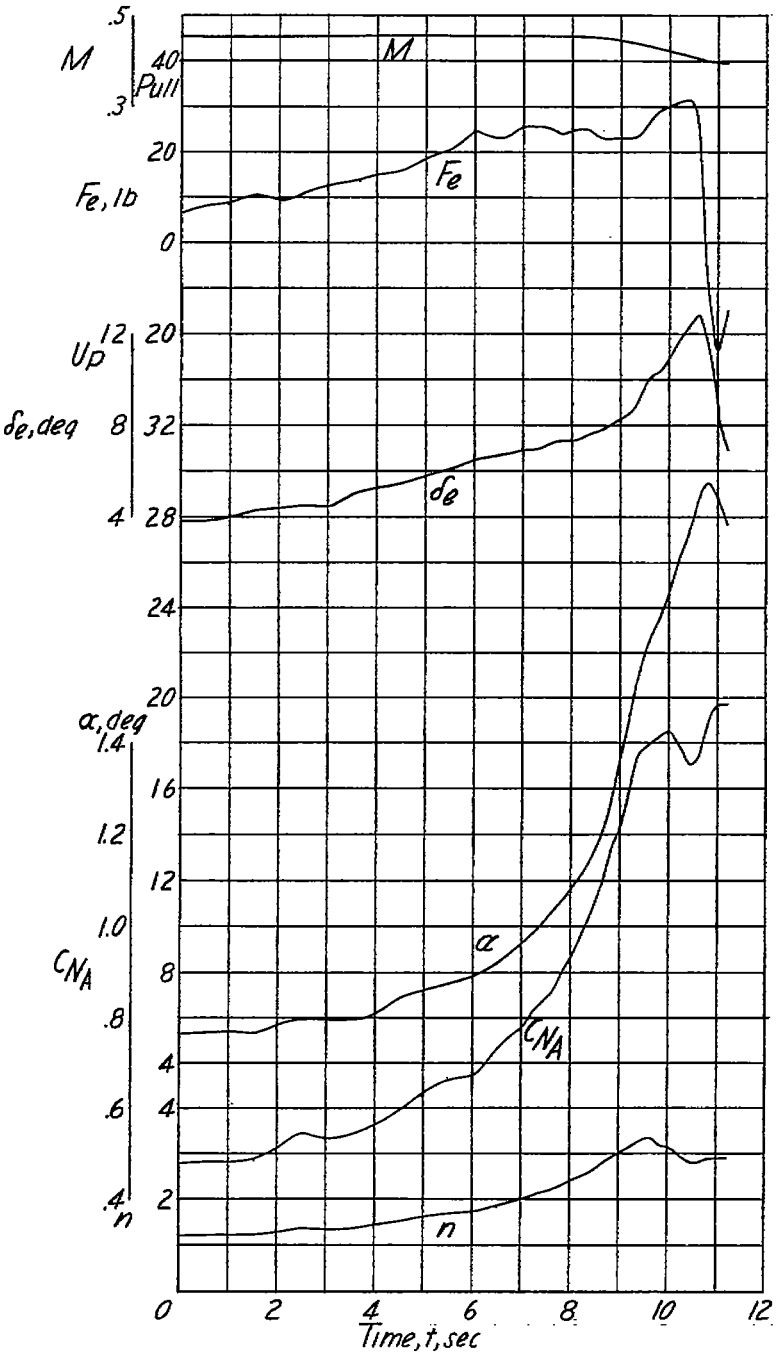

(d) $h_p \approx 15{,}500$ feet; $i_t = 1.5^\circ$; center of gravity at 26.5 percent mean aerodynamic chord.

Figure 13.- Continued.

[redacted]

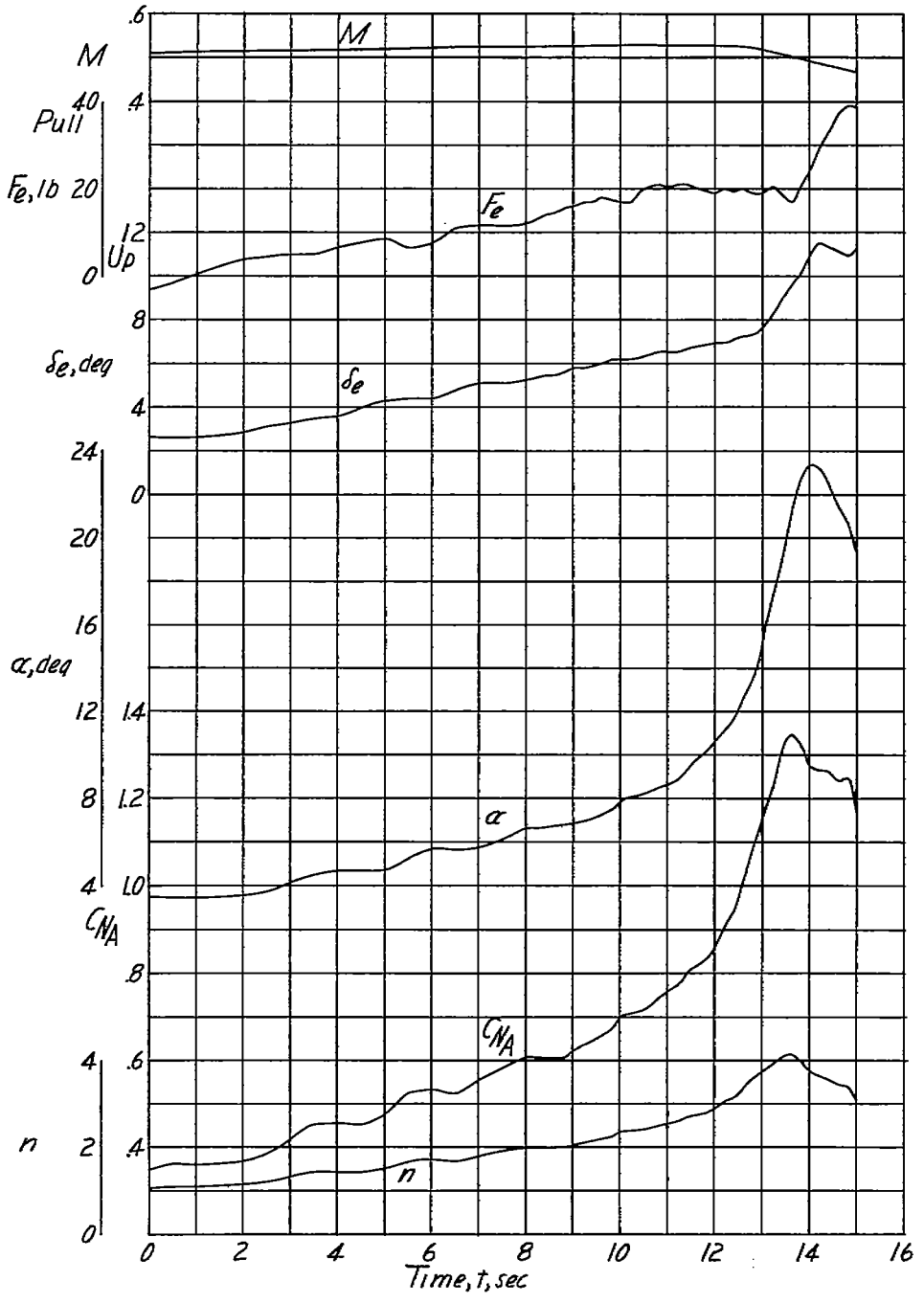

(e) $h_p \approx 16{,}500$ feet; $i_t = 1.5°$; center of gravity at 26.5 percent mean aerodynamic chord.

Figure 13.- Continued.

[redacted]

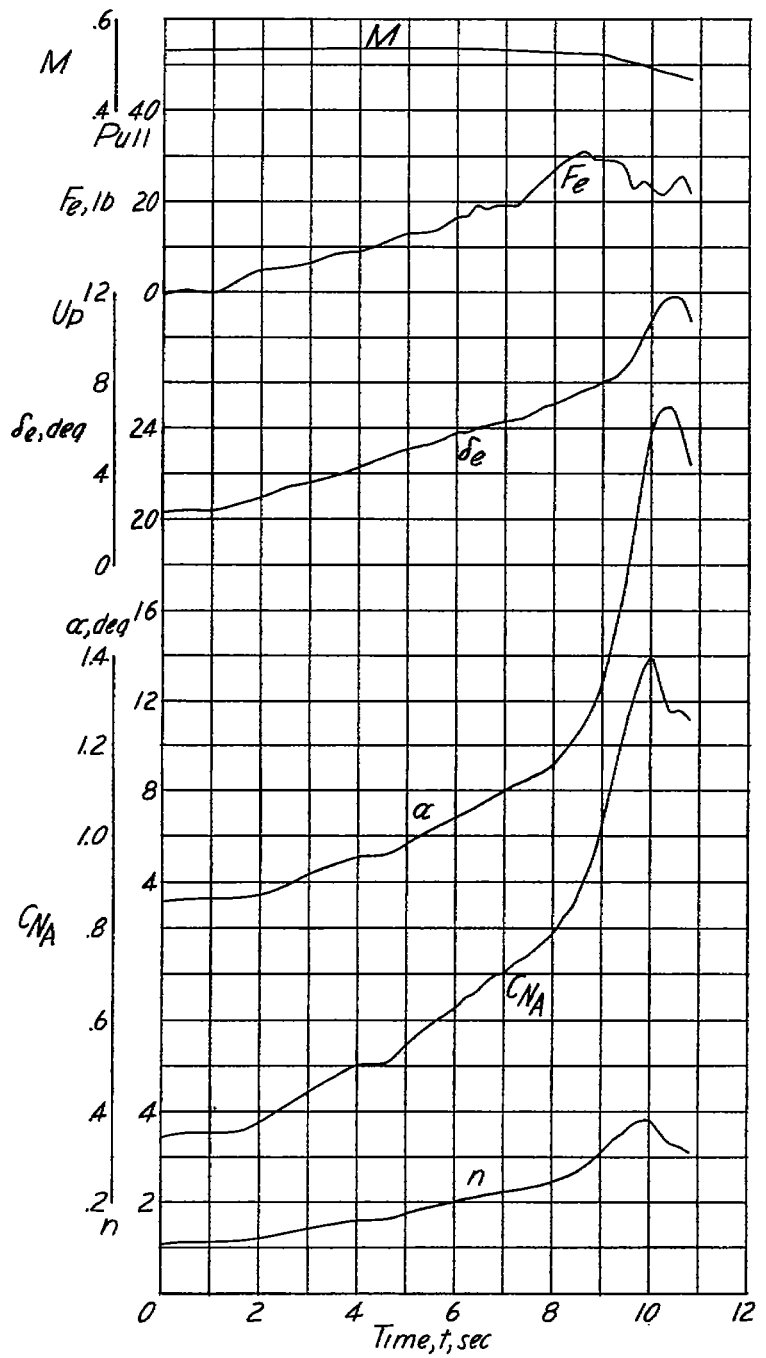

(f) $h_p \approx 18{,}000$ feet; $i_t = 1.5°$; center of gravity at 26.4 percent mean aerodynamic chord.

Figure 13.- Continued.

[redacted]

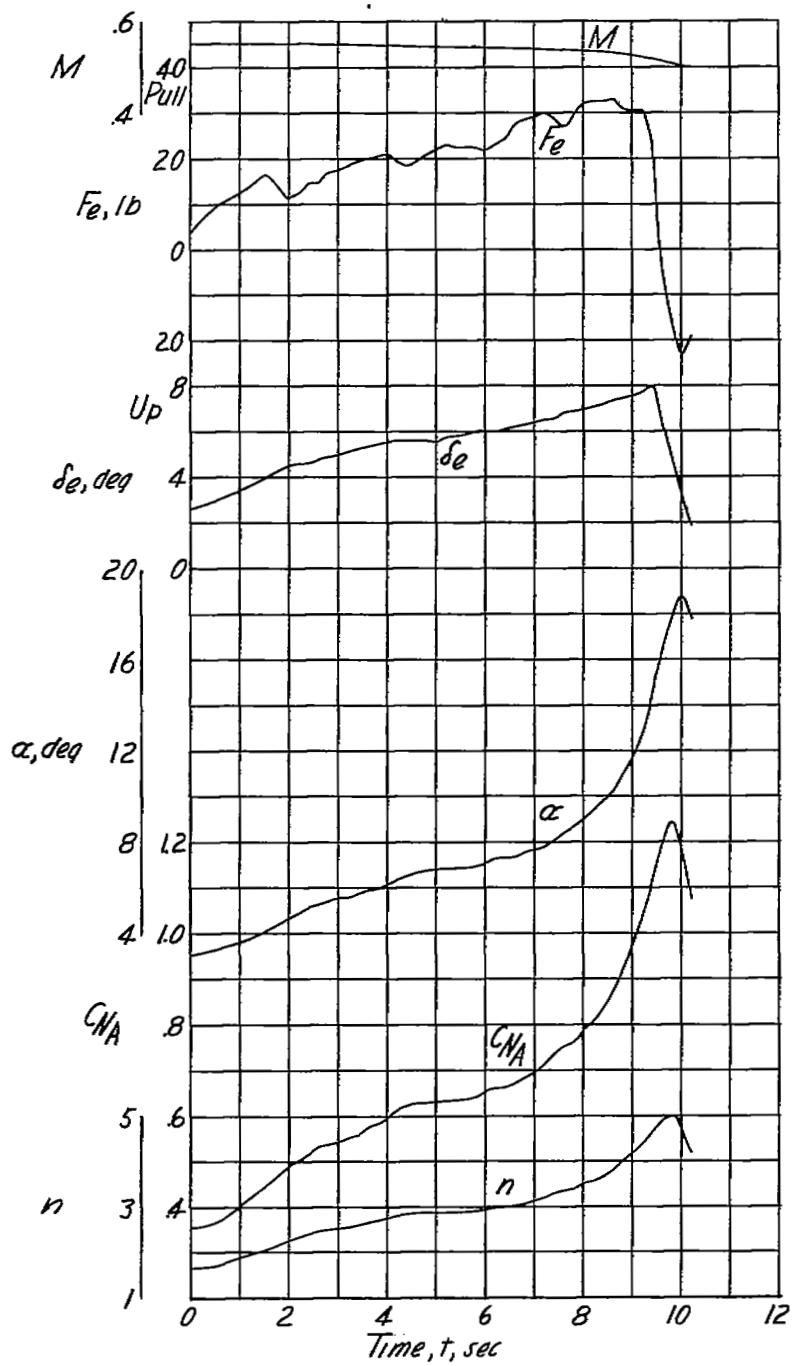

(g) $h_p \approx 10{,}800$ feet; $i_t = 1.5°$; center of gravity at 26.9 percent mean aerodynamic chord.

Figure 13.- Continued.

[redacted]

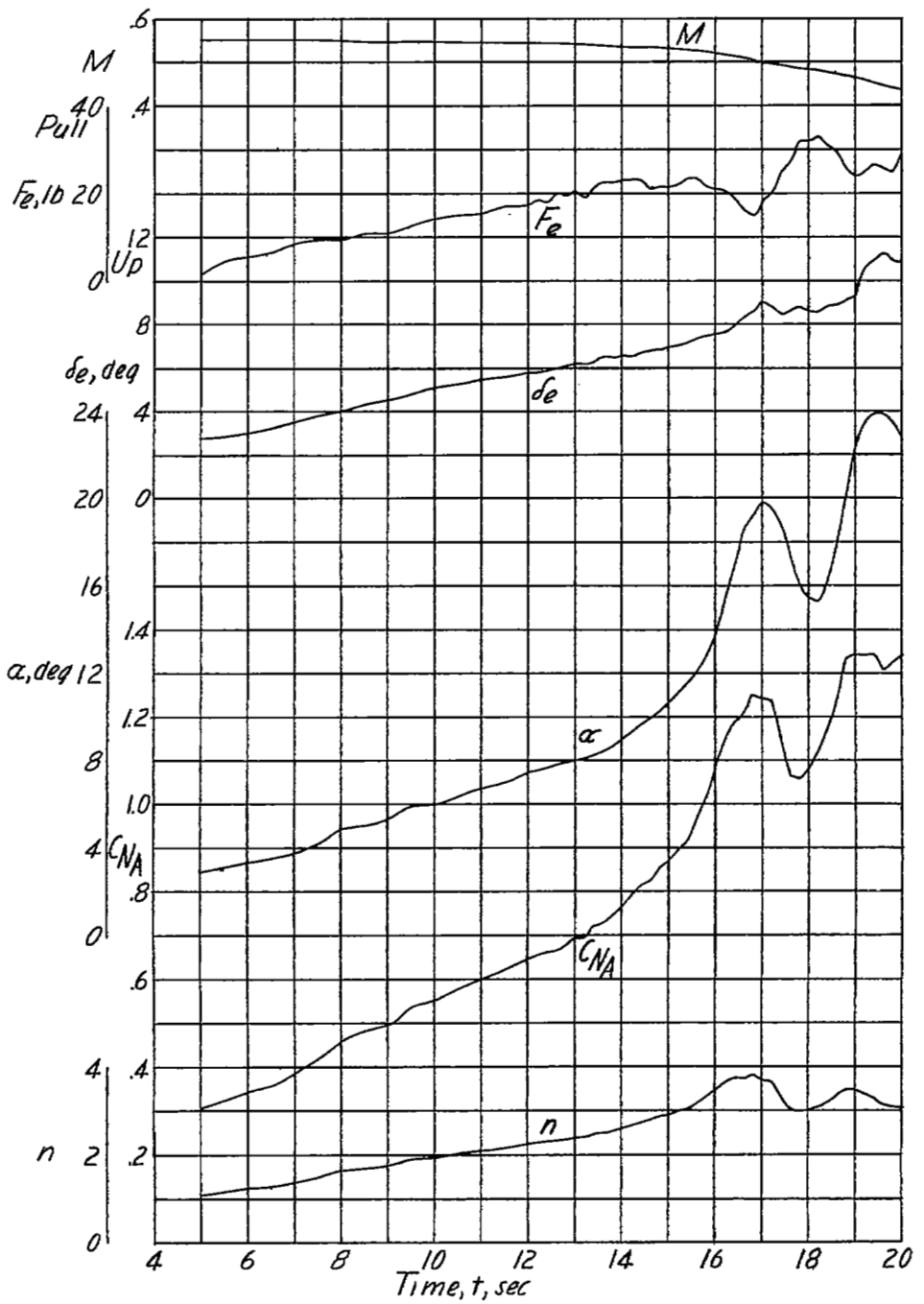

(h) $h_p \approx 16{,}100$ feet; $i_t = 1.6°$; center of gravity at 26.2 percent mean aerodynamic chord.

Figure 13.- Continued.

[redacted]

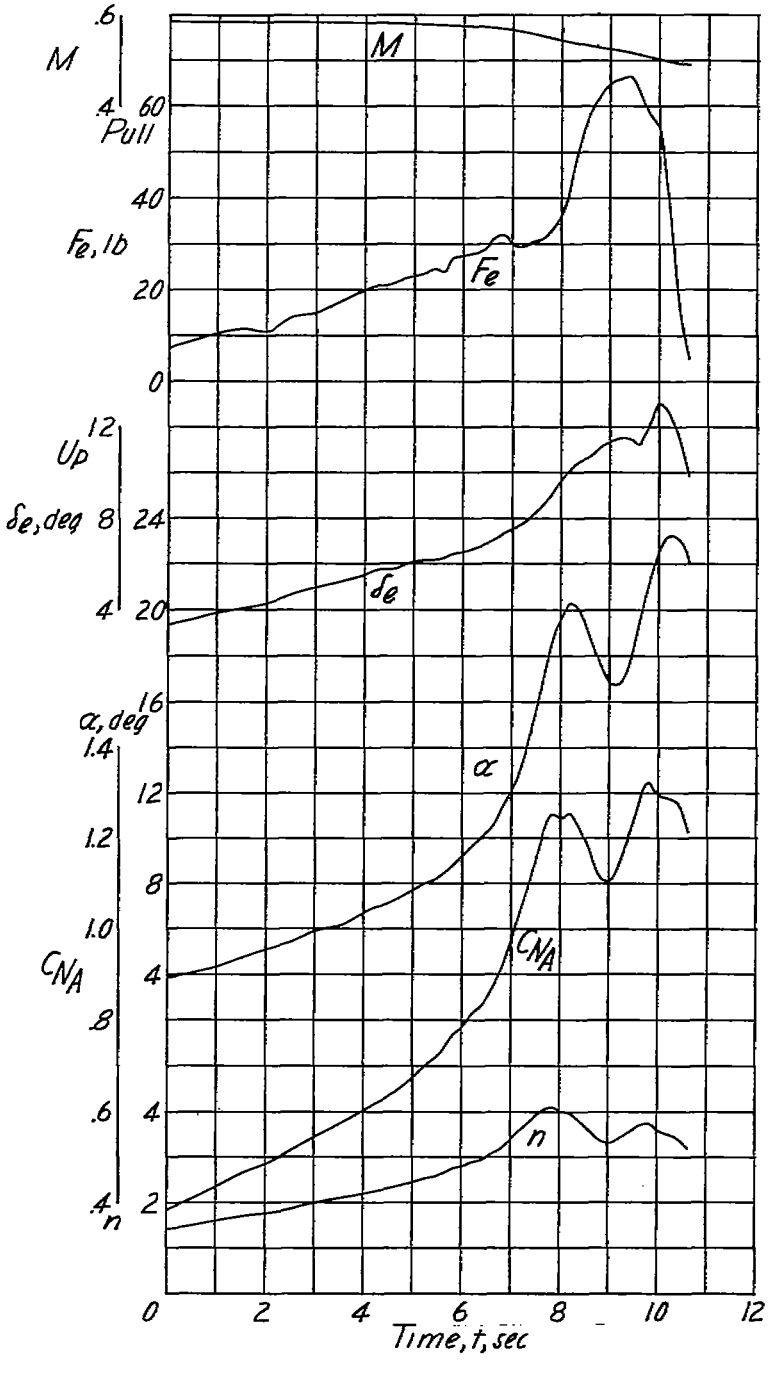

(i) $h_p \approx 18{,}300$ feet; $i_t = 1.6°$; center of gravity at 26.2 percent mean aerodynamic chord.

Figure 13.- Continued.

[redacted]

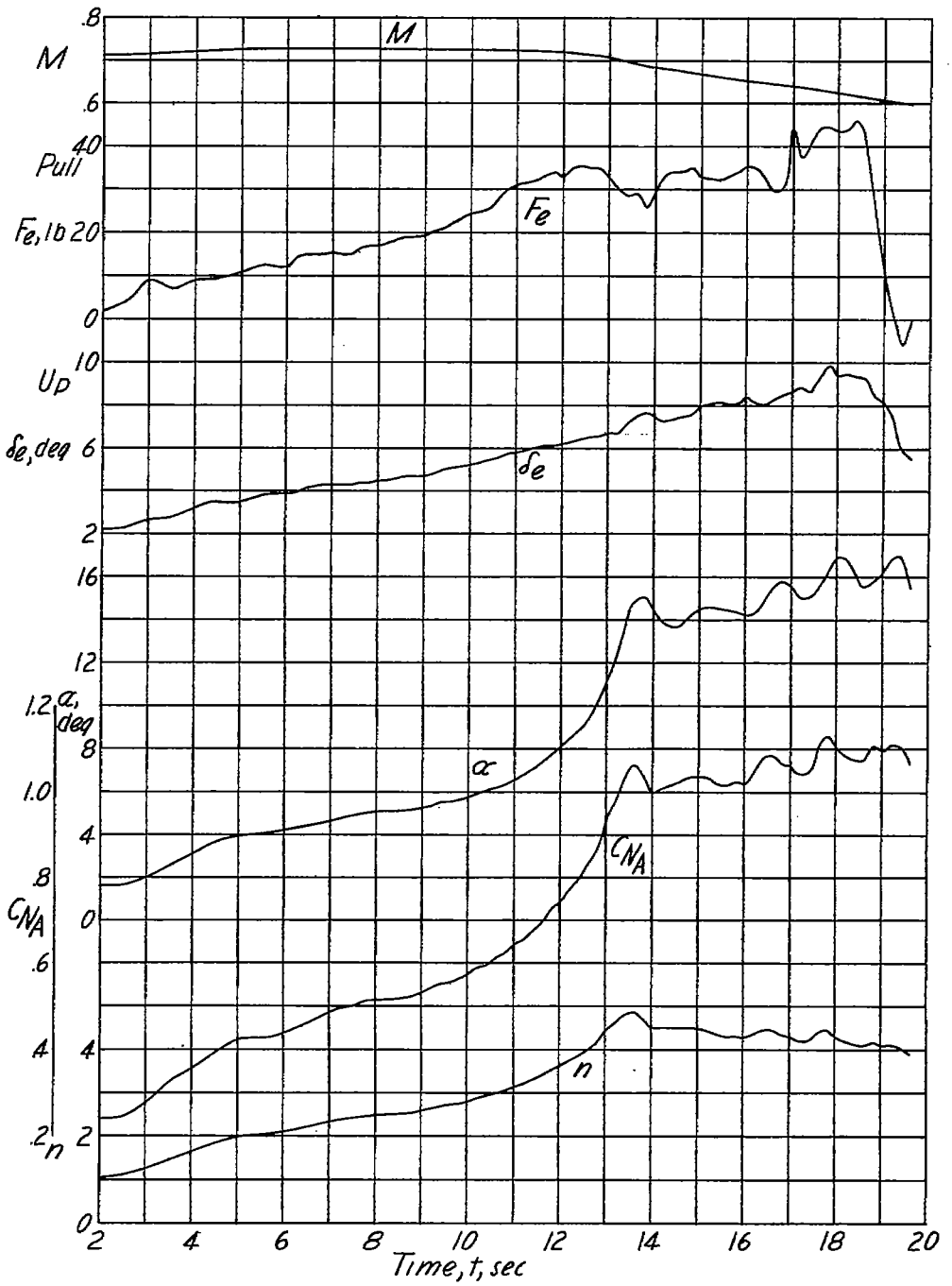

(j) $h_p \approx 22{,}000$ feet; $i_t = 1.6^\circ$; center of gravity at 26.1 percent mean aerodynamic chord.

Figure 13.- Continued.

[redacted]

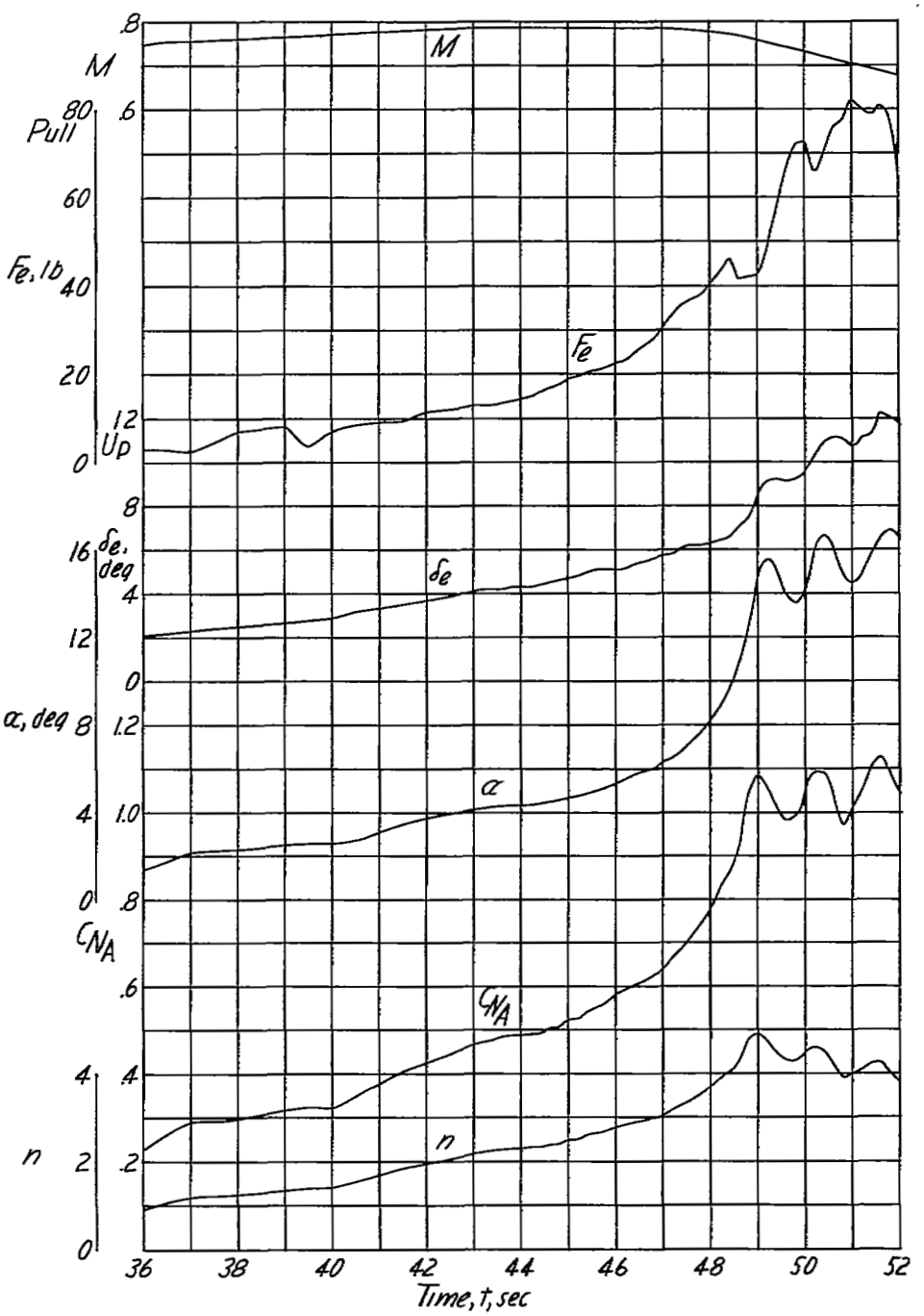

(k) $h_p \approx 26{,}500$ feet; $i_t = 1.6°$; center of gravity at 26.1 percent mean aerodynamic chord.

Figure 13.- Concluded.

[redacted]

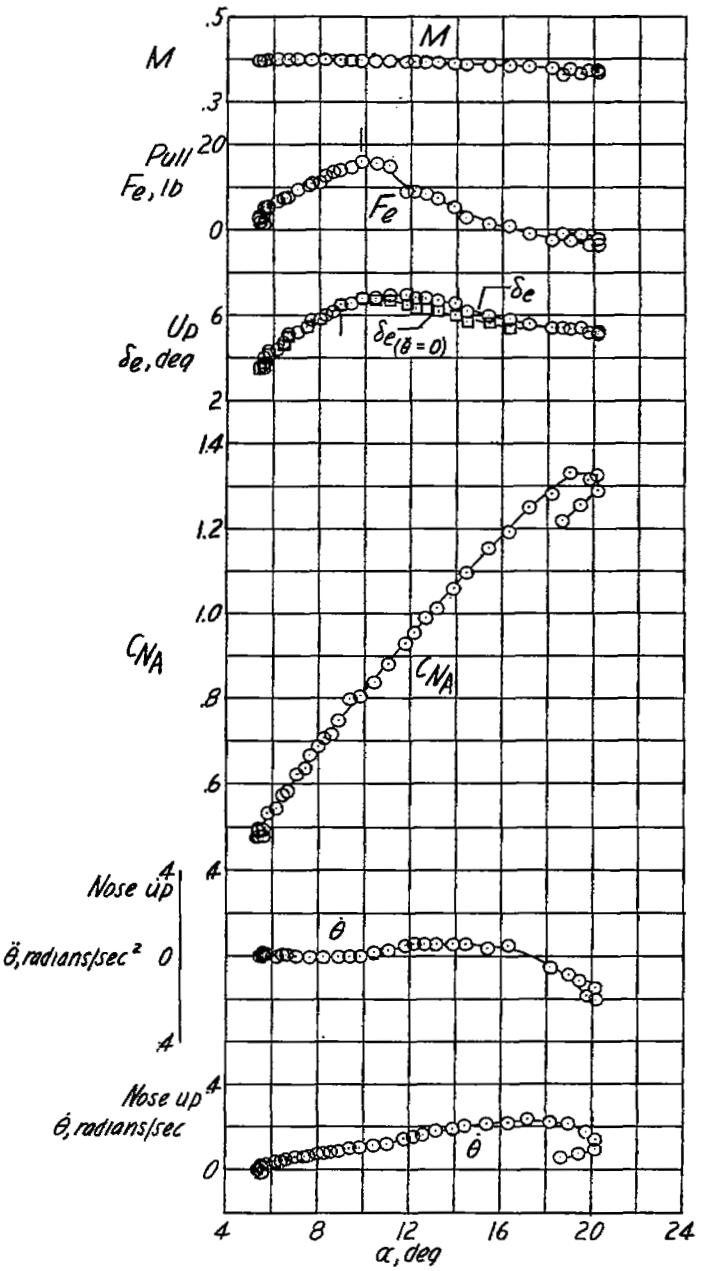

(a) $h_p \approx 12{,}700$ feet; $i_t = 1.5^\circ$; center of gravity at 26.6 percent mean aerodynamic chord.

Figure 14.- Static longitudinal stability characteristics of the Douglas D-558-II research airplane with slats fully extended, inboard wing fences removed, and a stiff bungee installed on the control column.

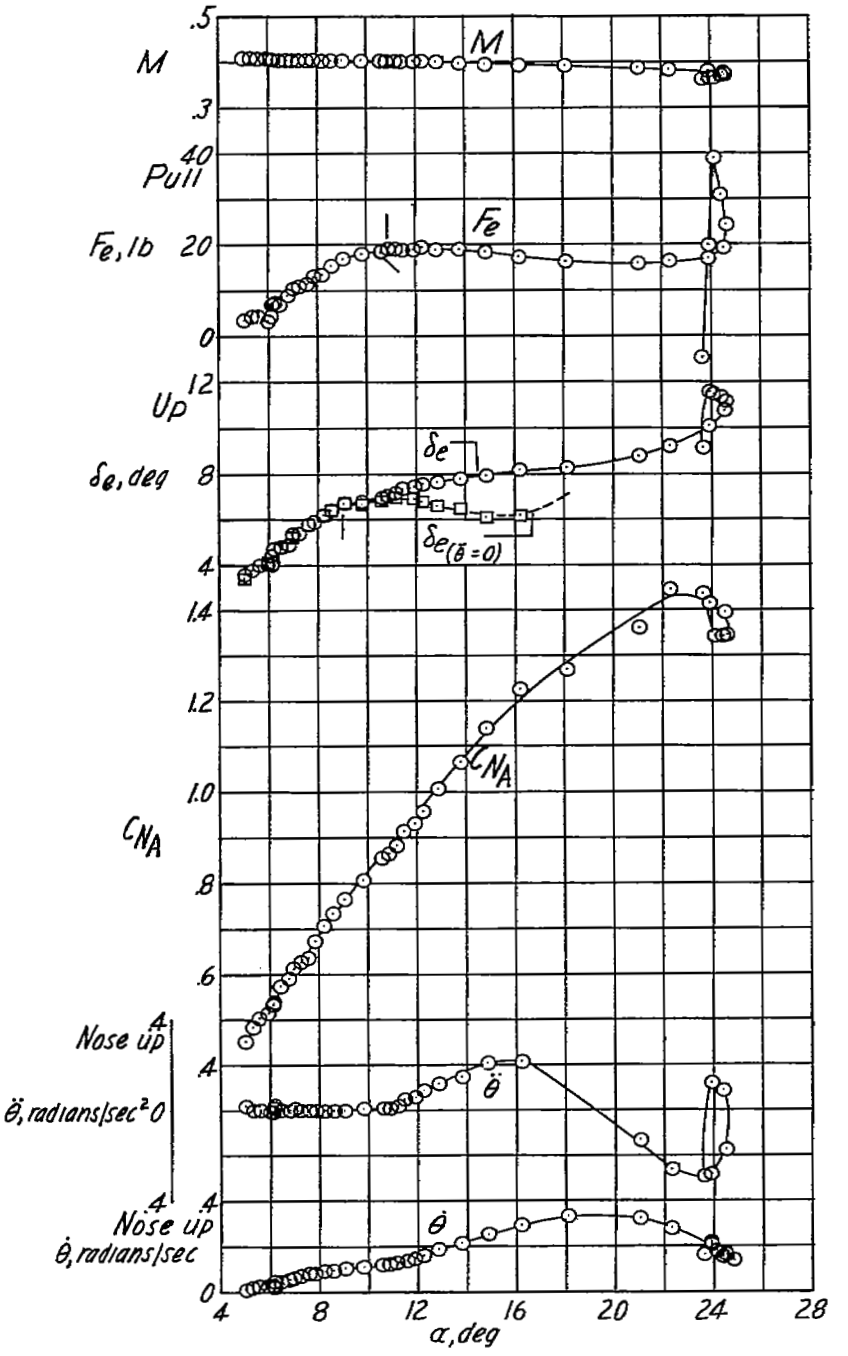

(b) $h_p \approx 13{,}600$ feet; $i_t = 1.5°$; center of gravity at 26.6 percent mean aerodynamic chord.

Figure 14.- Continued.

[redacted]

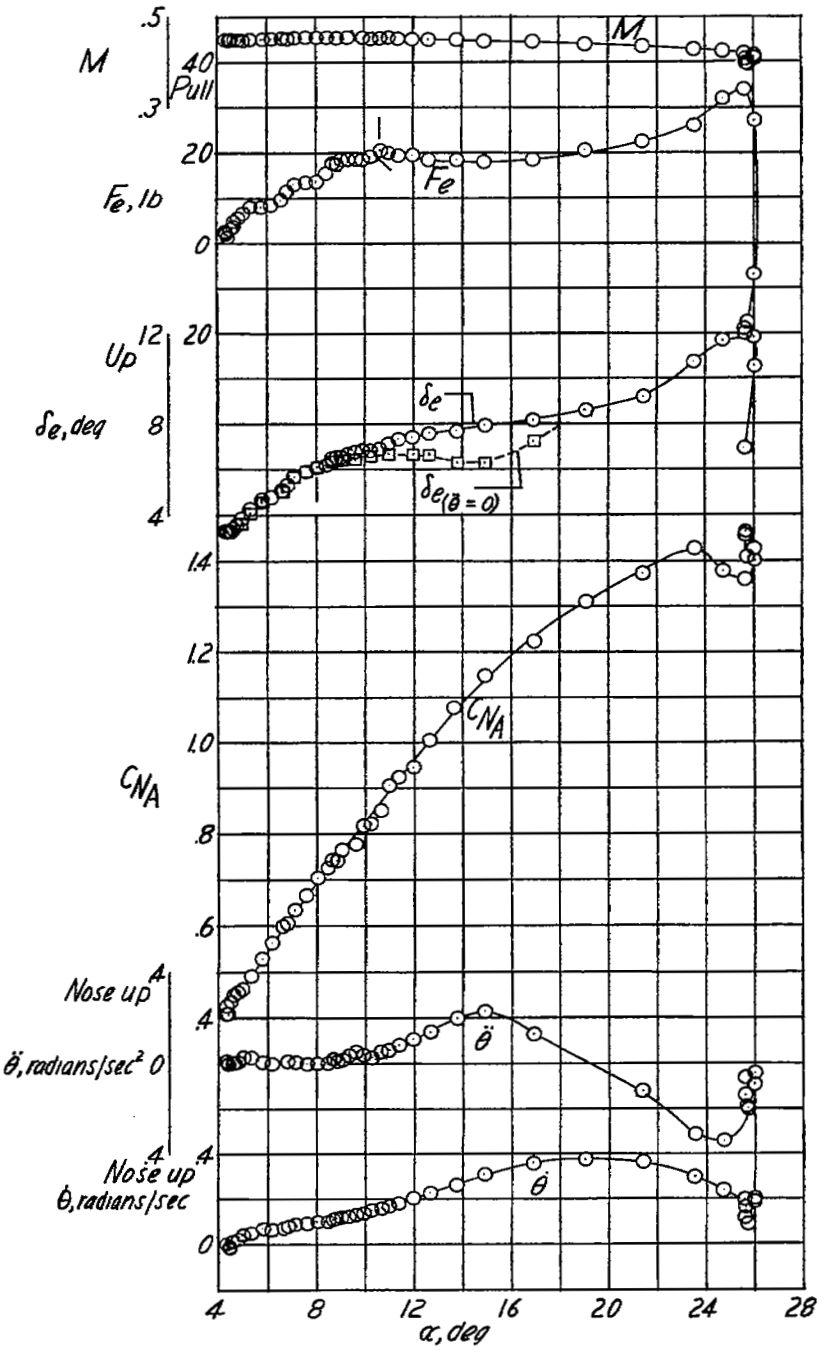

(c) $h_p \approx 14{,}200$ feet; $i_t = 1.5°$; center of gravity at 26.5 percent mean aerodynamic chord.

Figure 14.- Continued.

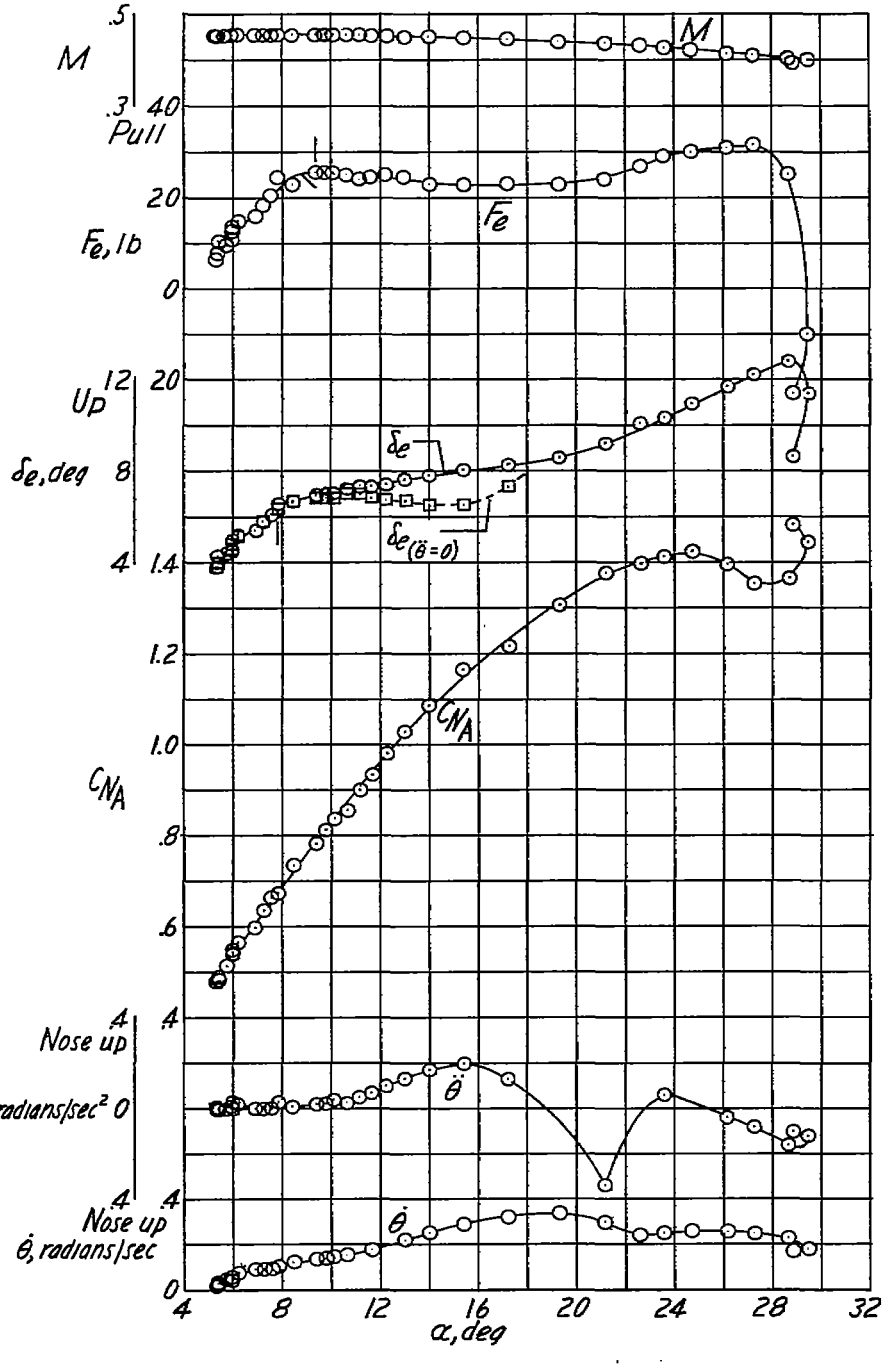

(d) $h_p \approx 15{,}500$ feet; $i_t = 1.5°$; center of gravity at 26.5 percent mean aerodynamic chord.

Figure 14.- Continued.

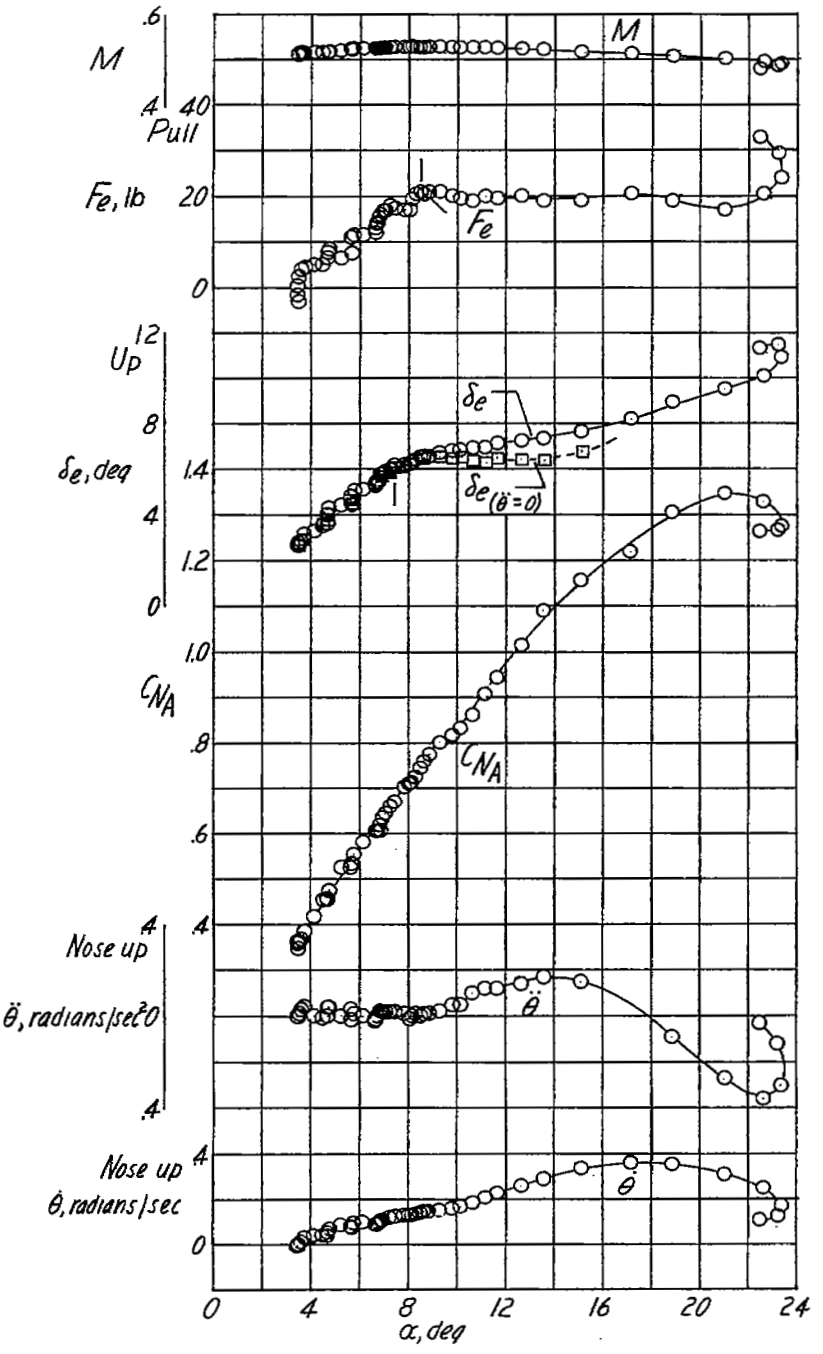

(e) $h_p \approx 16{,}500$ feet; $i_t = 1.5^\circ$; center of gravity at 26.5 percent mean aerodynamic chord.

Figure 14.- Continued.

[redacted]

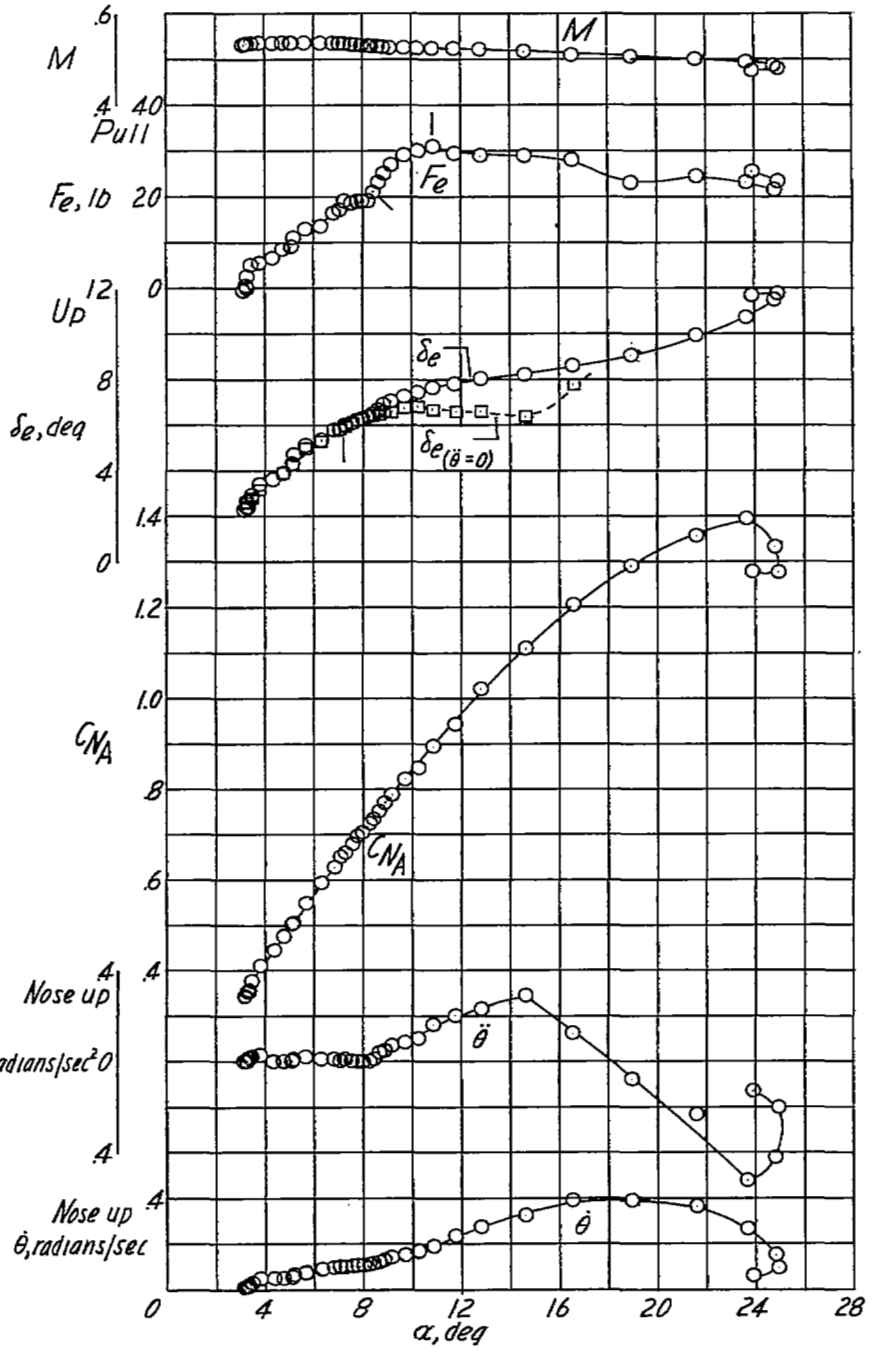

(f) $h_p \approx 18{,}000$ feet; $i_t = 1.5°$; center of gravity at 26.4 percent mean aerodynamic chord.

Figure 14.- Continued.

[redacted]

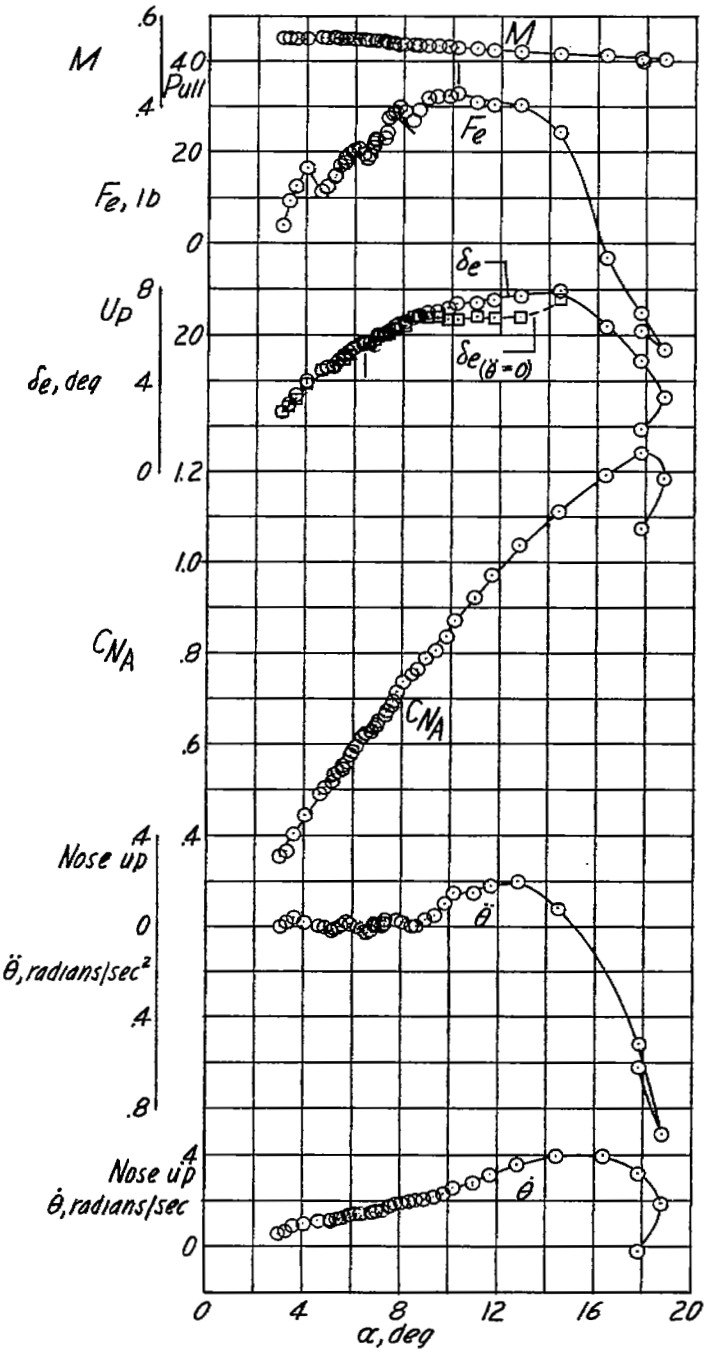

(g) $h_p \approx 10{,}800$ feet; $i_t = 1.5°$; center of gravity at 26.9 percent mean aerodynamic chord.

Figure 14.- Continued.

[redacted]

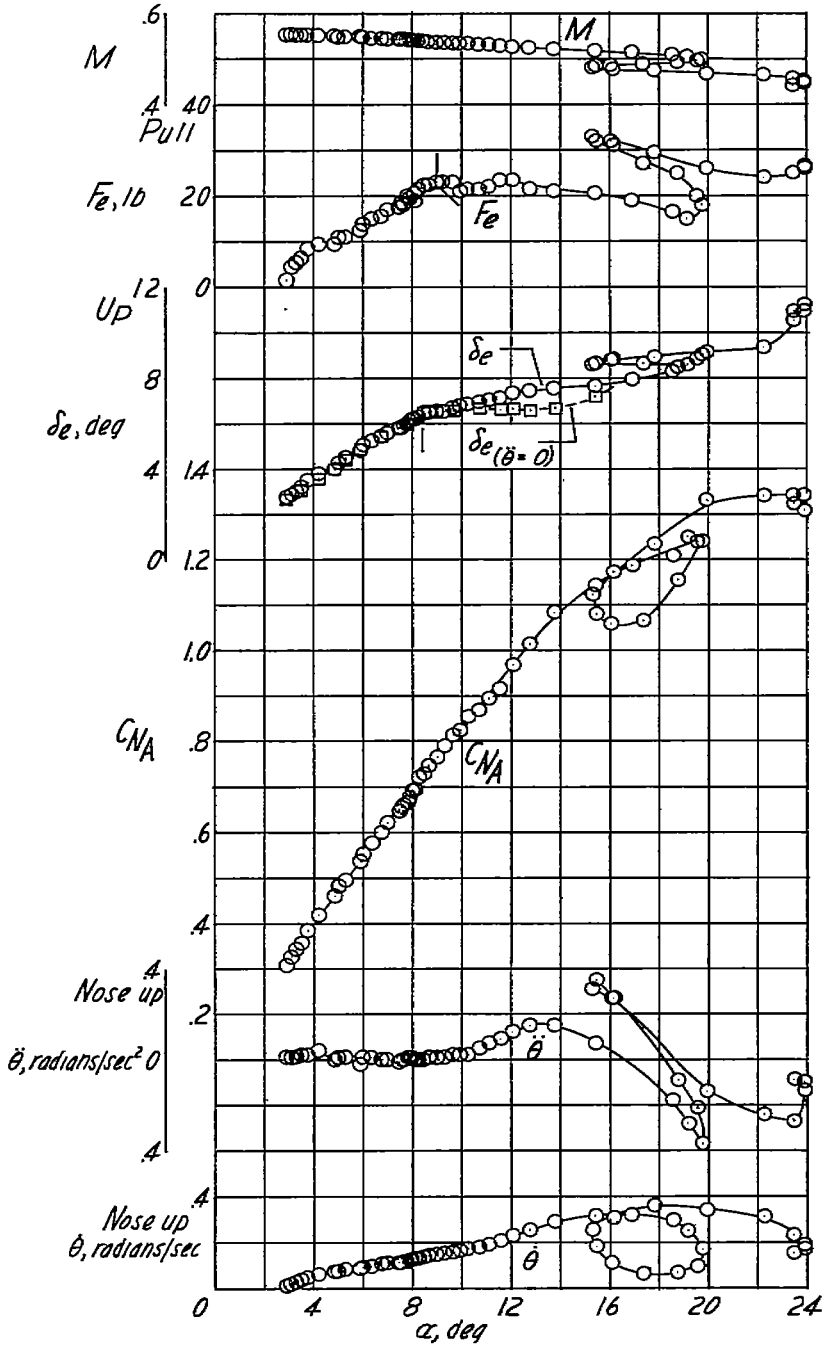

(h) $h_p \approx 16{,}100$ feet; $i_t = 1.6°$; center of gravity at 26.2 percent mean aerodynamic chord.

Figure 14.- Continued.

[redacted]

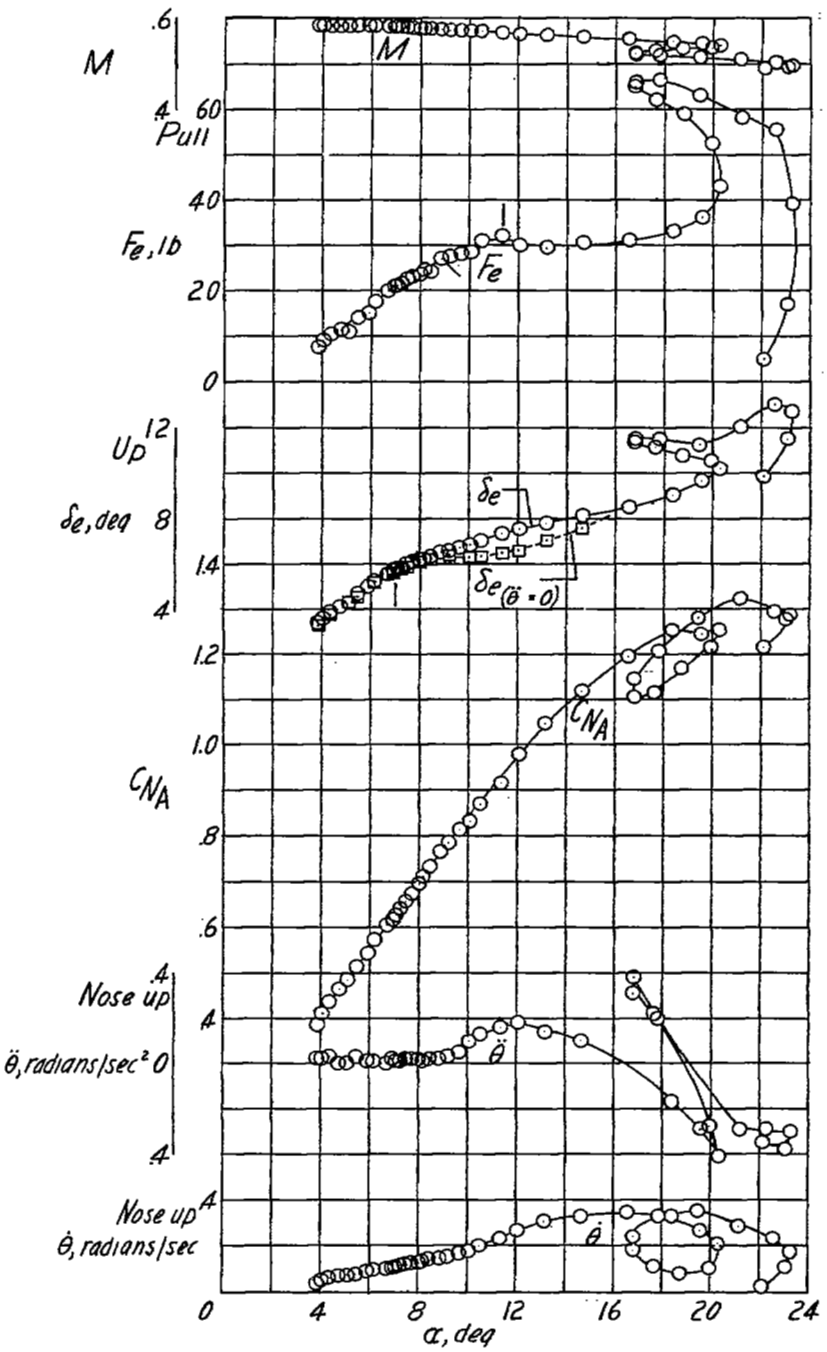

(i) $h_p \approx 18{,}300$ feet; $i_t = 1.6°$; center of gravity at 26.2 percent mean aerodynamic chord.

Figure 14.- Continued.

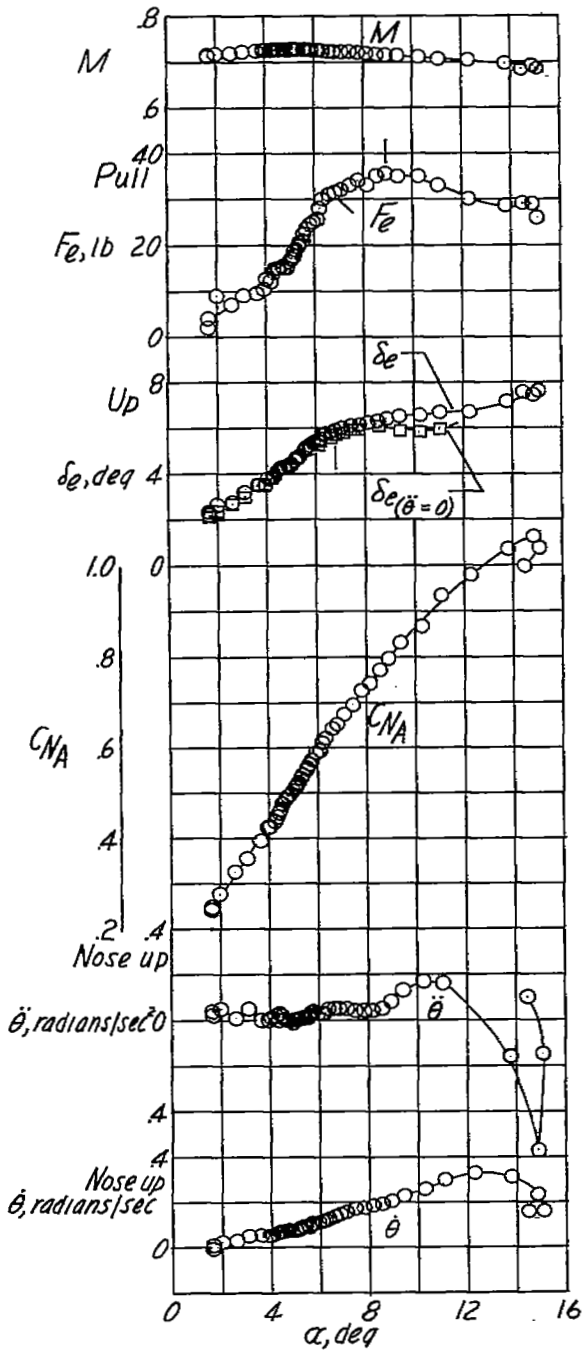

(j) $h_p \approx 22{,}000$ feet; $i_t = 1.6°$; center of gravity at 26.1 percent mean aerodynamic chord.

Figure 14.- Continued.

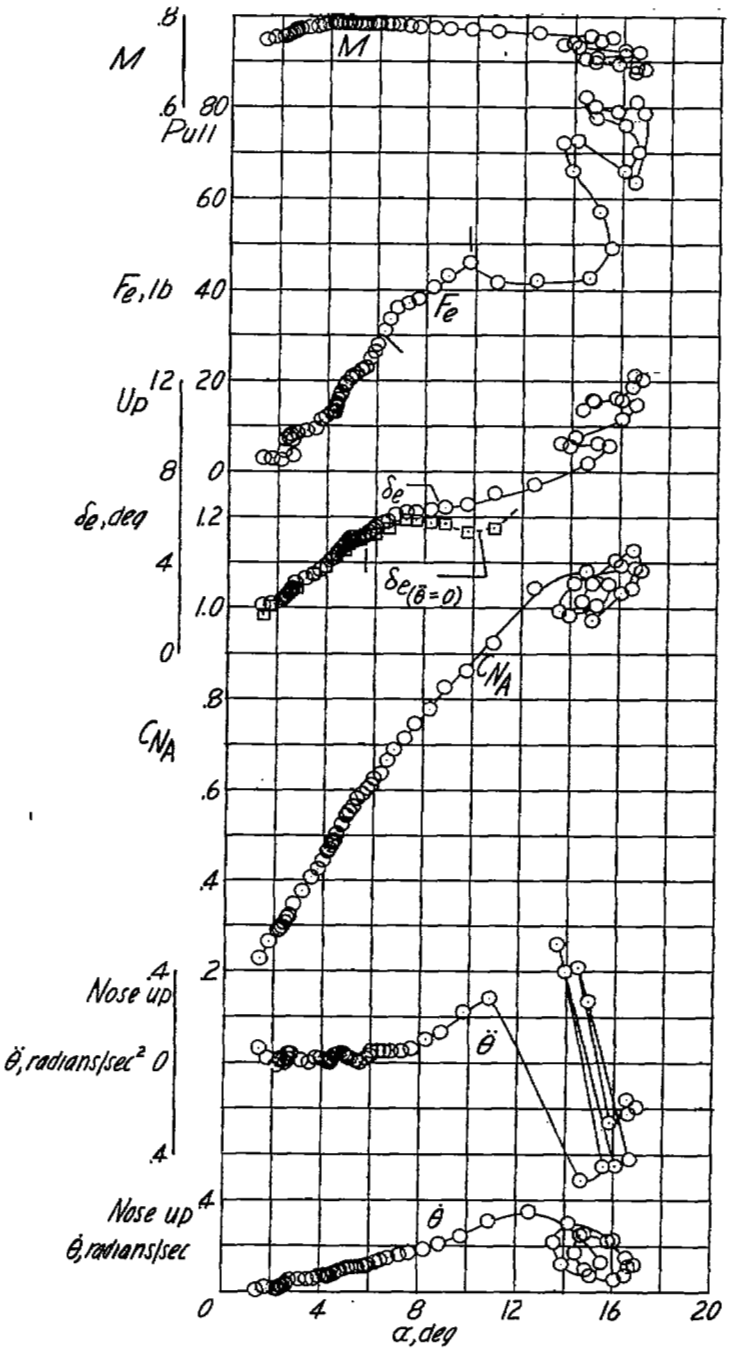

(k) $h_p \approx 26{,}500$ feet; $i_t = 1.6°$; center of gravity at 26.1 percent mean aerodynamic chord.

Figure 14.- Concluded.

[redacted]

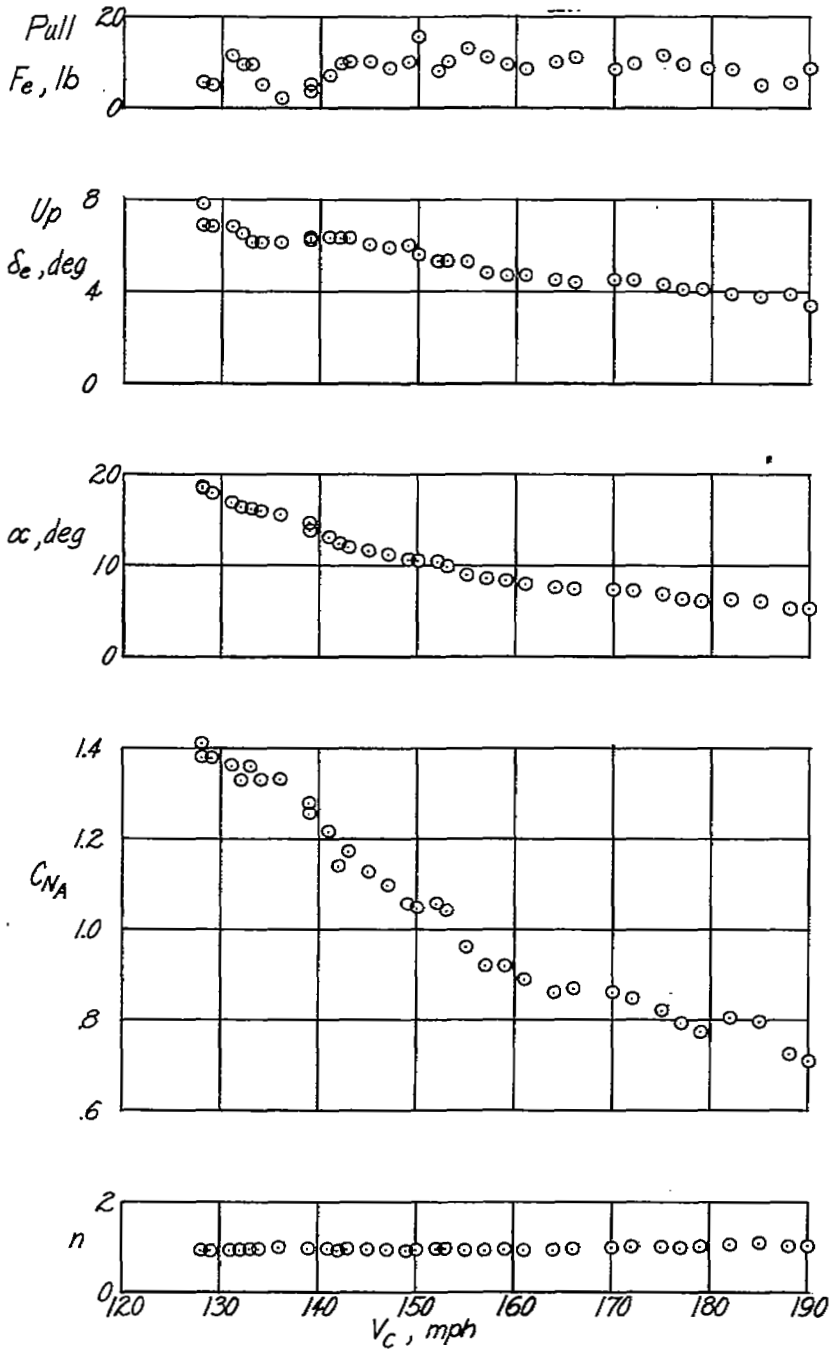

Figure 15.- Low-speed steady-flight static longitudinal stability characteristics of the Douglas D-558-II research airplane with slats fully extended and inboard wing fences on. Flaps and landing gear extended; $h_p \approx 20{,}000$ feet; $i_t = 1.6^\circ$; center of gravity at 25.2 percent mean aerodynamic chord.

[redacted]

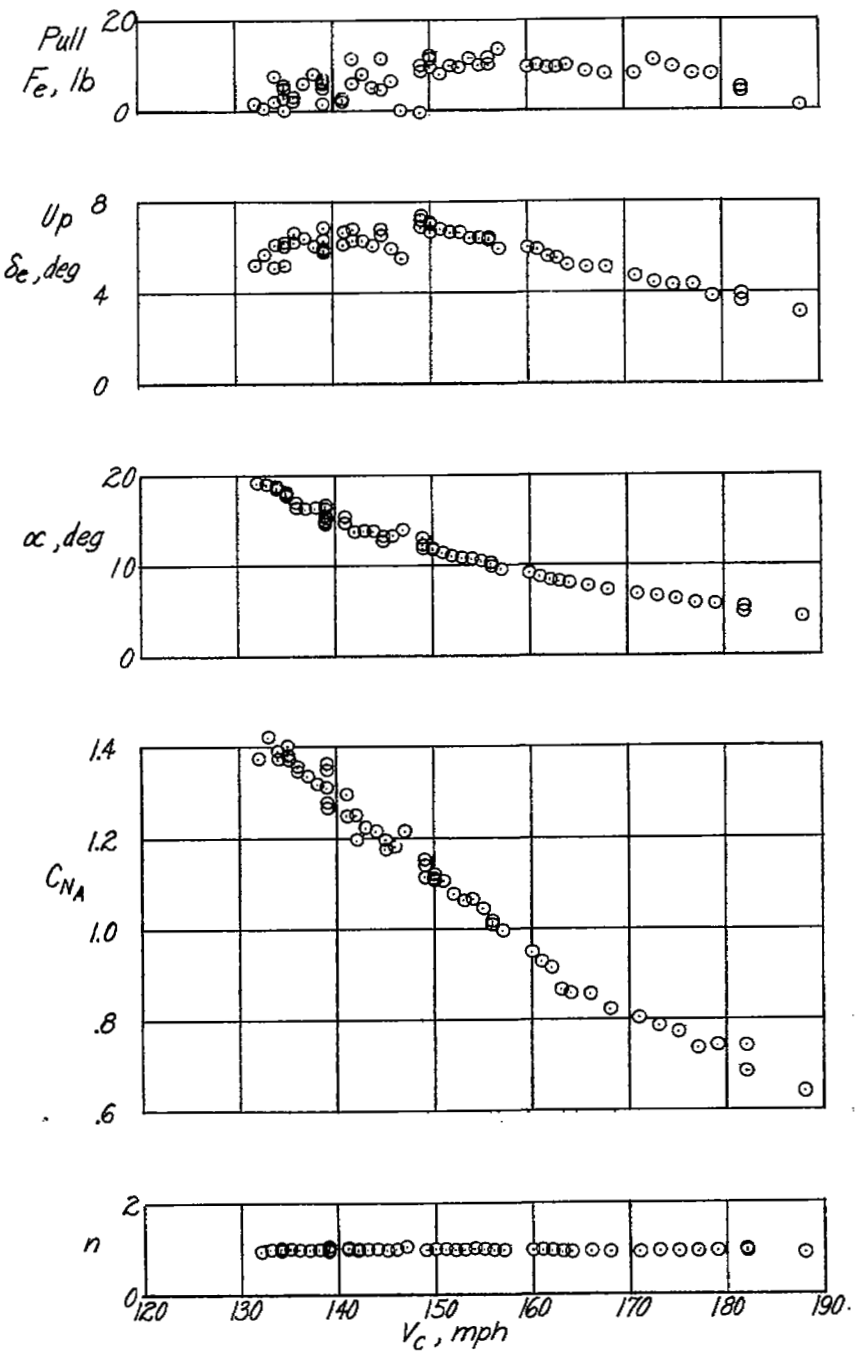

Figure 16.- Low-speed steady-flight static longitudinal stability characteristics of the Douglas D-558-II research airplane with slats fully extended and inboard wing fences removed. Flaps and landing gear extended; $h_p \approx 19{,}250$ feet; $i_t = 1.6°$; center of gravity at 24.9 percent mean aerodynamic chord.

[redacted]

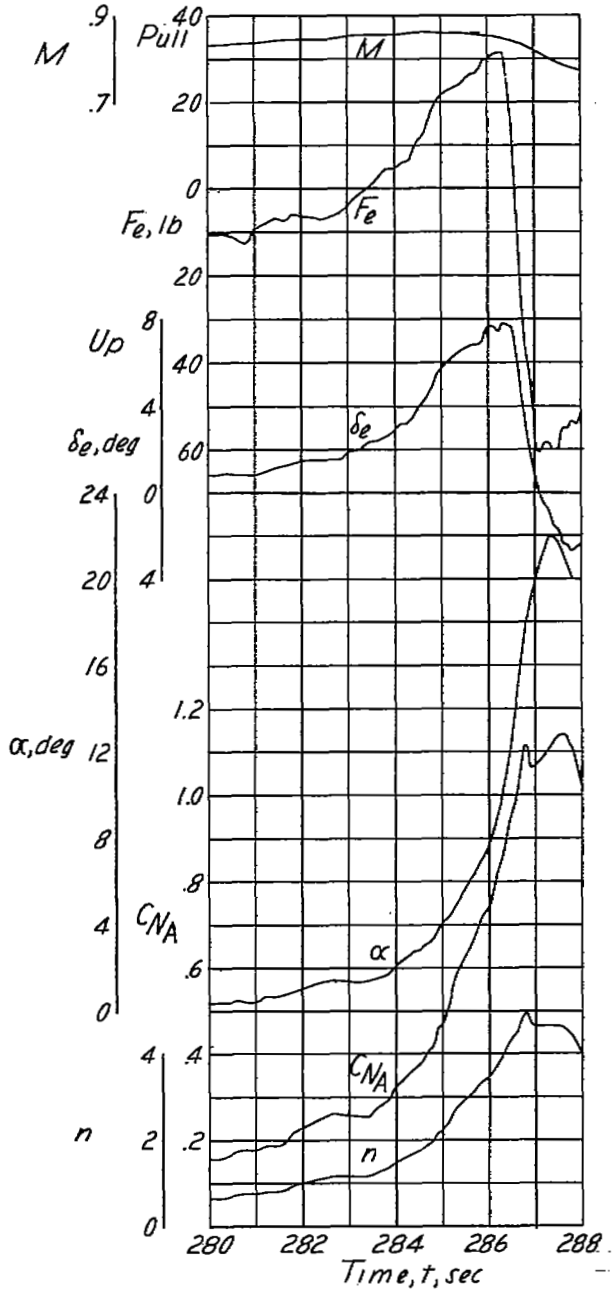

(a) $h_p \approx 29{,}000$ feet; $i_t = 1.6°$; center of gravity at 28.6 percent mean aerodynamic chord.

Figure 17.- Time histories of wind-up turns with the Douglas D-558-II research airplane with slats half extended and inboard wing fences removed.

[redacted]

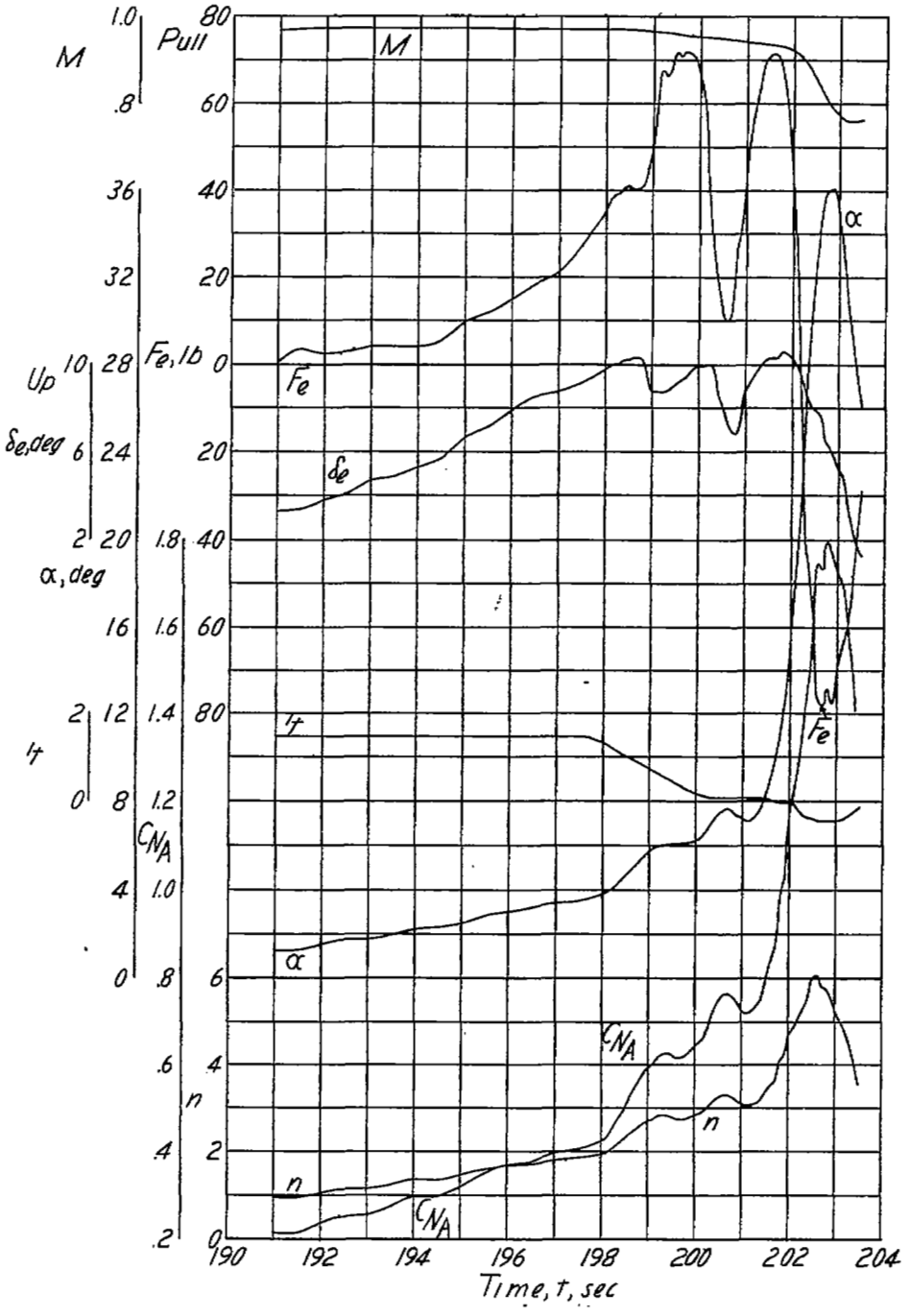

(b) $h_p \approx 35{,}000$ feet; center of gravity at 28.5 percent mean aerodynamic chord.

Figure 17.- Concluded.

[redacted]

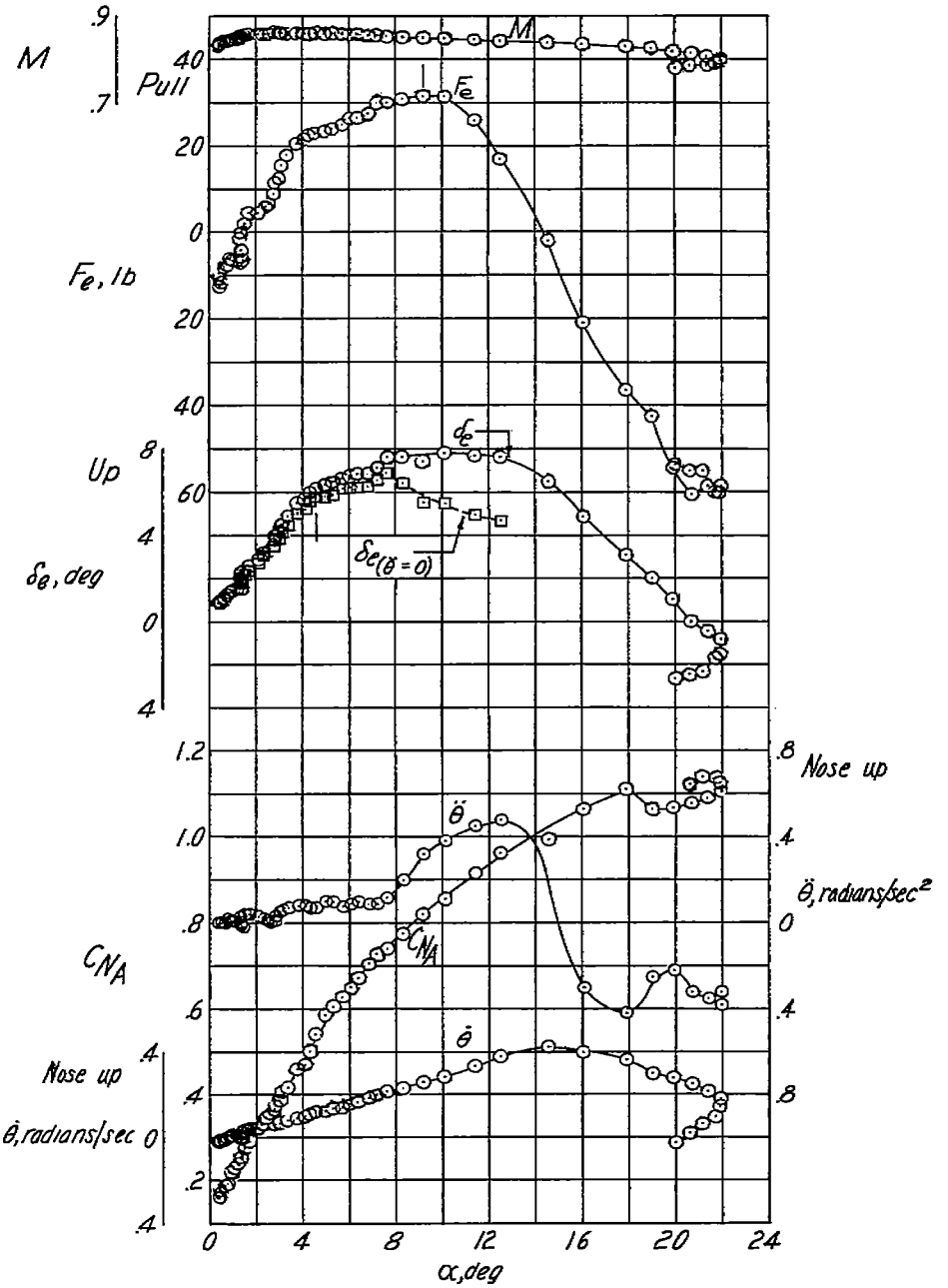

(a) $h_p \approx 29{,}000$ feet; $i_t = 1.6°$; center of gravity at 28.6 percent mean aerodynamic chord.

Figure 18.- Static longitudinal stability characteristics of the Douglas D-558-II research airplane, with slats half extended and inboard wing fences removed, in turning flight.

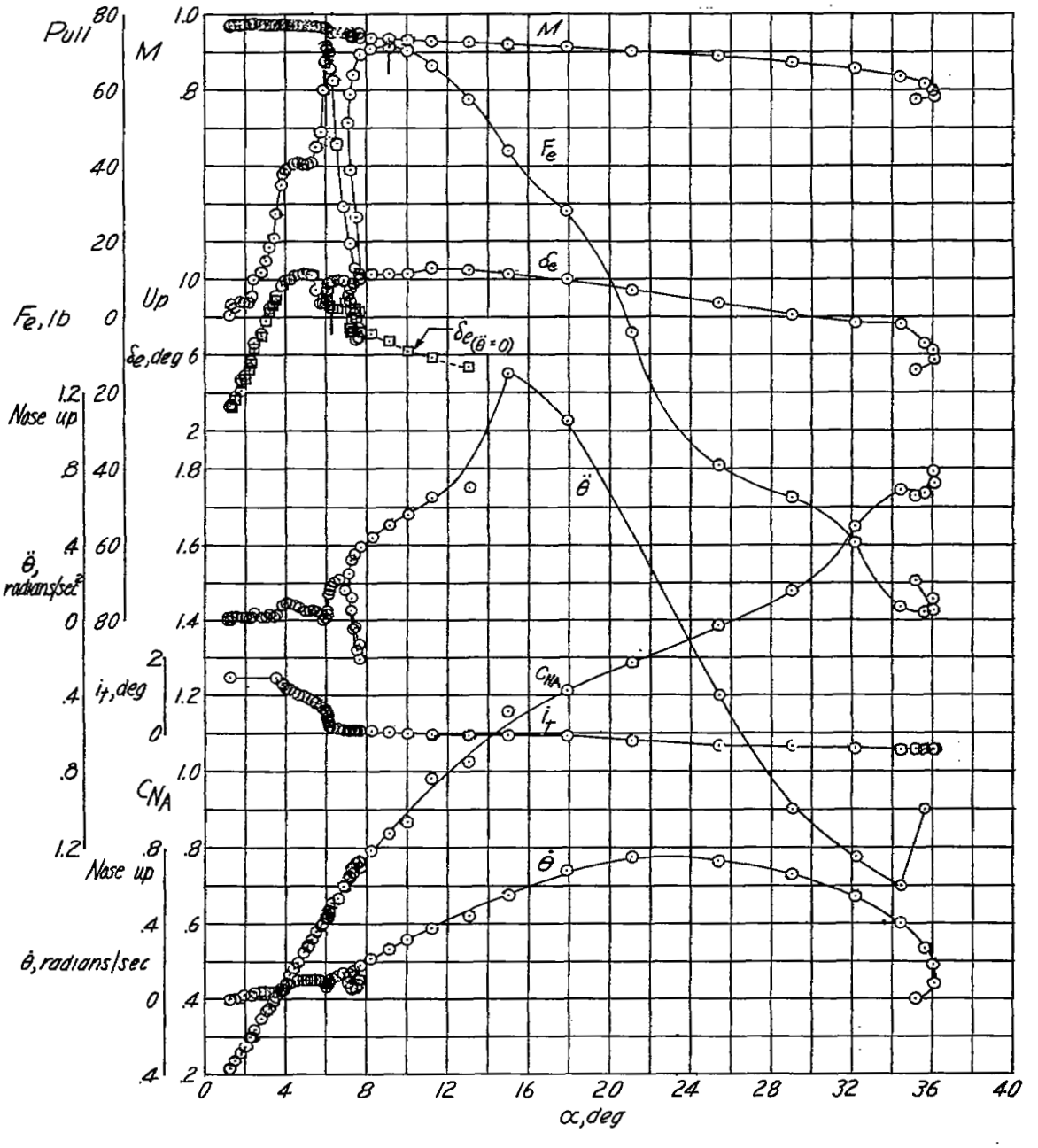

(b) $h_p \approx 35{,}000$ feet; center of gravity at 28.5 percent mean aerodynamic chord.

Figure 18.- Concluded.

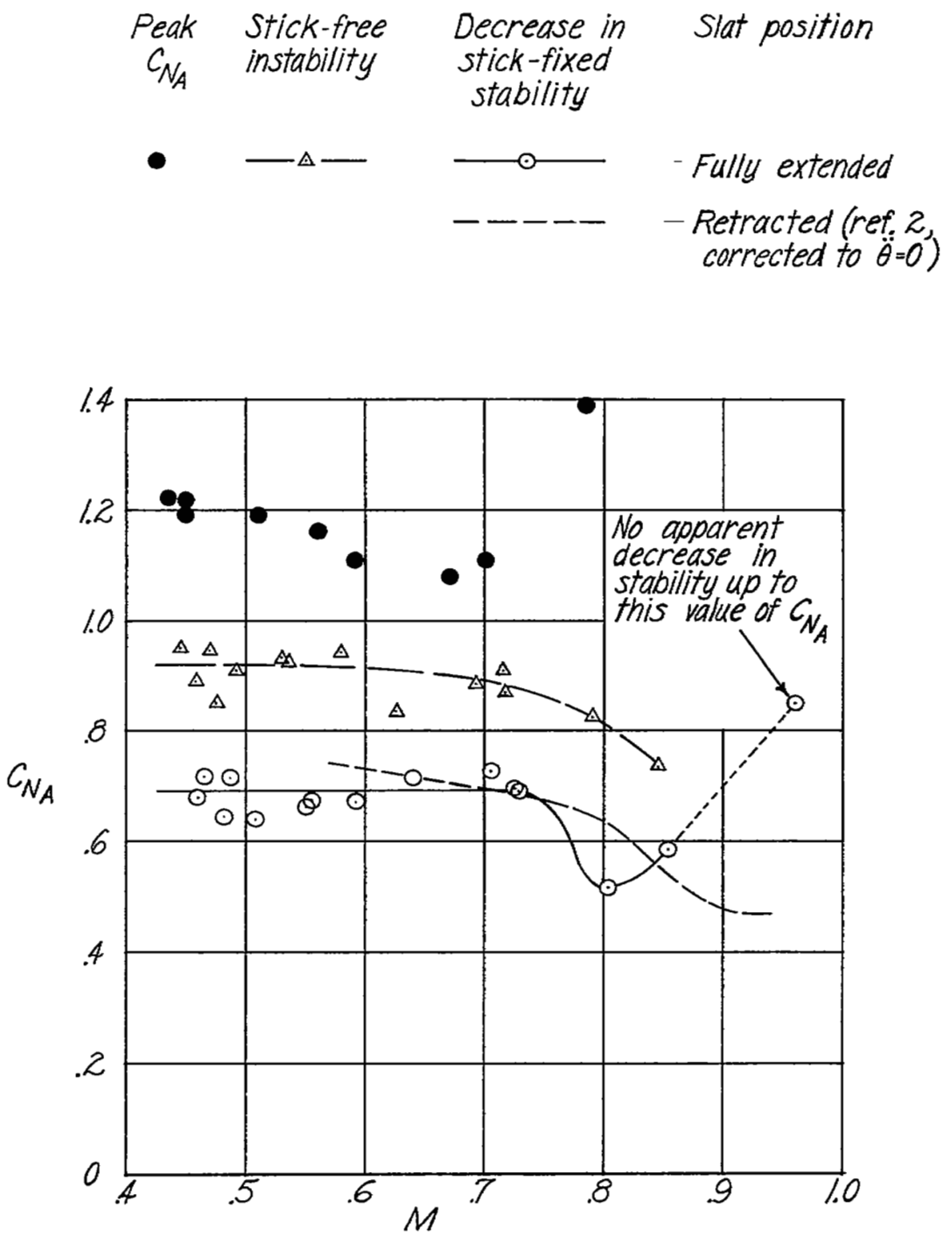

Figure 19.- Normal-force coefficient for decay in longitudinal stability as a function of Mach number for the airplane with inboard fences on the wing.

[redacted]

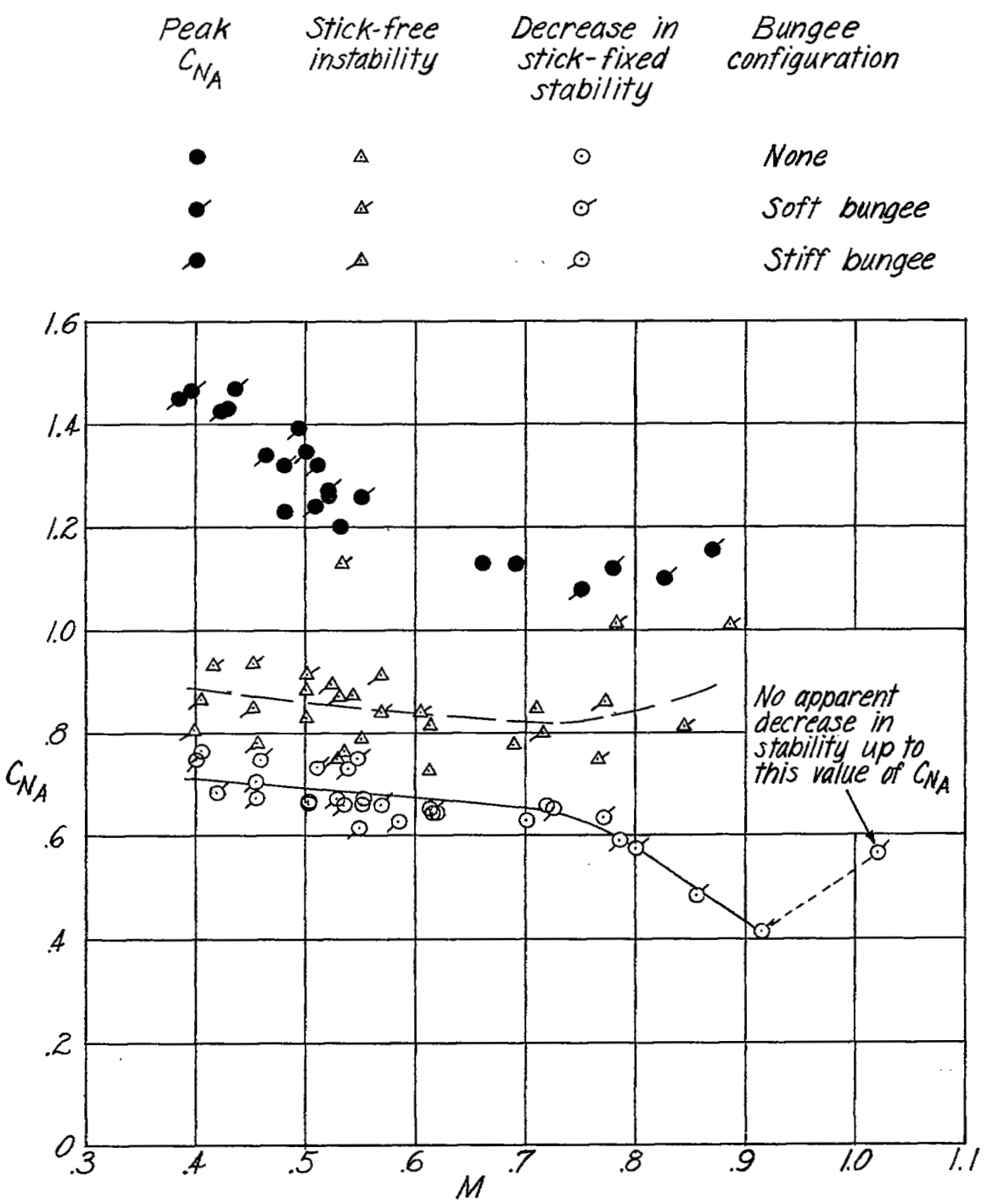

Figure 20.- Normal-force coefficient for decay in longitudinal stability as a function of Mach number for the airplane with fully extended slats and inboard wing fences removed.

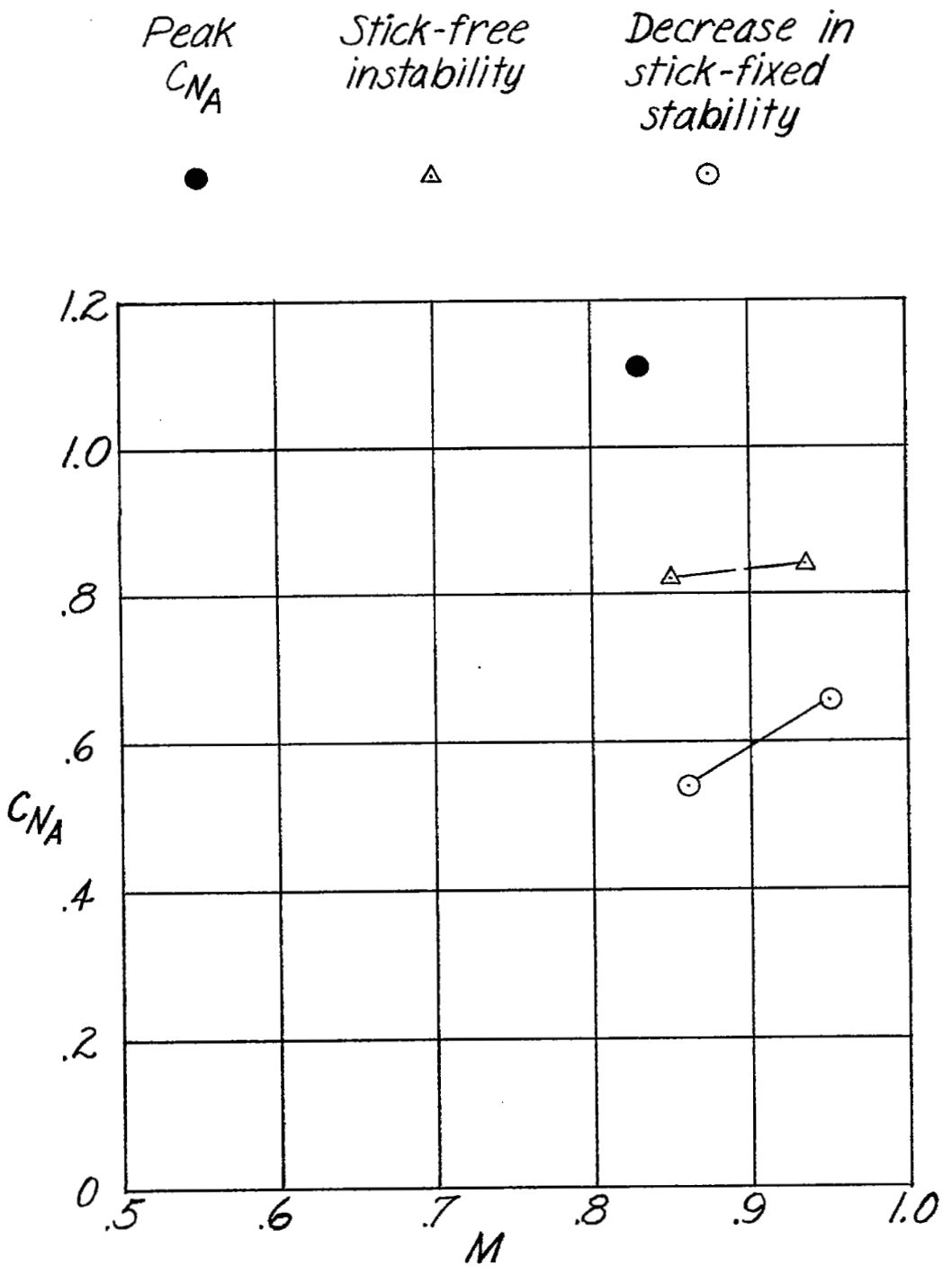

Figure 21.- Normal-force coefficient for decay in longitudinal stability as a function of Mach number for the airplane with half-extended slats and inboard wing fences removed.

[redacted]